NASA CR-54714
EOS Report 6981-Final

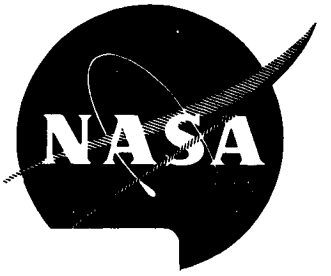

POWER SUPPLIES USING HIGH FREQUENCY MODULES

by
Peter Ramirez, Jr.

prepared for
NATIONAL AERONAUTICS AND SPACE ADMINISTRATION
CONTRACT NAS3-7926

ELECTRO-OPTICAL SYSTEMS, INC.
A Subsidiary of Xerox Corporation
300 N. Halstead St., Pasadena, California, 91107

Requests for copies of this report should be referred to

National Aeronautics and Space Administration
Office of Scientific and Technical Information
Attention: AFSS-A
Washington, D.C. 20546

1136

NASA CR 54714
EOS Report 6981-Final

FINAL REPORT

POWER SUPPLIES USING HIGH FREQUENCY MODULES

by

Peter Ramirez, Jr.

prepared for

NATIONAL AERONAUTICS AND SPACE ADMINISTRATION

February 1, 1967

CONTRACT NAS3-7926

Electro-Optical Systems, Inc. – Pasadena, California
A Subsidiary of Xerox Corporation

CONTENTS

CONTENTS (contd)

ILLUSTRATIONS

ILLUSTRATIONS (contd)

1. SUMMARY

The objective of Contract NAS3-7926 was twofold:

1. To develop three 100 watt power conditioning modules of the lowest possible weight, highest efficiency, and highest reliability.
2. To design a control system which provides power distribution, control, switching, and the necessary regulation to operate ion engines in a space environment.

These objectives were met successfully. As a result of the work on this program three, 100 watt, dc-dc converter modules (designated Module No. 1, Module No. 2, and Module No. 3) were developed and packaged in a flight hardware configuration. These modules utilize a 50 kHz switching frequency in order to minimize the size and weight of the magnetic and filtering components. In keeping with minimum size and weight, ferrite, square-loop core materials are used exclusively for all magnetic components and flat pack, 25 amp, power switching transistors (weighing 3.8 grams) are used for all power switches.

At an output power level of 100 watts, the efficiency of Module No. 1 (250 Vdc at 400 mA) is 88.7 percent with a total package weight of 12.0 ounces. The efficiency of Module No. 2 (5 Vdc at 20 amps) is 72 percent with a total package weight of 25.6 ounces. The efficiency of Module No. 3 (1000 Vdc at 100 mA) is 91.3 percent. The total package weight of this module is 12.0 ounces. The resulting package sizes for the converters are: Module No. 1 and No. 3 - 4.75 x 5.25 x 1.50 inches and Module No. 2 is 11.83 x 5.25 x 1.50 inches.

To achieve high reliability of the converter modules, the criteria employed were those of minimizing component parts and the use of low operating electrical stress levels on the components used. This resulted in a basic reliability number of 0.970 for each converter module. By

using 12 series modules in a one kW system, which includes two spares, the reliability number of the one kW unit will be 0.999. One important feature of these modules is that they provide system backups for component failures at fractional increases in size and weight.

Another important feature in using modular converters is the ability to provide power conditioning of any desired voltage and power level at a considerable reduction in size and weight compared to a more conventional approach. For example ten No. 1 modules can be assembled with outputs connected in series to provide 2500 Vdc at 1000 watts. The total weight of this power subsystem would be 120 ounces for a specific weight of 7.5 lb/kW.

The three converter modules have been designed with overload and short circuit protection. The modules will operate well within their capability when the load impedance is varied from an open circuit to a direct short circuit.

All of the modules have successfully passed the prescribed performance tests. This included periodic overloading and short circuiting of the modules for one hour periods at room pressure and temperature and in a vacuum of 10^{-4} torr or less. The modules also successfully passed a high potentiometer test of 10,000 Vdc applied from input to output terminals (in both polarities). The high voltage was applied while the units were operating normally; both in the unloaded and fully loaded conditions. The high potentiometer test was performed at room pressure and temperature and in a vacuum of 10^{-4} torr or less.

The packaging of the modules is unique in that they are designed for passive cooling. All modules will radiate the internally generated heat (into deep space) via the base plate. The use of other cooling techniques would significantly reduce weight. Use of beryllium oxide was utilized to maximize heat transfer from the power transistors and rectifier diodes to the base plate. While providing a low thermal impedance, the beryllium oxide pads used also provide the necessary high voltage insulation.

A control system was designed to operate the modules with an ion engine on a typical space mission. The control system provides automatic ion engine startup, steady state operation, shutdown, transient control, and voltage regulation. In addition, the control system provides failed module detection and module replacement. Integrated circuits are used exclusively throughout the system in the conversion of analog to digital information and in the detection of failed modules. The weight and power consumption of the complete control system, excluding the magnetic amplifiers is nominally 1.5 pounds and 2 watts for a 1-kW ion engine system. During certain switching conditions, the power requirements will reach 3.5 watts. For unit systems in the 1 to 5 kW range, the control system weight and power requirements should not increase significantly over that for the 1-kW unit.

2. INTRODUCTION

The goals of electric propulsion have placed stringent requirements on the weight, efficiency, and reliability of power conditioning and control systems, compelling designers to search for new and non-conventional designs.

In the past, power conditioning systems for electric propulsion were, for the most part, of a conventional nature, usually having individual dc-dc converters for each of the ion engine heater elements and electrodes. These conventional subsystems are relatively efficient, but are bulky and heavy, and complete redundancy cannot be readily incorporated. The main reason for heaviness and bulkiness is that they utilize state-of-the-art high current, slow switching power transistors to obtain high output power levels. Because of the power transistor limitations, relatively low switching frequencies had to be selected in order to achieve reasonable efficiencies.

Modular power conditioning provides several definite advantages over the conventional approach. It provides power subsystems of extremely small size, low weight, and high efficiency. In addition, high reliability is made possible through redundancy at fractional increases in system size and weight. The modular concept utilizes state-of-the-art, off-the-shelf components. The basic module or building block is a high frequency dc-dc converter which is lightweight, highly efficient, and very reliable. The modules can be connected with inputs in parallel and outputs in series or parallel to achieve the desired output voltage and power level.

3. SELECTION OF A REPRESENTATIVE SPACE MISSION

Work on this program began with the selection of a representative space mission. The selection of such a mission is important in that it defines many of the propulsion parameters and design constraints for the power conditioning. In particular, it defines:

1. Power level
2. Power profile, both voltage and current
3. Specific impulse and requirements for variation
4. Mission duration
5. Reliability required
6. Thrusting mode (cruise and coast phases, duty cycle, and number of cycles)
7. Space environment
8. Spacecraft environment (especially thermal balance)
9. Launch environment
10. Ground handling and checkout
11. Compatibility testing during integration with engines and spacecraft

The reduction in effort on the 300 kW SNAP 50 system, and the recent developments in improved solar-power sources, have together increased the interest in solar-powered electric rockets. Mission studies for this type of propulsion are reported in Ref. 1 and elsewhere, but most of the published analyses have reported that the payload capability of solar-electric rockets was not high enough when the power systems would weigh 100 lb per kW or more.

The recent designs of solar-power systems in which the solar-array specific weight may be reduced from 50 to 25 lb/kW and the power conditioning weight from 15 to 5 lb/kW, make it possible to consider

---

Ref. 1 EOS Report 3830-Final, Vol. 2

not only the class of missions for which SNAP 50 had appeared attractive, but to consider other missions at widely differing power levels, because the solar power itself is based on a modular approach using an extremely small unit - the individual silicon cell. A brief discussion of these missions follows.

3.1 Earth-Centered Missions

Missions in which the spacecraft remains in the vicinity of the earth are characterized by essentially constant power, except for time spent in the earth's shadow or the slow degradation and minor sporadic losses of power through total damage of individual cells. Among the many missions that can be considered, three are particularly pertinent to the present considerations.

3.1.1 Orbit Sustaining Against Atmospheric Drag in Manned Orbiting Systems

The requirements for propulsion in systems such as the MORL include: (1) drag make-up, (2) desaturation of momentum storage attitude control systems, and (3) precession of the spin axis of manned laboratories with artificial-G produced by spacecraft rotation. In considering electric propulsion for such missions, it is recognized that addition of solar panels to provide propulsive power adds to the spacecraft total drag and becomes prohibitive at altitudes below about 150 nautical miles. At 200 nautical miles, electric propulsion in the 1000 to 2000 second range appears attractive and ion engines operating at 3000 seconds and above would be penalized by this additional drag in present MORL designs. This effect would not be present to such an extent with isotopic or reactor power sources (their radiators are somewhat smaller than the solar arrays), but these power sources are not relevant to the present study.

3.1.2 Station Keeping and Attitude Control in Synchronous Orbit

At present, there appears to be no large spacecraft requirement in synchronous orbit, other than perhaps a manned space station at a future date, and consideration should only be given to

unmanned spacecraft in the range of 200 to 2000 lb. The thrust level required for station keeping and attitude control for such satellites is less than one millipound for designs in which thrusting is performed by electric propulsion in a near optimum manner.

At this low thrust level, the power requirement of less than 200 watts is too modest to consider extensive modularization of the power conditioning system.

3.1.3 The Lunar Ferry

The use of electric propulsion to ferry slow freight from earth orbit to lunar orbit has received much consideration. It is clear that for really significant payload advantages, i.e., sufficient to offset the possible disadvantages of long trip time, the electric propulsion systems begin to be significant only for total power system weights of less than about 20 lb/kW.

Other earth-centered missions include: (1) orbit transfer from low altitude to higher altitude earth orbits; (2) station keeping to prevent bunching when a number of satellites are placed in the same orbit; (3) deployment of many small satellites during a spiral trajectory performed by the electric thrustors; (4) mapping of the environment in cislunar space; and (5) orbit control operations in lunar orbit. However, none of these missions can be considered definitive enough to be used as representative for the present study.

3.2 Sun-Centered Missions

Missions in which the electric propulsion system is used for heliocentric transfer include: (1) probe and capture missions to the near planets and their satellites, (2) probes of the asteroids and the sun itself, and (3) probes which rise significantly out of the plane of the ecliptic. Solar-powered electric propulsion does not yet (with present weights) offer attractive combined trajectories which would include earth escape spiral, heliocentric transfer and planetary capture spiral, and so we can consider the sun-centered missions to take

place entirely out of the shadow of occluding planets. Such missions are characterized by changing solar flux and changing thermal conditions which affect the efficiency of photovoltaic systems.

3.2.1 Asteroid and Cometary Probes

The energy requirements for missions of this type are not large enough to require the use of solar-electric propulsion, and there will be no payload advantages unless the power supply specific weight can be reduced somewhat below 25 lb/kW.

3.2.2 Solar Probe

An extremely attractive solar probe mission would consist of retrothrusting to achieve a first solar approach posigrade thrusting following the initial close approach in order to obtain a highly eccentric orbit and then using retrothrust a second time after aphelion to achieve a close approach at the second perihelion. This somewhat ambitious mission could be performed readily with solar power, providing the solar array can be protected from serious damage at the first solar approach. It would provide an interesting mission to study the method of handling the wide variation in power, but insufficient consideration has been given to the many environmental and operational problems involved and the study would appear to be too extensive to be performed for present purposes.

3.2.3 Out-of-the-Ecliptic Probe

The use of electric thrustors in the out-of-plane direction for a half period and reversing for a second half period, will result in inclination of the spacecraft orbit about the line joining the mid-thrusting positions. In performing such a mission following earth escape, the trajectory would be characterized by essentially constant solar flux with no earth shadow.

In order to incline the orbit more than 15 degrees in one year (a typical time considered for such a mission), the total power system weight would need to be less than 25 lb/kW in order to carry a significant scientific payload.

3.2.4 Probe and Capture Missions to the Near Planets

Missions to Venus and Mercury are characterized by such short flight time by chemical rocket that electric propulsion can only compete with very lightweight power supplies. The carrying of a payload into a capture orbit at Jupiter is of considerable interest in that it is a somewhat difficult mission to perform by chemical rocket, and electric propulsion appears to offer a payload advantage (a factor of 3 to 10) in comparable trip time. The Mars orbiter mission, on the other hand, offers a payload advantage over chemical rockets only at the cost of some increase in flight time and the final choice of a preferred reference mission for solar electric propulsion rests between the Jupiter probe or orbiter and the Mars orbiter mission.

In choosing between the above two missions, the deciding factor is that the Mars orbiter mission has already received extensive study so that the thrusting parameters, the environment, and the spacecraft integration factors are already well understood. Both missions would give typical environments, power profiles, thrusting modes and reliability requirements, but the Jupiter missions have not yet been studied in detail. This is true not only of the electrically propelled missions, but also of the chemically propelled alternative.

It is therefore concluded that the Mars orbiter mission, which is the subject of joint NASA/USAF/JPL studies, should be used as the reference mission for the present studies.

3.3 Characteristics of Reference Mission

The particular Mars orbiter mission selected is that based on a Saturn-Centaur launch vehicle using solar-powered ion propulsion to effect a transfer from earth escape to a high altitude eccentric Mars orbit in 350 days.

1. The power level at earth into the power conditioning system is approximately 45 kilowatts and falls inversely as the 1.7 power of the distance. The solar cell output voltage increases with distance from the sun by approximately 25 percent on reaching Mars.

2. The specific impulse is nominally 5000 seconds at earth but can increase to accommodate the changing voltage with distance.
3. The thrusting mode can be considered as continuous thrust starting a few days after orbit injection, with shutdown of the propulsion system at 325 days. No cyclic operation of the thrustors is required, although the protective circuitry will provide for shutdown/restart, as required, if serious arcing occurs between thrustor electrodes.

The requirements on reliability and on the external local and launch environments will be taken directly from the NASA/USAF/JPL studies.

4. HIGH FREQUENCY DC-DC CONVERTER MODULES

This section will discuss the design, development and testing of the high frequency dc-dc converter modules.

4.1 Module Change

For the Mars Orbiter mission, the power level at earth into the power conditioning system is approximately 45 kilowatts and falls inversely as the 1.7 power of the distance. State-of-the-art bombardment ion engines such as the EOS DF engine or the NASA-Lewis Hg engine could be utilized for such a mission.

Consideration was given to the power conditioning requirements for both engines. Table I shows the power requirements for minimum thrust levels for a DF type engine over the specific impulse range from 3000 to 10,000 seconds. These limits are imposed by simultaneous attainment of optimum efficiency and lifetime with the engine adjusted for a nominal operating specific impulse of 7000 seconds. Table II shows the power conditioning requirements for the NASA-Lewis Hg engine.

A look at the power requirements for both engines indicated that Module No. 1 which would normally be used to supply the positive high voltage provided excessive current (1 A nom.) at 100 Vdc. A more suitable output was 250 Vdc at 400 mA. This would enable series connection of the module outputs and fewer modules would be required. This change in Module No. 1 was discussed and agreed to by Mr. Russ D. Shattuck, the NASA Technical Monitor. A formal request for change in Module No. 1 was submitted and received by EOS.

Modules No. 2 and No. 3 remained unchanged at 5V at 30A and 1000 Vdc at 100 mA respectively.

TABLE I

MINIMUM THRUST LEVELS

EOS DF ENGINE*

Positive High Voltage, V_+ (kV)	0.87	1.38	2.06	3.80	6.10	7.5
Negative High Voltage, V_- (kV)	1.50	1.00	1.80	0.50	0.50	0.50
Negative HV Current, I_- (amp)	0.003	0.002	0.002	0.002	0.005	0.006
Beam Current, I_B (amp)	0.125	0.150	0.175	0.250	0.450	0.650
Arc Voltage, V_A (volt)	6.5	6.6	6.7	6.9	7.0	7.0
Arc Current, I_A (amp)	7.7	9.1	10.4	14.5	25.7	37.1
Beam Power, P_B (kW)	0.109	0.207	0.360	0.950	2.745	4.870
Drain Power, P_D (kW)	0.007	0.005	0.006	0.011	0.030	0.052
Magnet Power, P_M (kW)	0.012	0.012	0.012	0.012	0.012	0.012
Arc Power, P_A (kW)	0.050	0.060	0.070	0.100	0.180	0.260
Total Power, P_T (kW)	0.178	0.284	0.448	1.073	2.967	5.194
Thrust, T (mlb)	1.39	2.10	3.00	5.80	13.30	21.20
Power to Thrust Ratio, P/T (kW/lb)	128.0	135.2	149.3	185.0	223.1	245.0
Power Efficiency, η_p (%)	61.2	72.9	80.4	88.5	92.5	93.8
Mass Efficiency, η_M (%)	83.0	88.0	90.0	93.0	94.0	94.0
Overall Engine Efficiency, η_E (%)	50.8	64.2	72.4	82.3	86.9	88.2
Specific Impulse, I_{sp} (sec)	3000	4000	5000	7000	9000	10,000

*Ref. 2. F. S. Osugi, "Analysis of Electrical Propulsion Electrical Power Conditioning Component Technology," EOS Report 5401-M-11

TABLE II

OVERALL ENGINE PERFORMANCE (NASA-LEWIS ENGINE)*
(Nonuniform magnetic field)

Ion chamber potential V_I, v	Accelerator potential V_A, v	Beam current (common ground), J_B, amp	Magnetic-field potential difference, ΔV_M, v	Magnetic-field current, J_M, amp	Ion-chamber potential difference, ΔV_I, v	Current collected by anode, J_A, amp	Current collected by accelerator, J_A, amp	Filament heating potential difference, ΔV_F	Filament heating current, J_F	Energy dissipated in discharge per beam ion, ev/ion	Specific impulse, sec	Overall power efficiency, η_P, P_B/P_T	Thrust, lb
4000	1100	0.250	7.0	6.5	55	3.35	0.0025	6.5	10.0	682	6300	0.772	7.2
7000	1400	0.250	↓	6.1	50	3.10	0.0020	7.3	10.2	570	8400	0.863	9.4
4800	1250	0.250	↓	6.0	45	3.20	0.0030	7.6	11.3	531	6900	0.811	7.9
2500	1000	0.125	6.0	↓	50	1.51	0.0002	6.7	10.8	554	5000	0.637	2.9
2500	1000	0.125	6.0	↓	55	1.43	0.0002	6.6	10.7	574	5000	0.636	2.9
5500	1250	0.340	7.0	↓	62	4.30	0.0040	7.6	11.0	722	7400	0.824	11.4
5800	1250	0.405	↓	↓	74	4.80	0.0040	7.6	11.0	803	7600	0.831	14.0
6500	1250	0.400	↓	↓	68	5.00	0.0042	8.4	11.0	782	8080	0.844	14.8
4000	1400	0.350	9.0	6.5	55	5.00	0.0050	10.0	20.0	731	6300	0.721	10.0
3500	500	0.510	7.0	5.6	47	8.40	0.0065	9.0	22.0	727	5900	0.738	13.8
6250	1750	0.250	↓	6.3	50	2.30	0.0022	7.1	10.4	410	7900	0.867	9.0
6000	1500	0.250	↓	↓	↓	2.15	0.0022	6.9	10.5	380	7750	0.868	8.8
5500	1500	0.250	↓	↓	↓	2.40	0.0025	7.1	10.7	430	7400	0.848	8.4
5000	1500	0.250	↓	↓	↓	2.55	0.0050	7.2	10.9	460	7070	0.822	8.2

*Ref. 3. P. D. Reader, "Investigation of a 10-Centimeter Diameter Electron Bombardment Ion Rocket," NASA TND-1163

4.2 Design Objectives for the Power Conditioning Modules

The program objective was to develop ion engine power conditioning systems of the lowest possible weight, highest efficiency, and highest reliability. Variations from this objective were dictated by overall system considerations, and final module specifications were dictated by system optimization. All variations were submitted to the NASA Project Manager for approval prior to fabrication. The following defined the nominal design base.

4.2.1 Electrical Specifications

Modules

Input voltage:	56 Vdc or less with ±5 percent regulation
Output voltage:	
Module 1:	250 Vdc at 0.40A nominal
Module 2:	5 Vdc at 20A nominal
Module 3:	1000 Vdc at 0.100A nominal
Output ripple:	10 percent rms
Regulation:	25 percent NL to FL and 10 percent 1/2 load to FL

Overload Protection

The modules shall either (1) be able to tolerate a load in the form of any value of resistor or capacitor or (2) shut down in sufficient time to prevent damage to any portion of the circuit after the application of any of the above overload conditions. Emphasis shall be on the latter.

Insulation

The output of each module shall be capable of withstanding a dc potential test of ±10,000 volts with respect to the input and to all heat sinks.

Efficiency

Module 1: 89 percent

Module 2: 75 percent dc, 91 percent ac

Module 3: 90 percent

Weight

Module 1: 7.4 oz

Module 2: 12.0 oz

Module 3: 7.4 oz

Package Sizes

Module 1: 4-1/4 x 5-1/4 x 1-1/2 inches

Module 2: 5-1/4 x 10-1/2 x 1-1/2 inches

Module 3: 4-1/4 x 5-1/4 x 1-1/2 inches

NOTE: The output transformers shall be constructed with a thermocouple near the most probable hot spot. Insulation shall be suitable for 155°C operation or greater.

Mechanical Base Design

Modules 1 and 3 shall have the same overall package size and shall be designed to fit interchangeably in a honeycomb type of housing as shown on EOS Drawing 31-1004 incorporated herein by reference. The base plate of each module measures 4-1/4 by 5-1/4 inches, and the outside shell is 4 by 5 inches by 1-1/2 inches high; thereby providing a lip on all sides to grip the edges of the honeycomb. Module 2 shall occupy three spaces, with an overall package size of 5-1/4 x 10-1/2 x 1-1/2 inches high. Each module shall be held in place by a clip engaging holes in the module base plate, with a captive type fastener engaging a quick-connect receptacle in each honeycomb intersection. Input and output electrical connections to the module shall be provided by push-in type terminals engaging sockets in the top of the module shell.

4.2.2 Testing Specifications

Static overload testing of the modules shall be performed as follows:

Test No. 1

With the unit operating normally, but with no load, a dummy load consisting of resistors and capacitors shall be connected to the output terminals by means of a relay closure. Peak and average currents and voltage shall be measured on all semiconductors by means of oscilloscope photographs and meters to record the transient and steady state data. This test shall be conducted at a repetition rate of two to ten times per minute for one hour without failure or measurable degradation in performance of the unit.

Test No. 2

With the unit operating at rated load, Test 1 shall be repeated in its entirety.

Test No. 3

With the unit operating normally, but with no load, a potential of 10,000 Vdc shall be applied between the input and output terminals and between output terminals and the heat sinks for ten minutes. Leakage current shall not exceed 100 microamperes with the dc potential of either polarity. There shall be no measurable degradation or failure due to this test.

Test No. 4

With the unit operating into its rated load, Test 3 shall be repeated in its entirety.

All tests shall be conducted both in air, at normal temperature and pressure, and in a vacuum at 10^{-4} torr or lower.

For vacuum tests, the modules shall be mounted with five sides insulated by double walls of mirror finished stainless steel. The radiator surface shall be exposed facing the LN_2 ($77^{o}K$)

cooled plate of sufficient area to give an essentially infinite view factor. The place shall be coated with "Parsons Optical Black Lacquer" which has a calibrated α at $77^{o}K$. Both the radiator and receiver shall be instrumented with thermocouple so that radiation efficiencies in space may be calculated.

4.2.3 Quality Assurance

1. In support of the fabrication of the power conditioning modules, the contractor shall implement applicable provisions of EOS Product Assurance Manual — Volume 1, dated May 1964, in compliance with provisions of NASA Quality Publication NPC 200-3. Particular emphasis shall be placed on the receiving and in-process inspection of those parameters that cannot be verified after assembly. In order that the above be accomplished effectively, the contractor shall prepare a processing and inspection instruction that defines the inspection points and details the actual inspection operation. This instruction shall be used as the record document to provide evidence of quality for the fabrication of the item. The instruction shall be submitted to NASA for approval 2 weeks prior to fabrication of the first module.
2. NASA Quality Document NPC 200-4 shall be complied with during the fabrication and design phases of this contract.

4.2.4 Reliability

All parts shall be selected from one of the following preferred parts lists in order of decreasing preference:

1. MSFC M-ASTR-TSR-PPL-1 Electrical
2. JPL ZPP-2061-PPL-F Electrical
3. MIL-R-38100A Reliability Assurance
4. MIL-T-38099 Test Methods
5. MIL-R-38101 Resistors
6. MIL-C-38102 Capacitors
7. MIL-S-38103 Semiconductors

In the event a required part is not listed, it may be used upon approval of the NASA Project Manager. The following general rules shall apply:

1. Semiconductors, except high voltage rectifiers, shall be operated at not greater than 1/2 their voltage and not greater than 1/2 their current ratings for their operating temperature. Semiconductors, except high voltage rectifiers, shall be operated at estimated junction temperatures at least 5°C below their rated temperature. The junction temperature shall be estimated with the aid of heat sink temperature measurements made close to semiconductor in question.
2. High voltage rectifiers shall be rated at peak inverse voltages at least 2-1/2 times their use rating and for current at least 2-1/2 times their use rating. In the event of overloads, the rectifiers shall not be stressed above 1/2 their peak voltage and current ratings for the overload conditions.
3. Other components shall be operated at no greater than 1/2 their voltage or current rating.

4.3 Design Considerations

Since the prime power source selected for the Mars Orbiter mission was a solar array, the basic problem was that some type of dc-to-dc conversion was required. This assumed that the prime source power was not directly usable.

In static converter design, a fundamental tradeoff exists between weight and efficiency. For example, as the frequency is increased the weight of the converter may be decreased mainly because of the reduction in weight of the magnetic and filtering components. However, as the switching frequency is increased, the efficiency of the circuit is reduced because of increased transistor switching losses. In the frequency range of interest here, the transformer

losses actually decreased as the switching frequency was increased, but the increasing transistor switching losses more than cancel this effect. The transformer losses decrease because of reduced copper losses and because at higher switching frequencies the transformer may be operated at a low flux density without the penalty of a large number of primary turns.

Transistor losses are a function of switching time and it is therefore desirable to use as fast a switching device as is possible. However, as the required output power level is increased, large power transistors must be used and these are typically characterized by inherently slower switching speeds than those of the lower power class. The result is that conventional, large power converters are usually operated at low switching frequencies and have relatively high efficiencies, but are very bulky and extremely heavy.

The modular approach utilizes extremely fast switching transistors in the light to medium power level, together with highly efficient magnetic materials, to produce extremely lightweight, highly efficient, and highly reliable high frequency power converter modules. These modules can then be used as "building blocks" to assemble larger power systems that are much smaller, weigh considerably less, and are as efficient as a conventional power converter.

Before the design of the high frequency converters could be initiated, considerable attention was given to the following areas:

1. Second breakdown effects
2. Storage time effects
3. Fast switching power transistors
4. Fast recovery rectifiers
5. Transformer designs
6. Circuit selection

4.3.1 Second-Breakdown Effects

Second breakdown is a factor that must be considered in the design of high speed, high power converters. In general,

second breakdown is a condition in a junction transistor that causes the output impedance to change instantaneously from a large positive value to a negative value and then a final small positive value. In some respects, second breakdown appears similar to a normal avalanche breakdown, either collector-to-base (BV_{CBO}) or collector-to-emitter $V_{CE(SUS)}$. There are however, two major differences: (1) the second-breakdown final limiting voltage is always in the 5 to 30 volt range, while BV_{CBO} and $V_{CE(SUS)}$ usually have much higher limiting values, and (2) second breakdown is energy dependent while BV_{CBO} and $V_{CE(SUS)}$ are independent of energy to a first order approximation.

Physically, second breakdown is a local thermal runaway effect induced by severe current concentrations. These concentrations can result from biasing conditions, excessive transverse base fields and defects in the base region or junctions or both. It can be found to some degree in all junction transistors. In many transistors, primarily small signal and low frequency power types, the maximum steady state dissipation rating limits the voltage-current product to something less than the critical value necessary to produce second breakdown. Results show that transistors with higher frequency characteristics undergo second breakdown at lower power ratings. This behavior is attributed to a narrower, active base spacing, which increases the severity of transverse base fields, amplifies biasing effects and raises the defect level relative to the greater tolerances required.

If the on time of the transistor is decreased or the frequency of operation is increased, the critical voltage-current product necessary to produce second breakdown becomes greater. This condition results from the fact that the rate of localized heating is governed not only by current concentration, but by the thermal time constant of the semiconductor material; therefore high frequency, high power transistors can safely handle large power dissipation without incurring second breakdown in high speed switching circuits.

High frequency, high power transistors are rated for second breakdown in two ways: (1) a safe operating range curve for forward-bias drive conditions, with time as the running variable, and (2) a safe operating range curve showing second breakdown energy as a function of reverse-bias voltage and inductances. Forward bias second breakdown can be analyzed as follows: During the turnon time the transistor is subjected to high dissipation in the active region. A plot of the experimentally determined load line superimposed on the transistor safe operating region curve for the appropriate time duration, t_{ON}, will determine whether the circuit is operating in the safe operating region for second breakdown.

Reverse bias breakdown can be analyzed as follows: During the fall time, t_f, the transistor is subjected to high energy as a result of energy stored in the output transformer leakage inductance. This leakage inductance can be made small by careful winding of the transformer to obtain close coupling. An approximation of the value of leakage inductance can be obtained by measuring the primary inductance with the secondary winding short-circuited. The leakage inductance value and the peak collector current can be used to provide an analysis of reverse-bias second breakdown.

4.3.2 Storage Time Effects

As operating frequency increases, limiting factors such as power dissipation, core loss, frequency response and storage effect become more severe on converter operation. At high frequencies, the most severe limiting factor is the storage time effect. Figure 1 shows a typical two transformer converter circuit. During the storage period, while the transistor on one side of the push-pull circuit begins to conduct, the transistor on the other side remains on; thus the two simultaneous collector currents cause magnetic fluxes that oppose each other. Therefore high current spikes are produced.

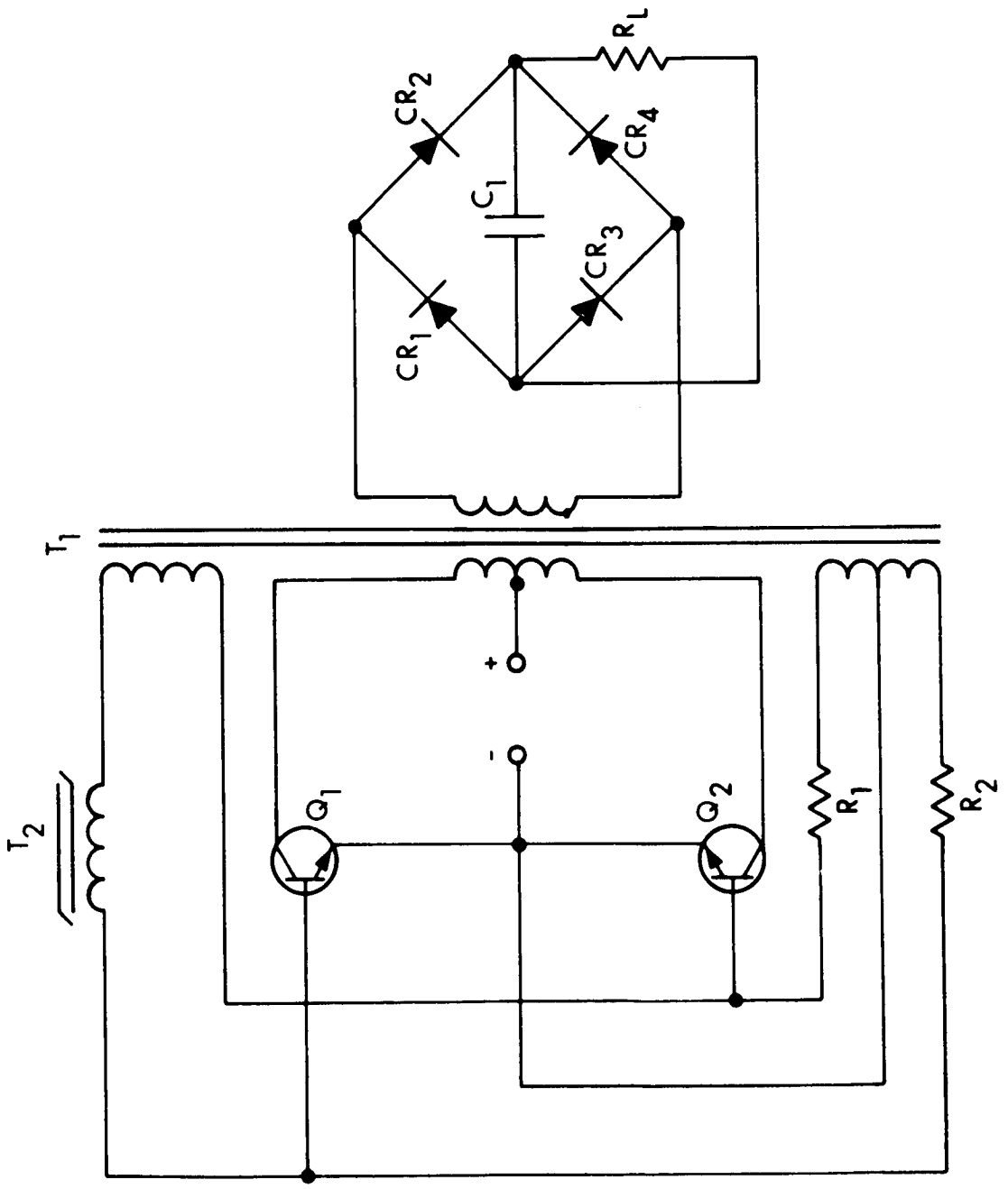

FIG. 1 TYPICAL TWO-TRANSFORMER CONVERTER

The collector current is determined to a first approximation by the base current times beta. The collector-to-emitter voltage (V_{CE}) is at its maximum at this time, therefore transistor dissipation is extremely high until the stored charge is cleared in the opposite transistor. Since the storage time is directly proportional to overdrive, these losses are even greater at lighter loads than at rated loads of the converter.

The high collector currents also cause excessive voltage spikes at switchover which could destroy the transistors. The voltage spikes are a result of the stored energy from the inductance of the circuit leads and leakage flux of the transformer.

It is imperative that the transistors of high frequency converters should have low thermal resistances and fast switching characteristics.

The converter transformer should have low core loss and low leakage inductance.

Converter circuits that receive their drive or are synchronized from a separate driver or inverter stage are also subject to the same problems. Figure 2 shows a converter circuit which provides compensation for storage time. The circuit prevents forward bias from being applied to one transistor while the other transistor is on. The polarities shown exist after base drive has reversed but before storage time has allowed the on transistor to turn off. Reverse bias is applied to Q1 but forward bias is shunted from Q2 through CR2, winding 1-2 and the collector-emitter circuit of Q1 to the return of the drive winding. When Q1 starts turning off and the emitter-collector voltage exceeds the bias winding voltage, forward bias is applied to Q2 and the next cycle of operation begins. The bias windings are necessary to overcome the forward drop of the diodes.

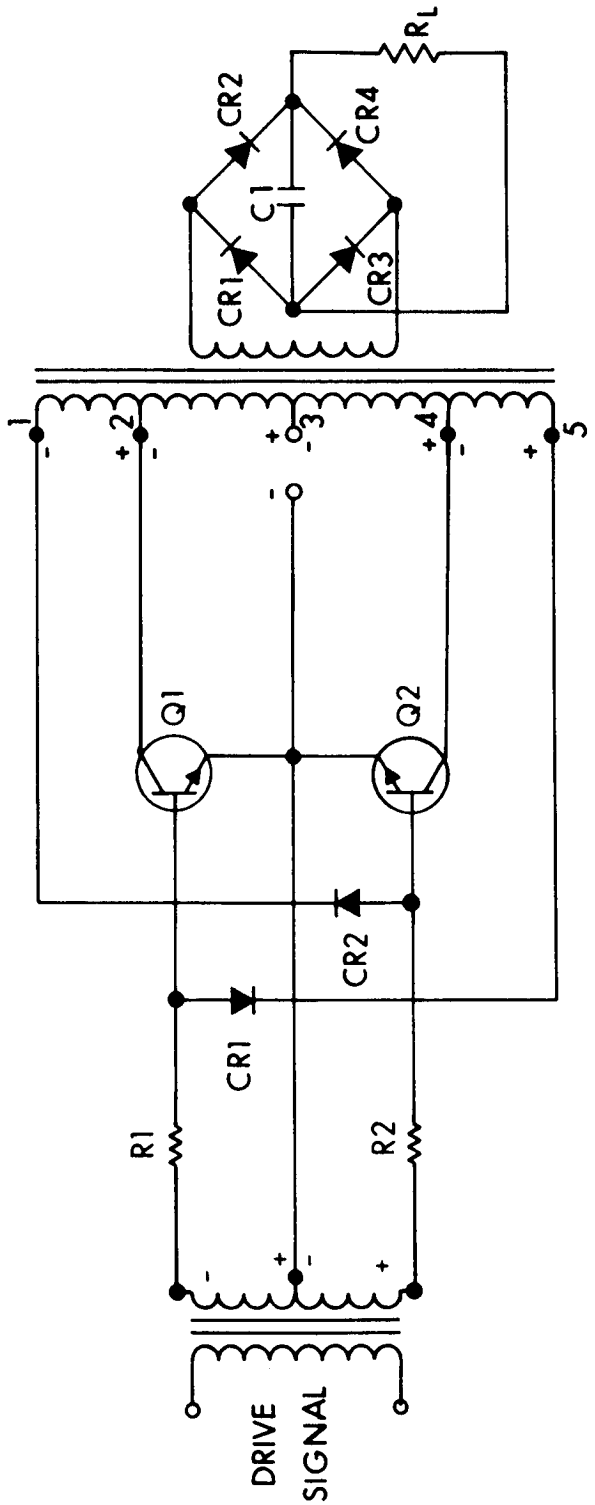

FIG. 2 CONVERTER WITH COMPENSATION FOR STORAGE TIME

The methods discussed automatically compensate for storage time regardless of load or environmental conditions. There are other means to accomplish the same end, but most of them do not adjust for changing load or temperature.

4.3.3 Transistors Considerations

In order to design efficient high frequency converters, fast switching power transistors are necessary. A survey of state-of-the-art power switching transistors was made early in the program. During the evaluation phase, the following manufacturers were contacted:

Honeywell
RCA
Texas Instruments
Westinghouse
Bendix
Silicon Transistor Corporation
Transitron
TRW Electronics
Fairchild
General Electric
Delco

Honeywell

Honeywell has several 10 ampere planar transistors that could have been used in the converter circuits. These transistors are the 2N2814 (TO-61 case) and the MHT7403 (TO-5 case). The design limits and performance specifications are shown in Table III.

These devices represent the state of the art in a 10 ampere power switching transistor. One inherent advantage of both of these devices is the flat gain characteristics.

TABLE III

TYPE NUMBER	T_s °C max.	θ °C/W max.	P_t watts 100°C case	BV_{cEo} volts min.	BV_{cEo} volts min.	BV_{EBo} volts min.	hFE at IC=10A min.-max.	$V_{BE(sat)}$ volts IC=10A	$V_{cE(sat)}$ volts IC=10A	I_{cBo} ma V_{cB}=60v	f_T mc min.
MHT7403	200	20	5	100	80	5.0	40-120	1.2	0.5	1.0	30
2N2814	200	2.5	40	120	80	8.0	40-120	1.2	0.5	0.1	30

	Rise Time (microseconds)	Storage Time (microseconds)	Fall Time (microseconds)	Weight (grams)	Price
MHT7403	0.140	1.8	0.600	1.28	$ 50.00
2N2814	0.140	1.8	0.600	14.64	120.00

TABLE IV

	θ_{J-c} °C/W max.	V_{cBo} volts max.	$V_{cEo(sus)}$ volts max.	V_{EBo} volts max.	I_c amps max.	I_b amps max.	I_{cBo} ma max.
2N3263 2N3265	1.0	150	90	7.0	25	10	4.0

	$V_{cE(sat)}$ at 15A max.	$V_{BE(sat)}$ at 15A max.	hFE at 15A min.-max.	Turn-On Time at 15A microseconds	Storage Time at 15A microseconds	Fall Time at 15A microseconds	f_T min.	Weight
2N3263	0.75	1.6	25-75	0.5	1.5	0.5	20 mc	3.8 gm
2N3265	0.75	1.6	25-75	0.5	1.5	0.5	20 mc	

Price: $99.00

RCA

RCA presently has on the market a line of fast, epitaxial power transistors. These are the 2N3263-65. The 2N3263 is a flat pack version of the 2N3265, a 778 hexagonal double-ended stud package. The electrical characteristics for both devices are shown on Table IV.

These devices are rated for higher current than the Honeywell transistors, yet the 2N3263, flat pack model is a smaller, lighter unit.

Texas Instruments

Texas Instruments is also marketing the 2N3552, a 12 ampere flat pack. This is a triple-diffused mesa transistor and has an isolated collector. The electrical characteristics are shown on Table V.

This 12 ampere unit has the advantage of being obtainable in a flat pack (3.8 gms).

Fairchild

Fairchild has recently marketed a planar epitaxial transistor (FT34A). This unit is available only in a TO-59 package. The electrical characteristics are shown on Table VI.

This device looks attractive; however, the manufacturer does not give the gain variation as a function of collector current and temperature.

The other transistor manufacturers listed were also contacted regarding a high current (10 ampere or greater) fast switching power transistor. Nothing compared to the units listed above. As a result of the evaluation the RCA 2N3263 transistor was selected for use in the high frequency converters. These units are extremely lightweight (3.8 grams) and can easily switch the anticipated currents at very fast switching rates.

TABLE V

TYPE NUMBER	θ_{J-C} °C/W max.	BV_{EBo} volts min.	BV_{cEo} volts min.	V_{BE} volts at IC=10A max.	$V_{cE(sat)}$ volts at IC=10A max.	hFE at IC=10A min.-max.
2N3552	1.875	140	80	1.4	1.0	20-90

	Turn-On Time (microseconds) max.	Turn-Off Time (microseconds) max.	Weight (grams)	Price
2N3552	0.3	2.5	3.8	$112.50

TABLE VI

TYPE NUMBER	θ_{J-C} °C/W max.	BV_{CBo} volts min.	V_{CEo} volts min.	BV_{EBo} volts min.	$V_{CE(sat)}$ volts at 10A max.	$V_{BE(sat)}$ volts at 10A max.	hFE min.-max.
FT34A	35	150	80	6.0	1.2	1.8	40-120

	Turn-On Time (microseconds) max.	Turn-Off Time (microseconds) max.	Weight (grams)	Price
FT34A	0.5	1.0	6.21	$33.00

These devices, however, imposed constraints on the converter design: (1) they must be operated at 15 amperes or less if a suitable gain is to be realized; (2) the source voltage must be kept at 28 Vdc if a margin of safety in breakdown voltage is to be maintained (the collector-to-emitter voltage of each transistor will be equal to twice the supply voltage plus the amplitude of the voltage spikes generated by transient elements); and (3) the junction-to-case thermal resistance of the transistors must be low enough so that for the given ambient temperature and the available heat sink and cooling apparatus, the manufacturer's maximum ratings are not exceeded.

The maximum collector current, the dissipation, and the heat sink thermal resistance of the power transistors can be approximated on the basis of the following conditions:

The maximum collector current is given approximately by

$$I_C = \frac{P_{OUT}/\eta}{V_S - V_{CE(SAT)}}$$

where

V_S is the supply voltage

$V_{CE(SAT)}$ is the collector-to-emitter saturation voltage

P_{OUT} is the output power

η is the desired efficiency of the output transformer

The transistor dissipation can be approximated as follows (base dissipation was neglected here):

$$P_D = \frac{T_1}{T}\left(V_{CE(SAT)}\ I_C + 2\ I_{CEX}\ V_S\right) + \frac{t_{on} + t_f}{T}\frac{V_S I_C}{3}$$

where

V_S is the supply voltage

$V_{CE(SAT)}$ is the transistor saturation voltage

I_C is the collector current

I_{CEX} is the collector current with the base reverse-biased (for $V_{CE} = 2V_S$)

t_{on} is the transistor turn on time

t_f is the transistor fall time

T_1 is $1/2 \left[T - (t_{on} + t_f)\right]$

T is the period

The equation above is used only as a guide for the first stages of design; the exact dissipation is determined experimentally.

4.3.4 Rectifier Considerations

The rectifier circuits of the high frequency converters were an important design consideration. At high switching frequencies fast recovery silicon rectifiers are necessary if the converter efficiency is to be optimized.

At low frequencies, the losses normally associated with rectifier diodes are due to the forward voltage drop during the conduction cycle and to the reset current pulse leakage current. Normally, the largest percentage of the losses are attributed to the forward conduction characteristics.

Diodes with recovery times in the 10 to 20 microsecond region may have excellent loss characteristics up to 1 kHz. At the higher frequencies, the rectification efficiency is increasingly impaired and heat losses increase as a direct result of the increased recovery losses. To minimize the rectifier recovery losses, fast recovery rectifiers with recovery times of 150 nanoseconds were used in the output rectifier circuit of the converter.

4.3.5 Transformer Considerations

In the design of efficient high frequency converters, the transformer design is a very important consideration. Losses that could perhaps be neglected at lower frequencies become predominant at higher frequencies.

Practical transformers can be designed quite efficiently using Hi-Mu-80 and Supermalloy magnetic materials at switching frequencies up to 10 kHz. These materials exhibit reasonable losses in this frequency range. The optimum tape thickness for this frequency range is 1/2 mil, but the stacking factor is quite poor in this size. An additional factor is the fact that most magnetic material manufacturers will not guarantee the characteristics of core materials of 1/2 mil or less. With operating frequencies up to 10 kHz, 1 mil tape wound cores may be used very effectively and efficiently.

Some ferrite cores offer certain advantages over tape wound cores in the frequency range above 50 kHz. The major disadvantages of ferrite core materials are low curie temperature, low maximum flux density and considerable variance of maximum flux density with temperature. The advantages that this core material offers are the many different core configurations that are available, their low cost, and above all they exhibit low losses at frequencies extending into the RF spectrum.

At frequencies beyond 10 kHz the skin effect starts to become significant. For example, at 50 kHz a transformer can have more skin effect wire loss than the measured wire loss. Since Litz wire is not available in the large wire sizes that are required for power conversion, the alternative is to use parallel windings of smaller diameter wire which equal the cross-sectional area of the desired wire size.

The problems of leakage inductance and interwinding capacitance are also factors that affect the design of the transformer. For low voltage windings, the scarcity of turns on the transformer and leakage inductance can cause very poor coupling between windings and this can result in poor load regulation. Higher voltage windings are hindered by interwinding capacitance which causes increased losses in both the transformer and in the power transistors. The combination of both can cause spurious oscillations that can appreciably disrupt circuit operation.

The core of a transformer is selected on the basis of power handling requirements, frequency, and temperature of operation. Temperature is an important consideration in the selection of a ferrite core because the curie temperature for many ferrites is quite low. Magnetization is zero above the curie temperature. Another important consideration in the selection of core material is the desired transformer efficiency. The efficiency can be used to obtain an approximation for the magnetic power to be dissipated. The necessary volume of core material can then be estimated on the basis of the value of magnetic power and the core loss factor for the selected material at the operating frequency. The core loss factor is determined from the core-material data furnished by the manufacturer.*

In the design of the transformer, the curie temperature must be considered together with the variation of flux-density as a function of temperature and the desired operating value of flux density, B. For the base-drive transformer, a temperature rise results in a decrease in flux density and an ultimate increase in operating frequency. The ambient temperature and the maximum operating core temperature are used to compute the maximum permissible temperature rise, ΔT. A second estimate of the volume of core material must then be made on the basis of the magnetic power to be dissipated and the temperature rise ΔT. A rule of thumb for most ferrites is that the temperature rises according to 3.2 $mW/cm^3{}^oC$. This volume should be compared with the volume selected above on the basis of core losses. The final volume should satisfy both requirements.

The output power transformer is designed to satisfy the following familiar equation:

$$N_P = \frac{V_S \times 10^8}{4\ FAB}$$

*Ref. 4. H. T. Breece III, "Boosting dc Voltage with Silicon Transistors," Electronics, Nov 16, 1964

where

V_S is the source voltage in volts

F is the operating frequency in cps

A is the transformer core area in cm^2

B is the flux density in gausses

In the design of the output transformer for high frequency converters, excessive primary turns should be avoided to minimize power dissipation, to insure that the transformer can be fabricated using the proper wire size and the relatively small cores that are usually employed, and to insure that the leakage inductance effects are minimized. Good balance and close coupling between primaries can be achieved by means of bifilar windings. The flux density for the output transformer is determined by the usual compromise: The selected wire size on the basis of a 50 percent duty cycle must be large enough so that power dissipation will be low. If the wire size is inadequate, dissipation will be appreciable and a high transformer core temperature will result.

The design of the base-drive transformer is quite different from that of the output transformer. When the driver transformer saturates, a sharp drop in the applied primary voltage must be produced. The magnetizing current must then increase from a small value to one that is comparable to the primary current. The following equation may be used to arrive at the number of primary turns because of the saturation requirement:

$$H_S = \frac{1.26\ N_P I_m}{l}$$

where

H_S is the value of magnetizing field strength at saturation in oersteds

N_P is the number of primary turns

I_m is the value of magnetizing current at saturation in amperes

l is the length of magnetic path in centimeters

The equation presented above together with the basic transformer equation must both be satisfied for the proper design of the base drive transformer.

4.3.6 Circuit Selection

The converter circuit that was selected for the Mars Orbiter program is shown in Fig. 3. This circuit was selected for several reasons. First because of its simplicity and secondly because the converter circuit compensates for storage time without any modifications. Transformer T1 is a saturating type which determines the frequency of operation. T2 is the output transformer and does not saturate. When T1 saturates, base drive for both transistors falls to zero until the "on" transistor starts turning off. Stored energy in the core is then released which forward biases the opposite transistor, thus starting the next half cycle of operation. The paragraphs that follow will describe its operation and point out reasons for its selection.

In the circuit, a saturable base-drive transformer T1 controls the converter switching operation at base-circuit power levels, and a linear output transformer couples the output to the load. Because the core material of the output transformer, T2, isn't allowed to saturate, the peak collector currents of the transistor in the inverter are determined principally by the value of the load impedance. This feature makes possible high circuit efficiency. Operation of the circuit is as follows:

Because of a small inherent unbalance in the circuit, one of the transistors, say Q1, initially conducts more heavily than the other. The resulting increase in the voltage across the primary of the output transformer T2 is applied to the primary of the base-drive transformer T1 in series with the feedback resistor, R_{FB}. The secondary windings of transformers T1 are connected so that transistor Q2 is reversed biased and driven to cutoff while transistor Q1 is driven into saturation. As transformer T1 saturates, the rapidly

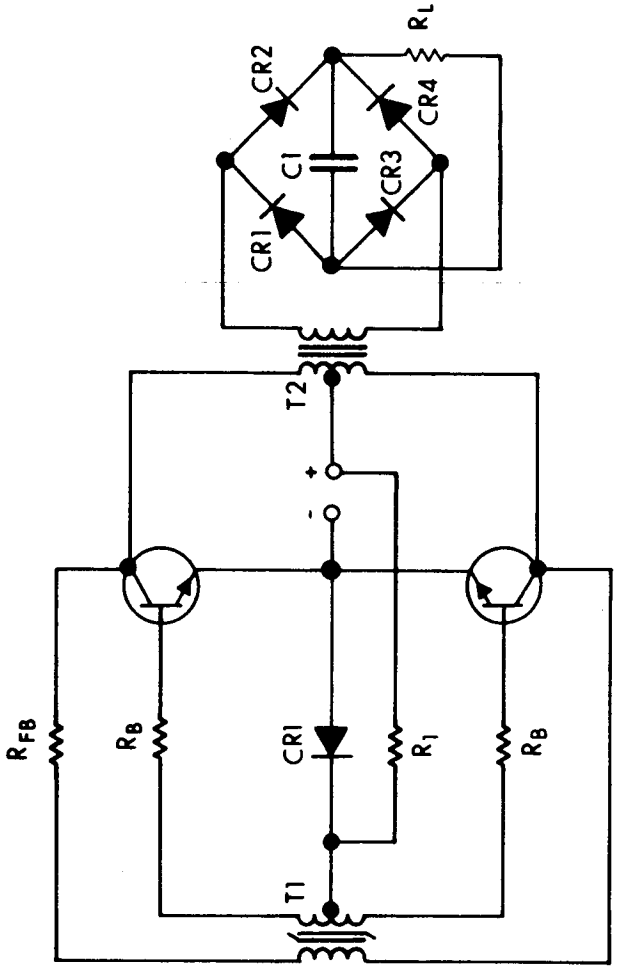

FIG. 3 BASIC DC-DC CONVERTER

increasing primary current causes a greater voltage drop across feedback resistor R_{FB}. This increase in voltage across R_{FB} reduces the voltage applied to the primary of transformer T1; thus the drive input and ultimately the collector current of transistor Q1 are decreased.

The decrease in the collector current of transistor Q1 causes a reversal of the polarities of the voltages across all the transformer windings. Transistor Q1, therefore, is rapidly driven to cutoff, and transistor Q2 is then allowed to conduct. The inverter operates in this state until the saturation of transformer T1 in the opposite direction is reached. The circuit then switches to the initial state and the cycle is repeated at a frequency determined by the design of transformer T1 and the value of feedback resistor R_{FB}.

The external base resistors, R_B, reduce the effect of the transistor base-to-emitter voltage, V_{BE}, on the operation of the circuit. These stabilizing resistors are needed because V_{BE} varies among individual transistors with temperature and operating time.

The collector current in each transistor must rise to a value equal to the load current plus the magnetization current of transformers T1 and T2 and the feedback current to produce the required drive. Because the output transformer is not allowed to saturate, the magnetization current is only a small fraction of the load current. In the switching operation, transistor Q1 will continue to conduct after the drive is removed because of the excessive charge that was stored in the base during saturation. However, transistor Q2 will not conduct until the core of transformer T1 has been reverse-magnetized and current has been injected into the base of transistor Q2. In the single transformer converter, both transistors conduct heavily during the switching. In the two-transformer circuit, neither transistor conducts during the switching time and thus very low power supply impedance is not necessary for fast switching.

The energy stored in the output transformer by its magnetizing current is sufficient to assure a smooth change-over from one transistor to the other with no possibility of the converter oscillations stopping.

Operation of the high frequency converter is relatively insensitive to small system variations that may result in a slight overloading of the circuit. Under such conditions, the base power losses will increase but these losses are so small that a slight increase in them will not noticeably affect circuit performance. The amount of energy stored in the output transformer will also be increased. Although this increase will result in a greater transient dissipation, the converter switching will still be smooth. Because the output transformer is not saturated, the collector currents are always determined by the circuit load impedance and not by small system variations.

A practical design of a high frequency converter should include a means of initially biasing the transistors into conduction to assure that the circuit will be started reliably. Such biasing networks can be readily added to the inverter, and are much more dependable than just assuming that the circuit unbalance will immediately shock the converter into oscillation.

4.4 10 kHz Design

The design of the high frequency modules began with the design of a 10 kHz dc-dc converter. The 10 kHz switching frequency served as the starting reference point.

Several models of a 10 kHz, 100 watt module were designed, breadboarded and tested. The circuits delivered 250 Vdc, 5.0 Vdc, and 1000 Vdc (modules No. 1, No. 2, and No. 3, respectively). Each design is discussed separately.

4.4.1 Module No. 1 (250 Vdc Output)

The module No. 1 design was approached with the idea of providing the highest possible efficiency and the lowest weight and volume.

Two types of transistors were selected for this circuit; these included the Honeywell MHT7016 (lower gain version of the 2N2814) and the RCA 2N3265. Both of these units were selected because of their excellent switching and saturation characteristics. The data obtained will show the results using both of these transistors.

Several output transformer designs were tested - each with a different volts/turn ratio. For the 10 kHz operation, tape wound cores were used exclusively. Hy-Mu-80 core material was used exclusively, because of its low core loss characteristics.

The circuit of module No. 1 is shown in Fig. 4. Circuit No. 1 used the MHT7016 transistor. Circuit No. 2 was the identical circuit, except for the power transistors; the 2N3265 transistors were substituted for the MHT7016. The efficiency was checked as a function of power and the results are shown in Fig. 5. The efficiency obtained at 100 watts output for circuit No. 2 was over 90 percent. However, the efficiency for circuit No. 1 fell below 90 percent at the 100 watt level. The decrease in efficiency was due to the decrease in gain of the power transistors. This problem was overcome by using a higher gain transistor at the required current level. The RCA transistor provided the added gain in circuit No. 2.

Circuits No. 3, No. 4, No. 5, and No. 6 were also fabricated and tested. Each of these circuits used the RCA 2N3265 transistors, but a different output transformer was used with each circuit. The results are also shown in Fig. 5. All but one design provided efficiency over 90 percent at the 100 watt level.

The component weights for the 10 kHz circuits are shown below.

Circuit No.	Weight (grams)
1	124.5
2	153.0
3	215.0
4	175.0
5	183.6
6	165.3

4.4.2 Module No. 2 (5 Vdc)

Four circuits of module No. 2 were fabricated and tested. Only the dc output is shown, as this is the worst efficiency expected. Dc-to-ac conversion of this module will be considerably better than the dc-dc case.

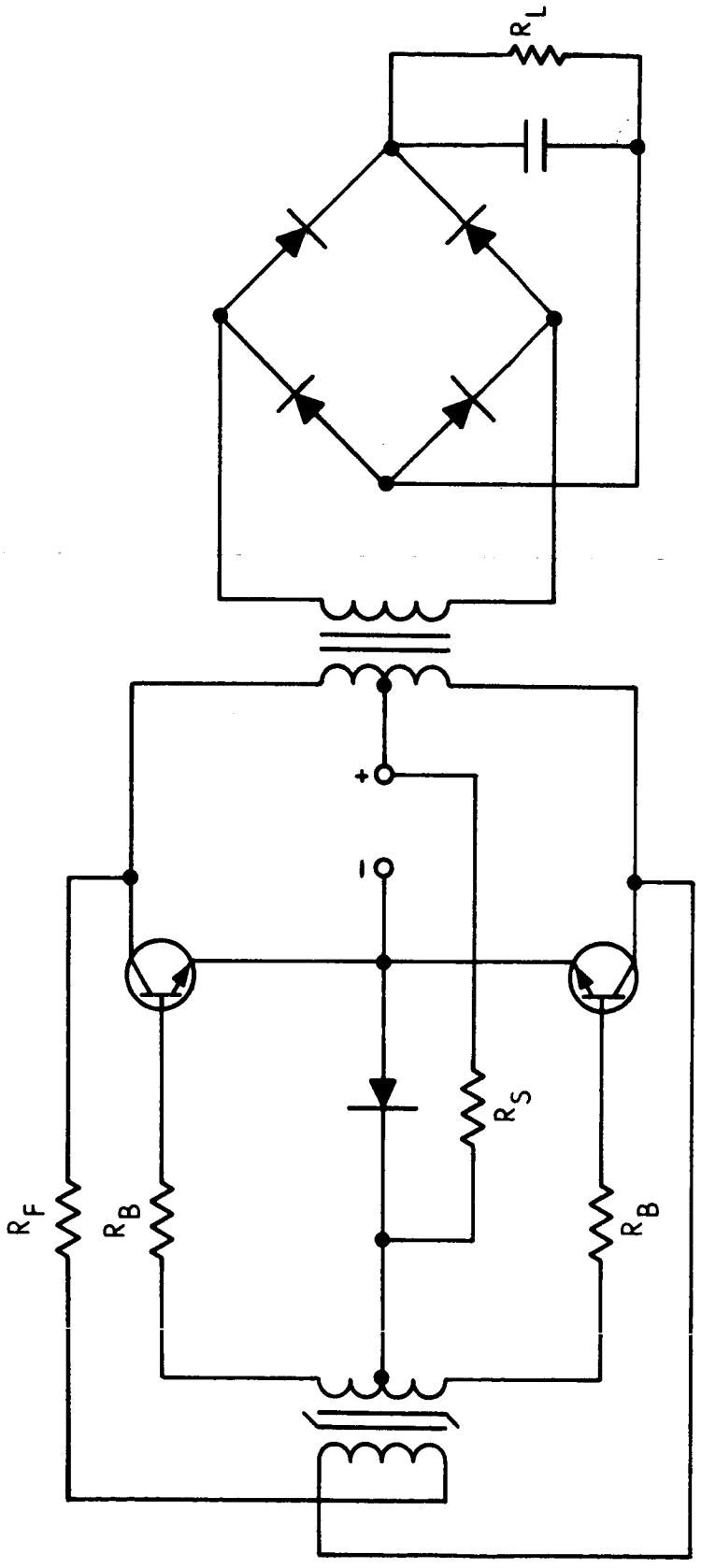

FIG. 4 MODULE NO. 1, 10 kHz CIRCUIT

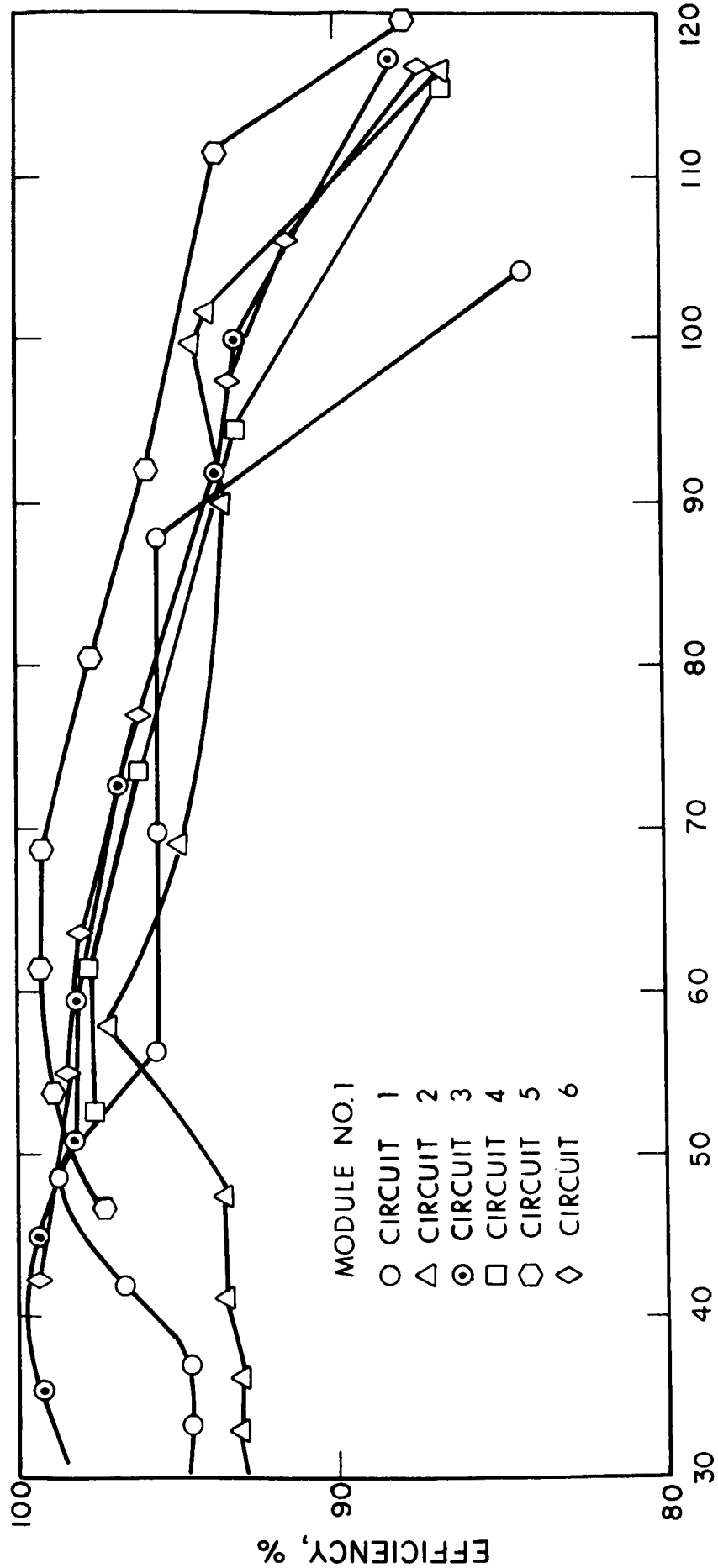

FIG. 5 EFFICIENCY RESULTS (MODULE NO. 1 – 10 kHz CIRCUITS)

Two transformers were used with two sets of output power transistors (the MHT7016 and the 2N3265). The results are shown in Fig. 6. Circuits No. 1 and No. 2 (using the same output transformer) rendered better efficiency than circuits No. 3 and No. 4. The component weights for the circuits are shown below.

Circuit No.	Weight (grams)
1	233.3
2	262.7
3	200.0
4	170.0

4.4.3 Module No. 3 (1000 Vdc)

Four separate module No. 3's were fabricated and tested. Circuits No. 1 and No. 3 employed the MHT7016 transistors and circuits No. 2 and No. 4, the 2N3265 transistors. The efficiencies of these circuits were lower than those of module No. 1. This was mainly due to the high turns ratio of the output transformers. Experimental data show that the switching times were adversely affected by the distributive capacity of the output transformer.

Circuit efficiencies as a function of the output power are shown in Fig. 7. Circuits No. 1 and No. 2 utilized the same output transformer but different power transistors. Circuits No. 3 and No. 4 used a different output transformer and the same power transistors used in circuits No. 1 and No. 2. The component weights for the circuits are shown below.

Circuit No.	Weight (grams)
1	205.9
2	235.3
3	162.5
4	191.9

4.5 50 kHz Converter Design

In order to realize a decrease in size and weight of the dc-dc converters, a 50 kHz design was investigated. The following converter design data is applicable to module No. 1.

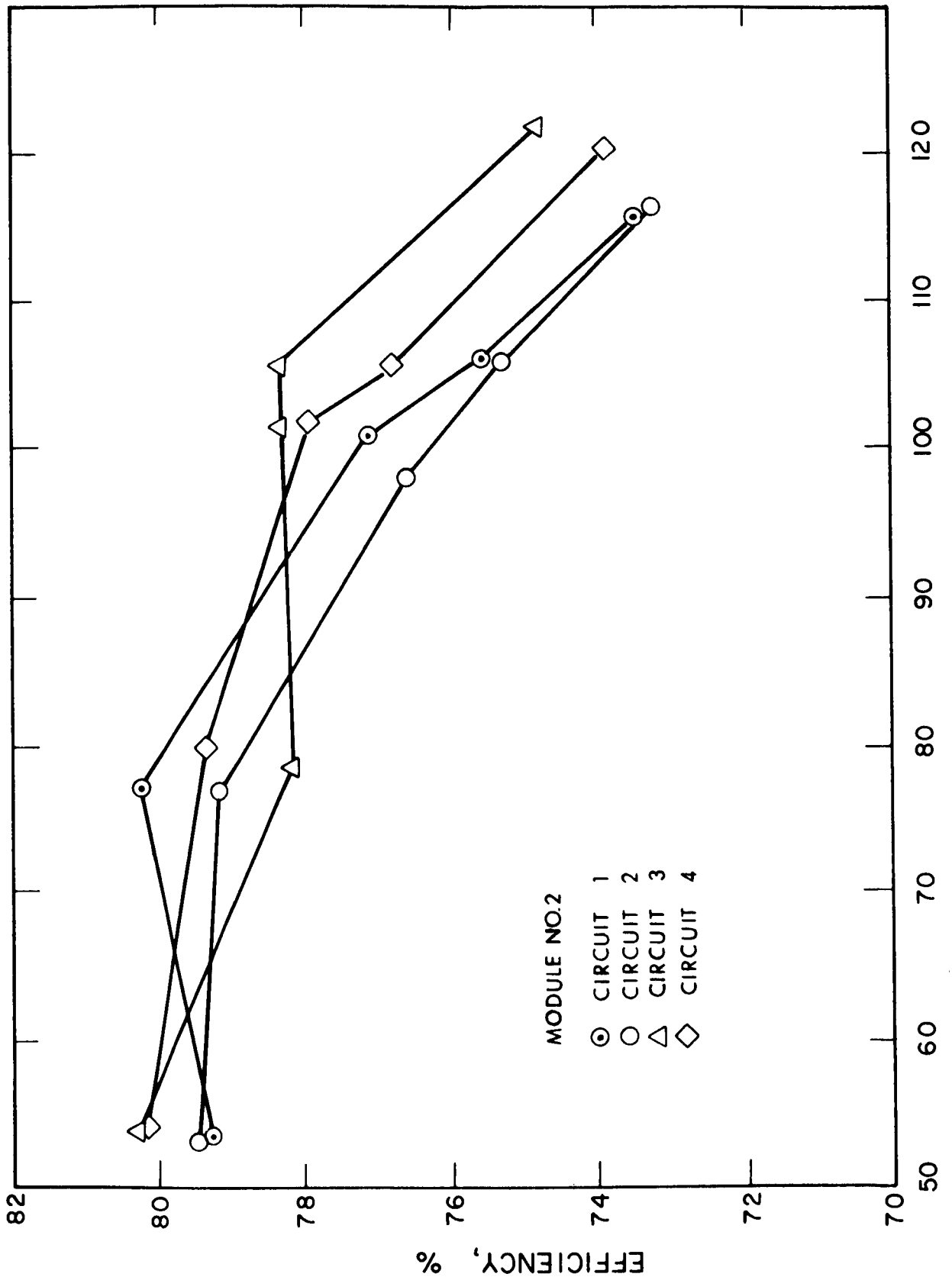

FIG. 6 EFFICIENCY RESULTS (MODULE NO. 2 - 10 kHz CIRCUITS)

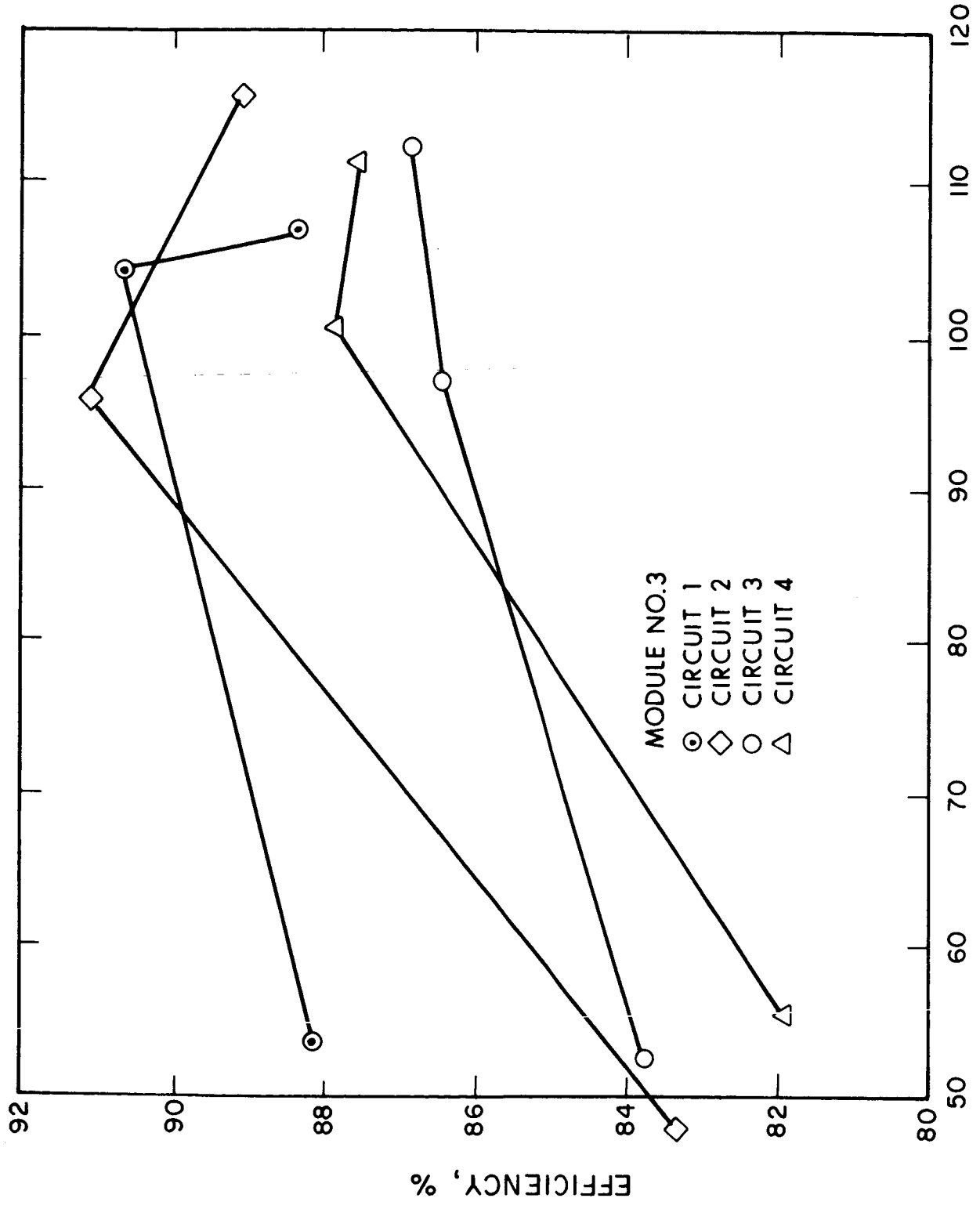

FIG. 7 EFFICIENCY RESULTS (MODULE NO. 3 - 10 kHz CIRCUITS)

4.5.1 50 kHz Converter Design

The operating requirements upon which the design is based are as follows:

Power output, P_{OUT}	=	100 watts
Operating frequency, f	=	50 kHz
Supply voltage, V_S	=	+28 Vdc
Load resistance, R_L	=	625 ohms
Ambient temperature, T_A	=	25°C

In order to properly select the power switching transistor for the converter, the power input to the output transformer, P_{OUT}, was computed. A transformer efficiency of 97 percent is assumed.

$$P_{OUT} = \frac{100 \text{ watts}}{0.97} = 103 \text{ watts}$$

An initial estimate of the transistor collector current that is necessary to produce the required output power is:

$$I_C = \frac{103 \text{ watts}}{28 \text{ Vdc}} = 3.68 \text{ amperes}$$

The transistors used in the converter circuit must have a collector-to-emitter breakdown voltage, V_{CEO}, equal to at least twice the supply voltage plus an additional 20 percent to allow for transient voltage spikes. Therefore:

$$V_{CEO} \geq 2 \times 28V \times 1.20 = 67 \text{ volts}$$

The RCA 2N3263 silicon power transistors selected for the converter circuit have a $V_{CEO(SUS)}$ of 90 volts, and a collector-to-emitter saturation voltage, $V_{CE(SAT)}$, of 0.75. This is given in the manufacturer's data for a collector, current I_C, of 15 amperes. At a

collector current of 3.68 amperes, the saturation voltage will be smaller to insure that the desired high operating efficiency can be obtained. A saturation voltage of 0.5V was assumed. The switching times for the 2N3263 transistor given by the manufacturer are:

Fall Time, t_f = 500 nanoseconds. (I_c = 15 amps)

On Time, t_{on} = 500 nanoseconds. (I_c = 15 amps)

These switching times are short in relation to the 20 microsecond period of the 50 kHz operating frequency.

The collector current, I', assuming 0.5V saturation voltage is:

$$I' = \frac{103 \text{ watts}}{28 - 0.5} = 3.75 \text{ amperes}$$

The data given for the 2N3263 transistor are used to determine the h_{FE} ratio and base-to-emitter voltage, V_{BE} of the transistor at this level of collector current. The minimum h_{FE} of 62 at a collector current of 4 amperes (95 percent of the transistors will meet this requirement) is close enough to the calculated value of I_c'. The forced value for this ratio, h_{FE}' is selected to be 20, which is small enough to assure that the transistor will saturate. The base-to-emitter saturation voltage, $V_{BE(SAT)}$, at the collector current of 4 amperes is 1.0 volt. The values of the following parameters were computed to be:

$$I_B = \frac{I_c'}{h_{FE'}} = \frac{3.75 \text{ amps}}{20} = 0.188 \text{ amperes}$$

$$R_{1N} = \frac{V_{BE(SAT)}}{I_B} = \frac{1.0 \text{ volt}}{0.188 \text{ amps}} = 5.32 \text{ ohms}$$

The total base-circuit input resistance, R_{1N}', is the sum of the quantity R_{1N} and the transistor bias resistor R_B. The value of R_B is selected as 3 ohms. Therefore, R_{1N}' is equal to 8.23 ohms. The base circuit input voltage V_{1N}' was determined from the product of R_{1N}' and I_B:

$$V'_{1N} = 8.23 \times 0.188$$

$$= 1.55 \text{ volts}$$

In the design of the converter circuit, the value of the feedback resistor is usually chosen so that the available voltage is divided equally across this resistor and the primary of the base-drive transformer. The voltage across the primary, V_{PR1}, was determined as follows:

$$V_{PR1} = 0.5 \times 2 \times \left(V_S - V_{CE(SAT)}\right)$$

$$= 0.5 \times 2 \times 27.5 = 27.5 \text{ volts}$$

The base-circuit input power, P_{1N} is then determined from the product of V'_{1N} and I_B:

$$P_{1N} = 1.55 \text{ volts} \times 0.188 \text{ amperes} = 0.292 \text{ watts}$$

If a transformer efficiency of 97 percent is assumed, the power input to the base-drive transformer is:

$$P'_{1N} = \frac{0.292 \text{ watts}}{0.97} = 0.301 \text{ watts}$$

The primary current is determined to be:

$$I_{PR1} = \frac{0.301 \text{ watts}}{27.5 \text{ volts}} = 0.011 \text{ amperes}$$

The feedback resistor, R_{FB}, is computed for magnetizing current equal to I_{PR1}:

$$R_{FB} = \frac{V_{PR1}}{I_{PR1}} = \frac{27.50 \text{ volts}}{0.011 \text{ amps}} = 2500 \text{ ohms}$$

The value of the bias resistor (a resistive voltage-divider starting circuit is assumed) required to produce 0.188 ampere of starting current is determined as follows:

$$R_1 = \frac{V_S - V_{BE(SAT)}}{I_B}$$

$$= \frac{28 - 1.0}{0.188} = 142 \text{ ohms}$$

The calculation of the transistor collector current was made on the basis of total power in the converter circuit, $P_{OUT} + P'_{IN}$:

$$I_c = \frac{(103 + 0.301) \text{ watts}}{27.5 \text{ volts}} = 3.76 \text{ amperes}$$

The impedance reflected into the primary of the output transformer, R'_L, is computed on the basis of this value of collector current:

$$R'_L = \frac{27.50 \text{ volts}}{3.76 \text{ amps}} = 7.32 \text{ ohms}$$

The ratio of the specified circuit load impedance, R_L = 625 ohms, and this reflected impedance defines the transformer ratio, N_2:

$$N_2^2 = \frac{R_L}{R'_L} = \frac{625}{7.32} = 85.4$$

On the basis of an assumed transformer efficiency of 97 percent, the magnetically dissipated power in the output transformer is given by:

$$P_m = P_{OUT} \text{ (100 - 97 percent)} = 3.09 \text{ watts}$$

For an operating frequency, f, of 50 kHz, the Ferroxcube 3E2A Ferrite material was selected. From the manufacturer's data sheets, the maximum usable core temperature is 150°C for the Ferroxcube material. For linear operation at these temperatures the flux density, B_M should be 1000 gauss.

The core-loss factor, ρ, for B_M = 1000 gauss and f = 50 kHz is given by:

$$\rho = 3.2 \frac{\mu w}{cm^3 \text{ cps}}$$

Therefore, at 50 kHz, the frequency dependent core loss ρ' is calculated as:

$$\rho' = \left(3.2 \frac{\mu w}{cm^3 \text{ cps}}\right) 5 \times 10^4 \text{ cps}$$

$$= 160 \frac{mw}{cm^3}$$

The maximum temperature rise is:

$$T = 150^oC - 25^oC = 125^oC$$

When the temperature-rise factor of $3.2 \frac{mw}{cm^3 {}^oC}$ is used,

$$\rho'' \; 3.2 = \frac{mw}{cm^3 {}^oC} \times 125^oC = 400 \frac{mw}{cm^3}$$

The minimum core volume can be determined from the core loss due to the temperature used and is given by:

$$\text{Volume} = \frac{P_m}{\rho''} = \frac{3.09 \text{ watts}}{400} = 7.7 \text{ cm}^3$$

To meet this requirement a pair of E cores, type 3E2A were selected. They have the following dimensions:

Volume = 4.4 cm^3
Area = 0.764 cm^2
Length = 2.3 inches = 5.84 cm

The number of primary turns were determined by the following calculations:

$$N_P = \frac{27.50 \times 10^8}{4 \times 5 \times 10^4 \times 0.764 \times 10^3} = 9.80 \text{ turns}$$

Use 10 turns, then:

$$N_S = 10 \times 9.25 = 92.5 \text{ turns}$$

From the manufacturer's data sheet, it is recommended that for linear operation the value of H = 1.0 oersted should be used. This value corresponds to a magnetizing current of:

$$I_m = \frac{5.84 \times 1.0}{1.26 \times 9.8} = 0.473 \text{ amperes}$$

Wire sizes for the transformer were selected to prevent excess power dissipation. The primary winding was wound in a bifilar manner. Polyester film tape was used as required to provide the high voltage insulation.

4.5.1.1 Thermal-Resistance Calculations

The average transistor dissipation was computed as follows:

$$P_D = \frac{T_1}{T}\left(V_{CE(SAT)}\ I_C + 2\ I_{CEX}\ V_S\right) + \frac{t_{ON} + t_f}{T}\frac{\left(V_S I_C\right)}{3}$$

where

V_S is the supply voltage

$V_{CE(SAT)}$ is the transistor saturation voltage (for a specific value of I_C)

I_C is the collector current

I_{CEX} is the collector current with the base reverse-biased (for $V_{CE} = 2\ V_S$)

t_{ON} is the transistor on time

t_f is the transistor fall time

$T_1 = Y_2\ T - (t_{ON} + t_f)$

$$P_D = \frac{(20 - 1)}{2(20)} \left[(0.5)(3.84) + 2(0.02)(28) \right] + \frac{1}{20} \frac{(28)(3.84)}{3}$$

$$= 3.235 \text{ watts}$$

For a junction temperature of 125°C, the maximum temperature rise is

$$\Delta T = 125^{\circ}C - 25^{\circ}C = 100^{\circ}C$$

The total junction-to-air thermal resistance including heat sink, mounting and junction to case thermal resistance is:

$$\theta_{j-A} = \frac{100^{\circ}C}{3.235 \text{ watts}} = 30.8 \ ^{\circ}C/W$$

For the 2N3263, the thermal resistance is

$$\theta_{j-c} = 1.5 \ C/W$$

The mounting thermal resistance is approximately 0.25 °C/watt. Therefore, the heat sink

$$\theta_{HS - A} = 30.8 \ ^{\circ}C/W - 1.75$$

$$\leq 29.05 \ ^{\circ}C/watt$$

4.5.1.2 Experimental Results

The output transformer was constructed and the leakage inductance was found to be 2.0 microhenrys. From previous calculations, the peak collector current is 3.84 amperes and the reverse base-to-emitter bias voltage is about -2 volts. Data for the 2N3263 power transistor for reverse-bias second breakdown are shown on Fig. 8. For the peak collector current and the measured transformer leakage inductance more than 90 percent of the 2N3263 transistors will operate without the risk of reverse-bias second breakdown. The operating conditions for the constructed output transformer are well within the safe area.

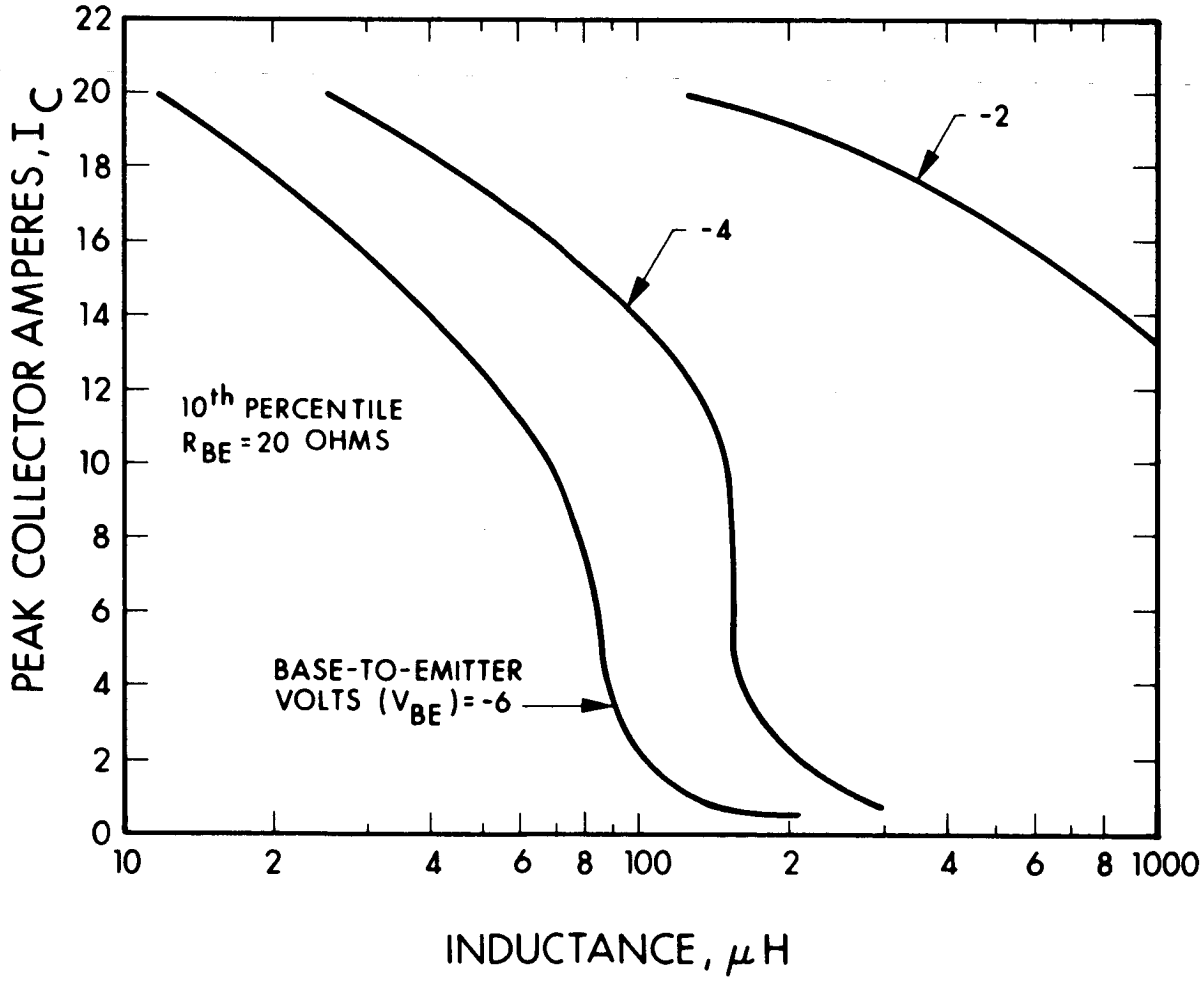

FIG. 8 COLLECTOR CURRENT AS A FUNCTION OF INDUCTANCE

From the manufacturer's data sheet, the safe operating area for forward-bias second breakdown as a function of pulse duration is shown in Fig. 9. At the maximum collector-to-emitter operating voltage of 67 volts, the design is well within the safe area for the forward-bias second breakdown for the 50 kHz operating frequency (10-microsecond pulse duration).

A similar design approach was used for Modules No. 2 and No. 3, utilizing different output transformer turn ratios.

Several circuits of a 50 kHz, 100 watt module were designed, breadboarded and tested. The circuits delivered 250 Vdc, 5.0 Vdc, and 1000 Vdc (Modules No. 1, No. 2, and No. 3 respectively). The various circuits are discussed separately.

4.5.2 Module No. 1 (250 Vdc Output)

Five converter circuits were designed, breadboarded and tested. Each circuit utilized a different output transformer with a different volt/turn ratio. The efficiency as a function of output power is shown in Fig. 10. Variations in efficiency occurred below and above the 100 watt level. At the 100 watt level the efficiencies were almost the same, approximately 89 percent.

The component weights for the circuits breadboarded and tested are listed below:

Circuit (No.)	Weight (grams)
1	89.1
2	90.2
3	92.4
4	100.4
5	96.5

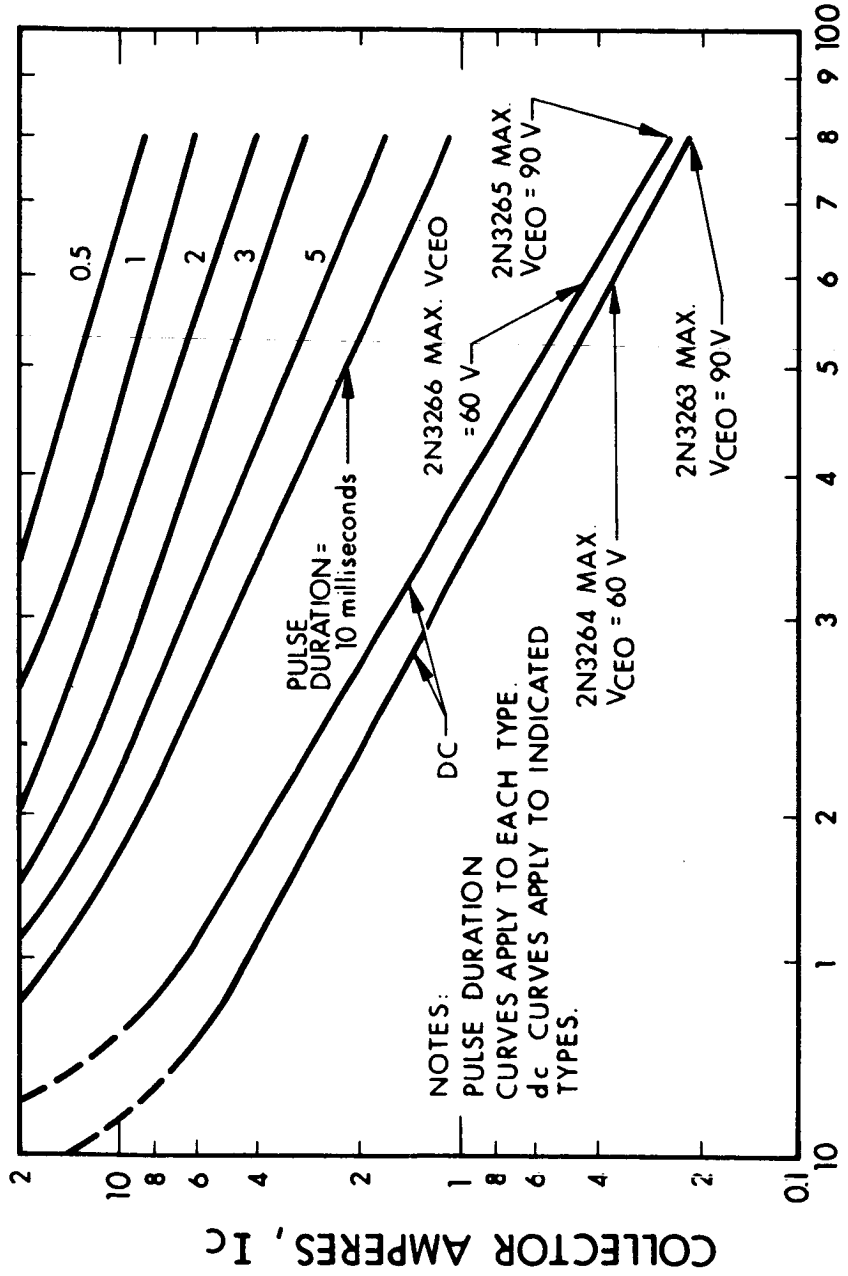

FIG. 9 SAFE OPERATING REGION AS A FUNCTION OF PULSEWIDTH

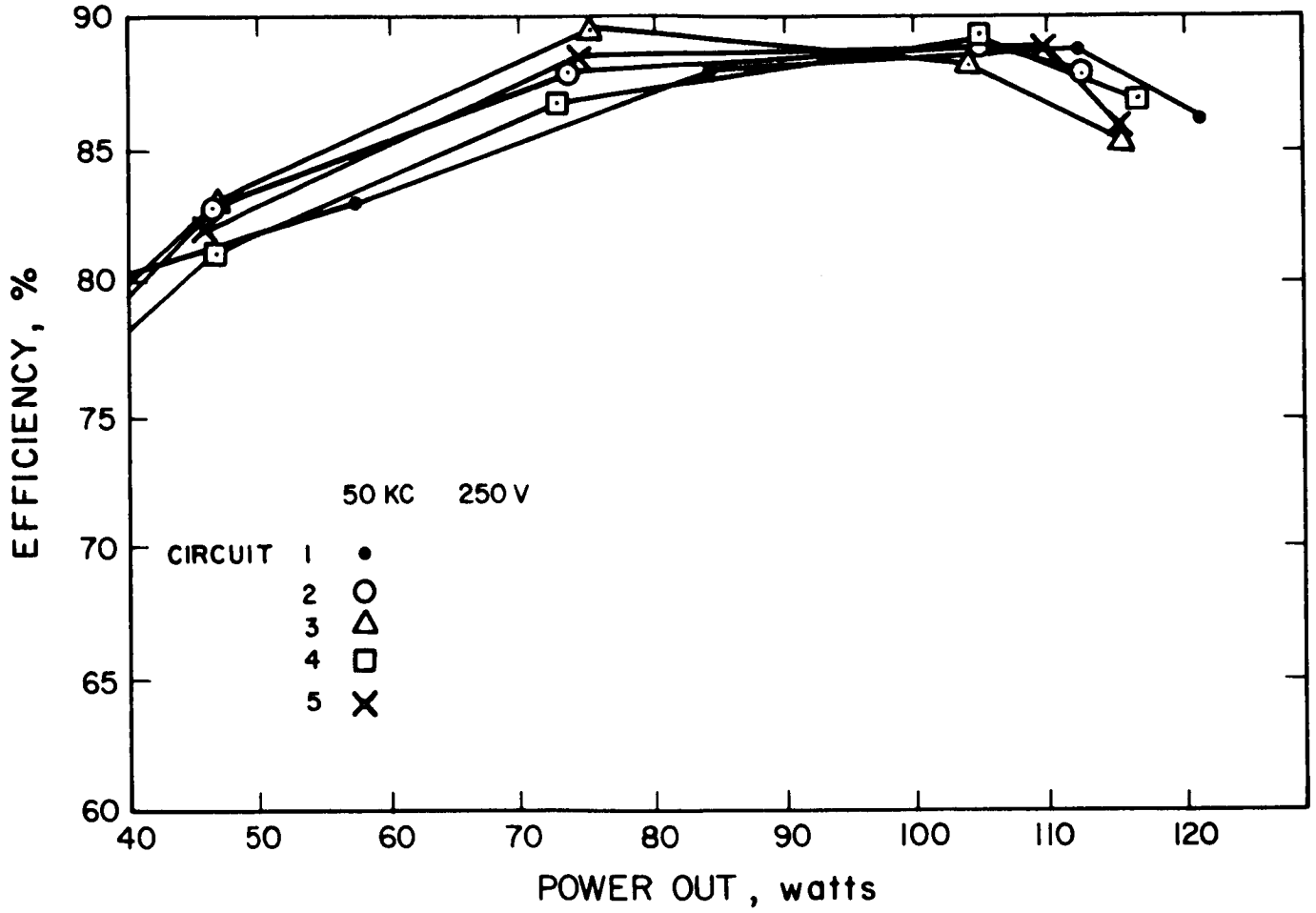

FIG. 10 EFFICIENCY VERSUS POWER OUTPUT (MODULE NO. 1 - 50 kHz CIRCUITS)

Circuit No. 2, shown in Fig. 11, was selected as the representative circuit at the 50 kHz switching frequency. This circuit was then subjected to further performance tests.

Figure 12 shows the variation of output voltage as a function of input voltage at constant power and at constant load.

Figure 13 shows the variation of output voltage as a function of output power.

Figure 14 shows the efficiency of Module No. 1 as a function of output power. The efficiency is fairly flat over the 100 watt design goal.

Figure 15 shows the change in efficiency of Module No. 1 as a function of ambient temperature at an output power level of 100 watts.

Figure 16 shows the switching frequency variation as a function of ambient temperature for temperature variations from $-50^{o}C$ to $+130^{o}C$.

Table VII shows a breakdown of the component weights for Module No. 1.

TABLE VII

MODULE NO. 1 – COMPONENT WEIGHT

Significant Components	Weight (grams)
Output Transformer	40.20
Driver Transformer	2.75
Current Transformer	2.85
Output Filter Capacitor	12.85
Output Power Transistors (2)	8.45
Basic Dc-Dc Converter Circuit	
Total Components	73.6 (or 2.59 oz)
Complete Module No. 1 Circuit with Overload and Short Circuit Protection	
Total Components	91.2 (or 3.21 oz)

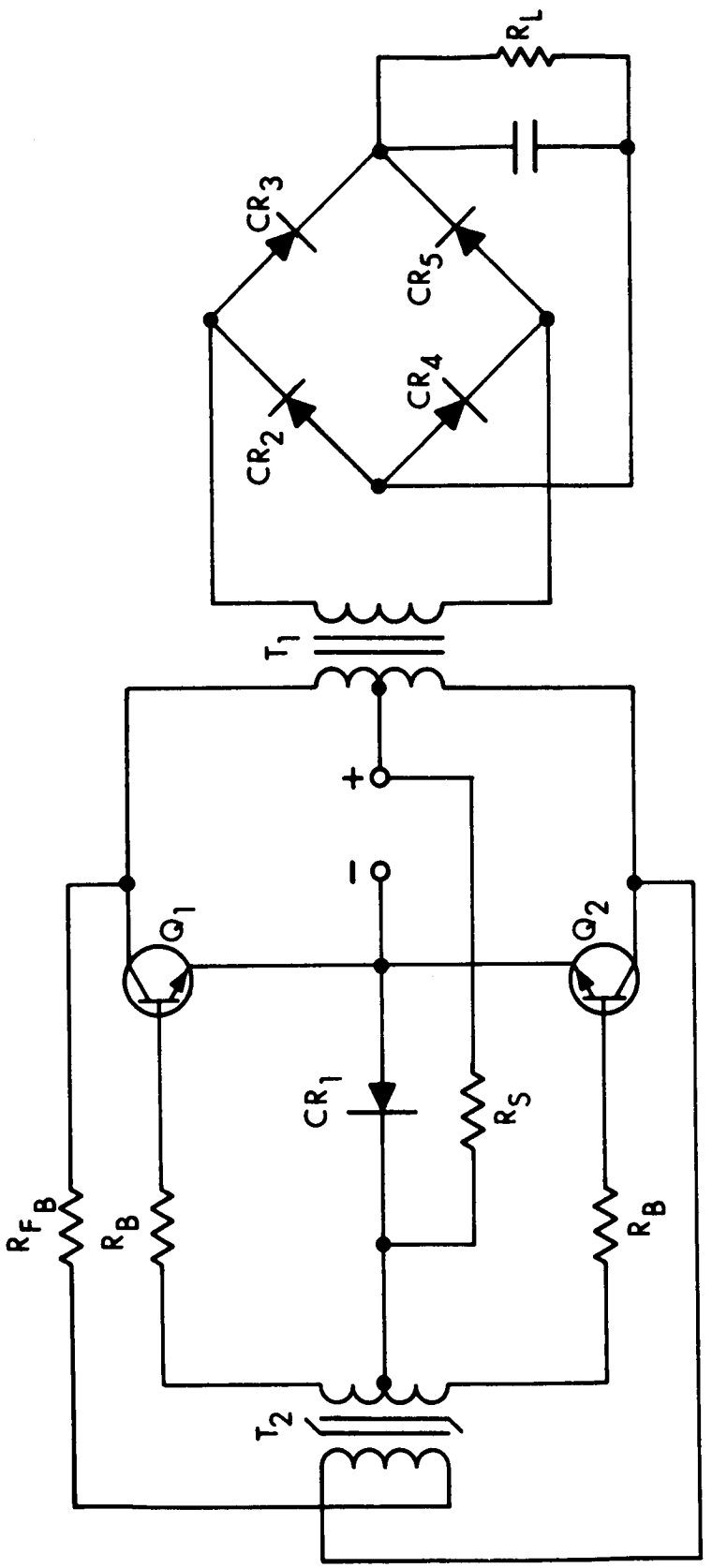

FIG. 11 MODULE NO. 1 - 50 kHz CIRCUIT

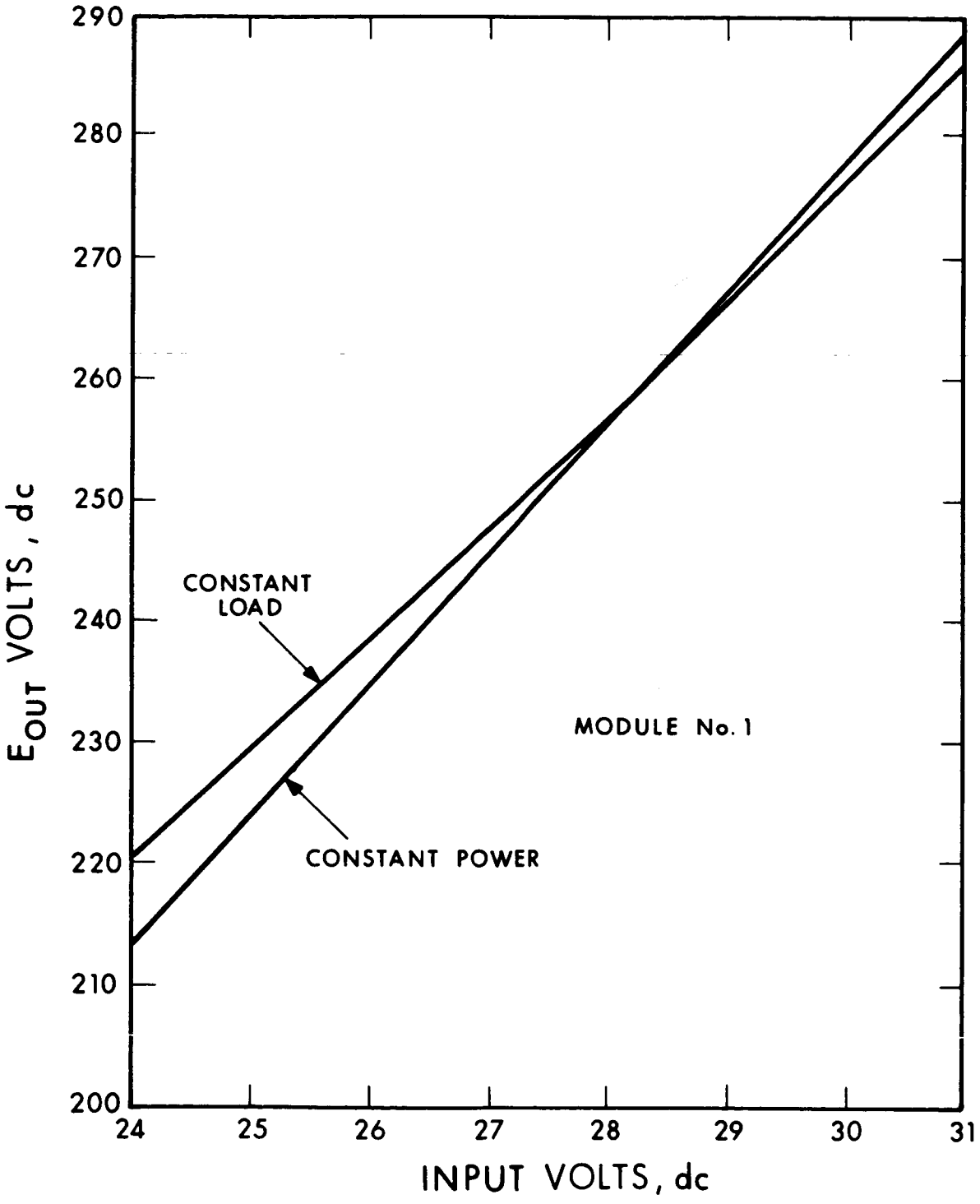

FIG. 12 OUTPUT VOLTAGE VERSUS INPUT VOLTAGE

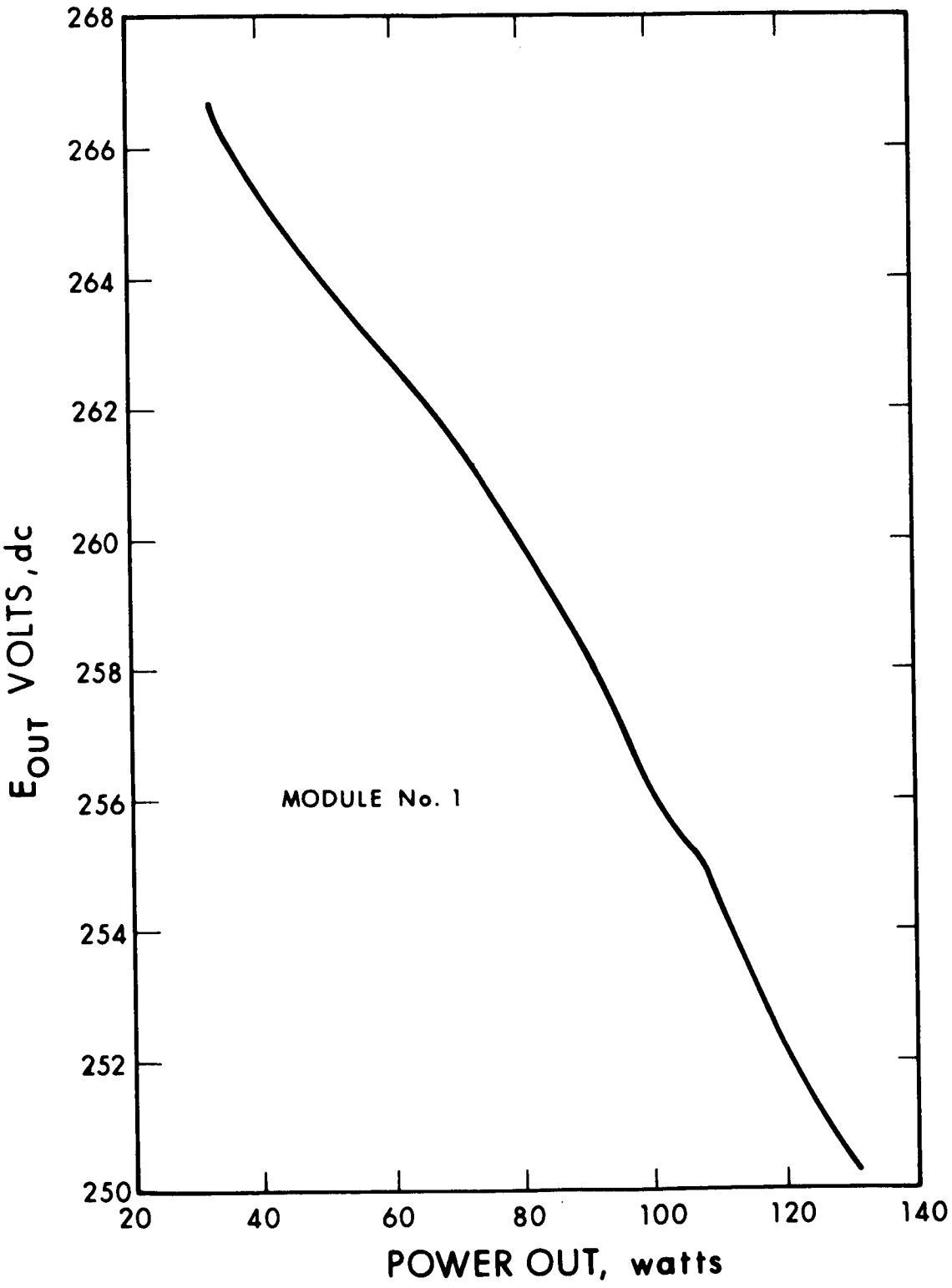

FIG. 13 OUTPUT VOLTAGE VERSUS OUTPUT POWER

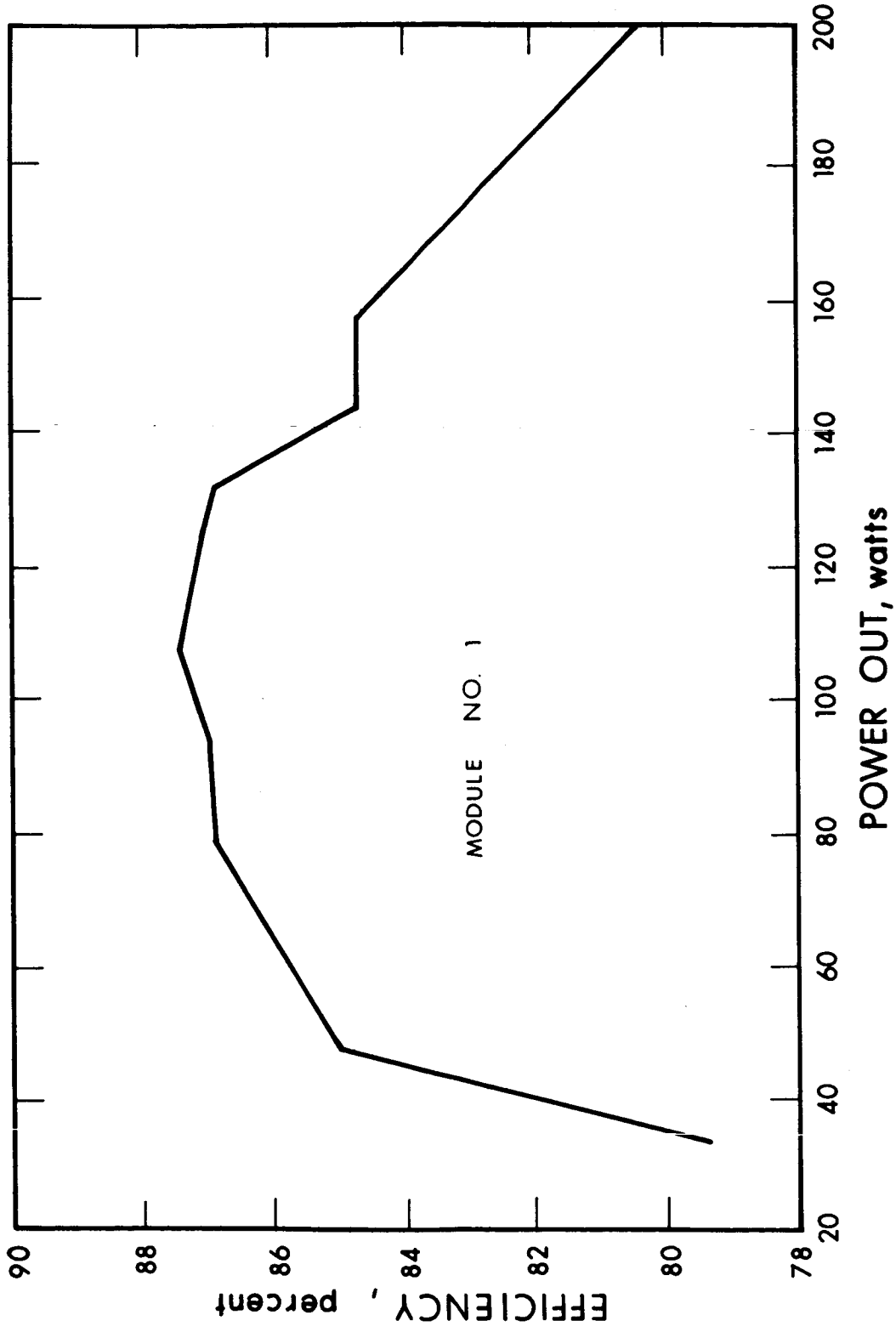

FIG. 14 EFFICIENCY VERSUS OUTPUT POWER

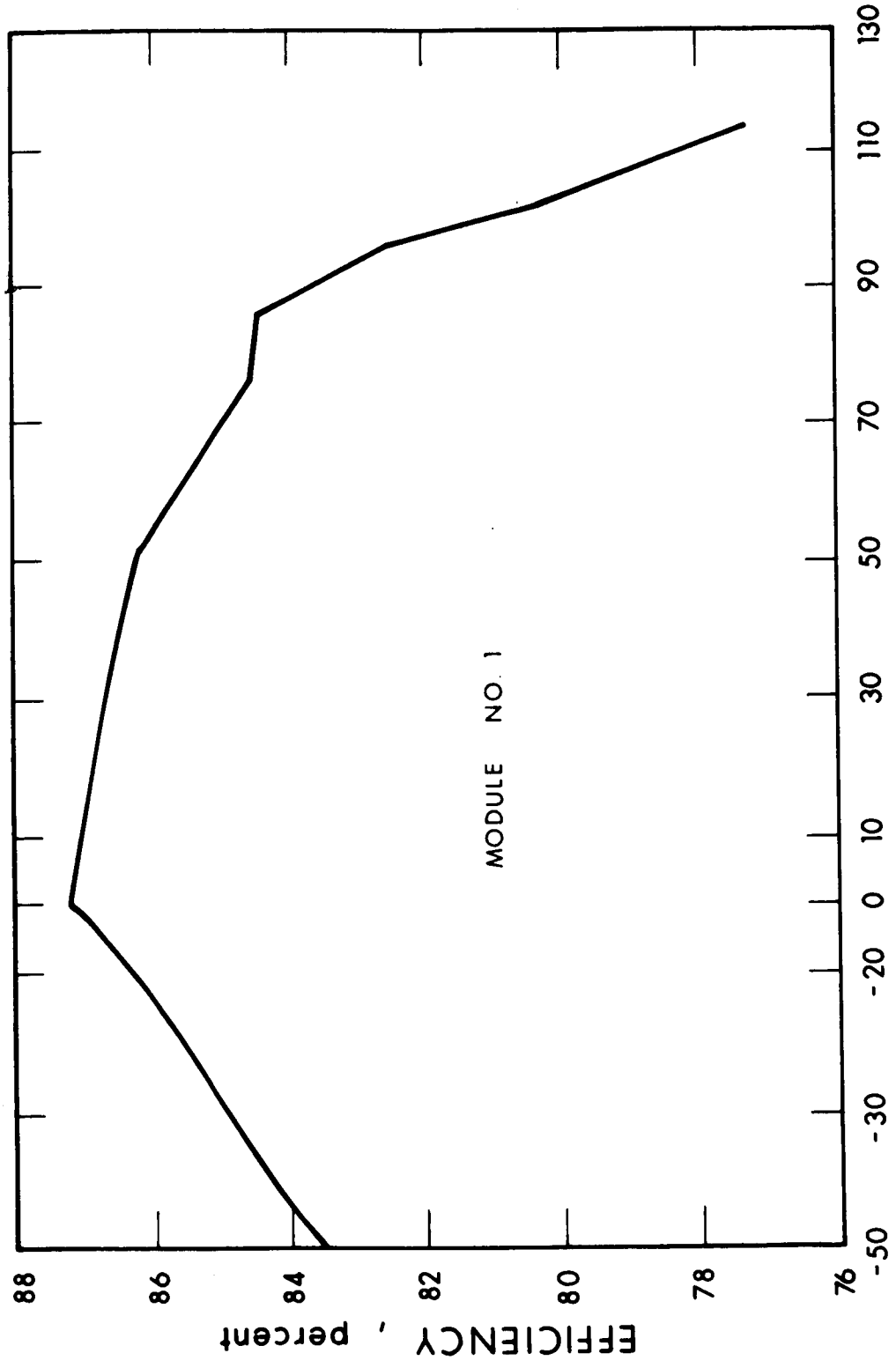

FIG. 15 EFFICIENCY VERSUS AMBIENT TEMPERATURE AT 100 WATTS OUTPUT

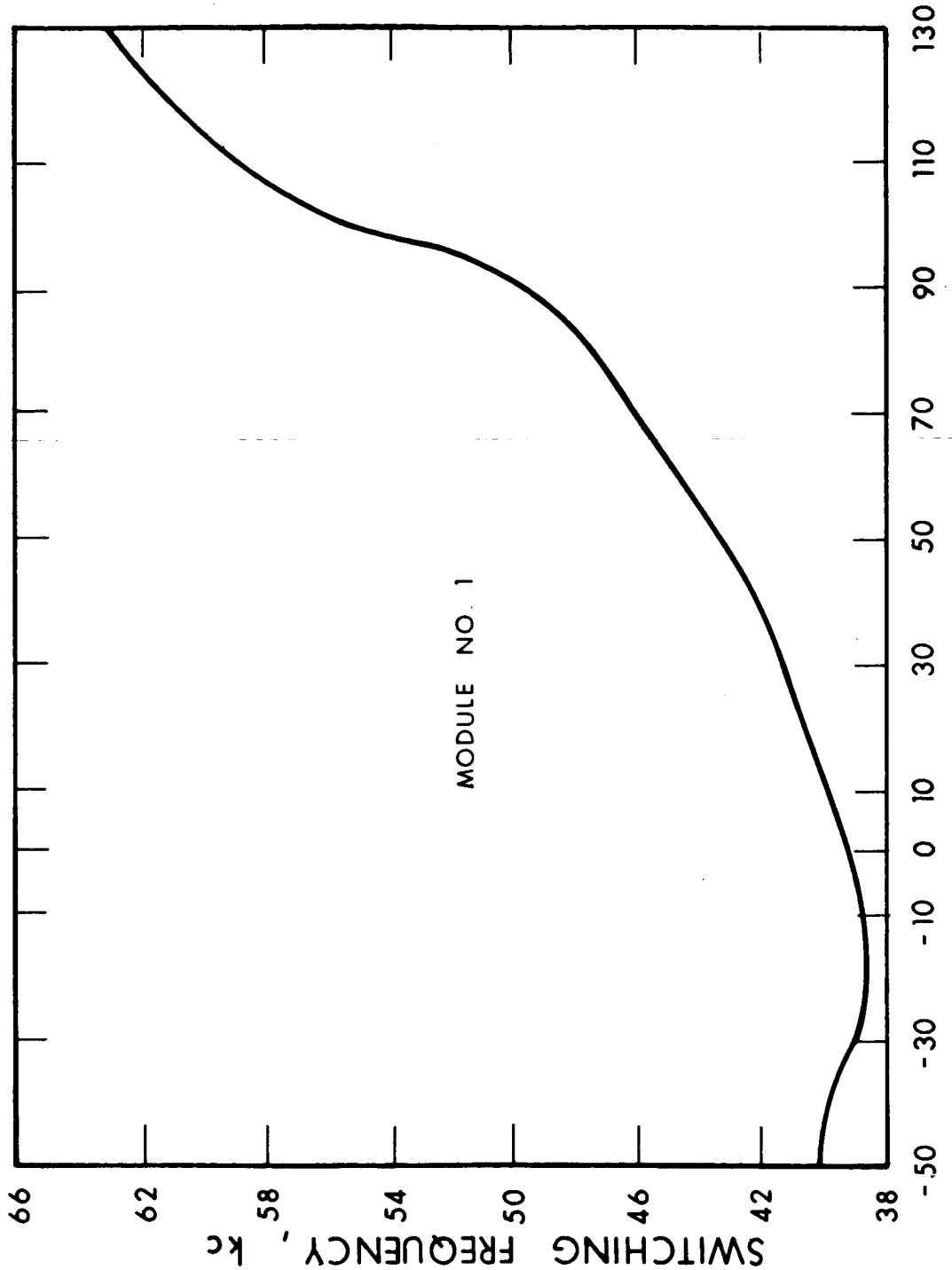

FIG. 16 SWITCHING FREQUENCY VERSUS AMBIENT TEMPERATURE

4.5.3 Module No. 2 (5 Vdc)

For Module No. 2, two separate designs were breadboarded and tested. For this unit, two separate output transformers were checked along with two different types of power transistors. The RCA 2N3265 and the Honeywell MHT7016 were used for this module. The plots of efficiency as a function of output power for the different circuits are shown in Fig. 17. All of the efficiencies obtained fell between 71.5 percent and 73 percent.

The component weights for the circuits breadboarded and tested are listed below:

Circuit (No.)	Weight (grams)
1	135.7
2	165.1

Circuit No. 2, shown in Fig. 18, was selected as the representative design and was subjected to the following performance tests.

Figure 19 shows the variation of module efficiency as a function of ambient temperature while delivering 100 watts of output power.

Figure 20 shows the variation of module efficiency as a function of output power.

Figure 21 shows the variation of output voltage as a function of output power.

Figure 22 shows the variation of switching frequency as a function of ambient temperature.

Figure 23 shows the variation of output voltage as a function of input voltage under constant load conditions.

Table VIII shows a breakdown of the component weights for Module No. 2.

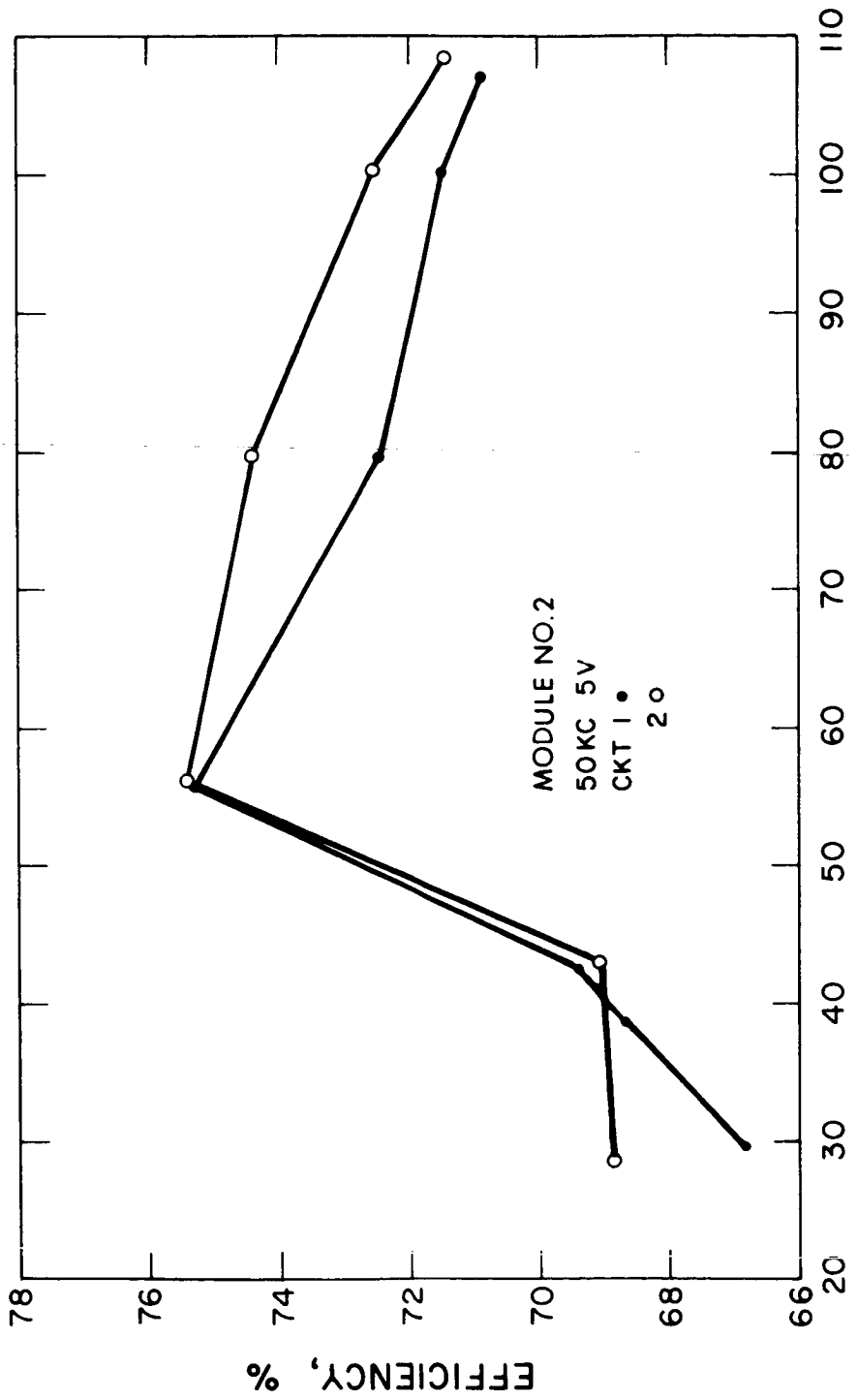

FIG. 17 EFFICIENCY VERSUS OUTPUT POWER, MODULE NO. 2 (50 kHz CIRCUITS)

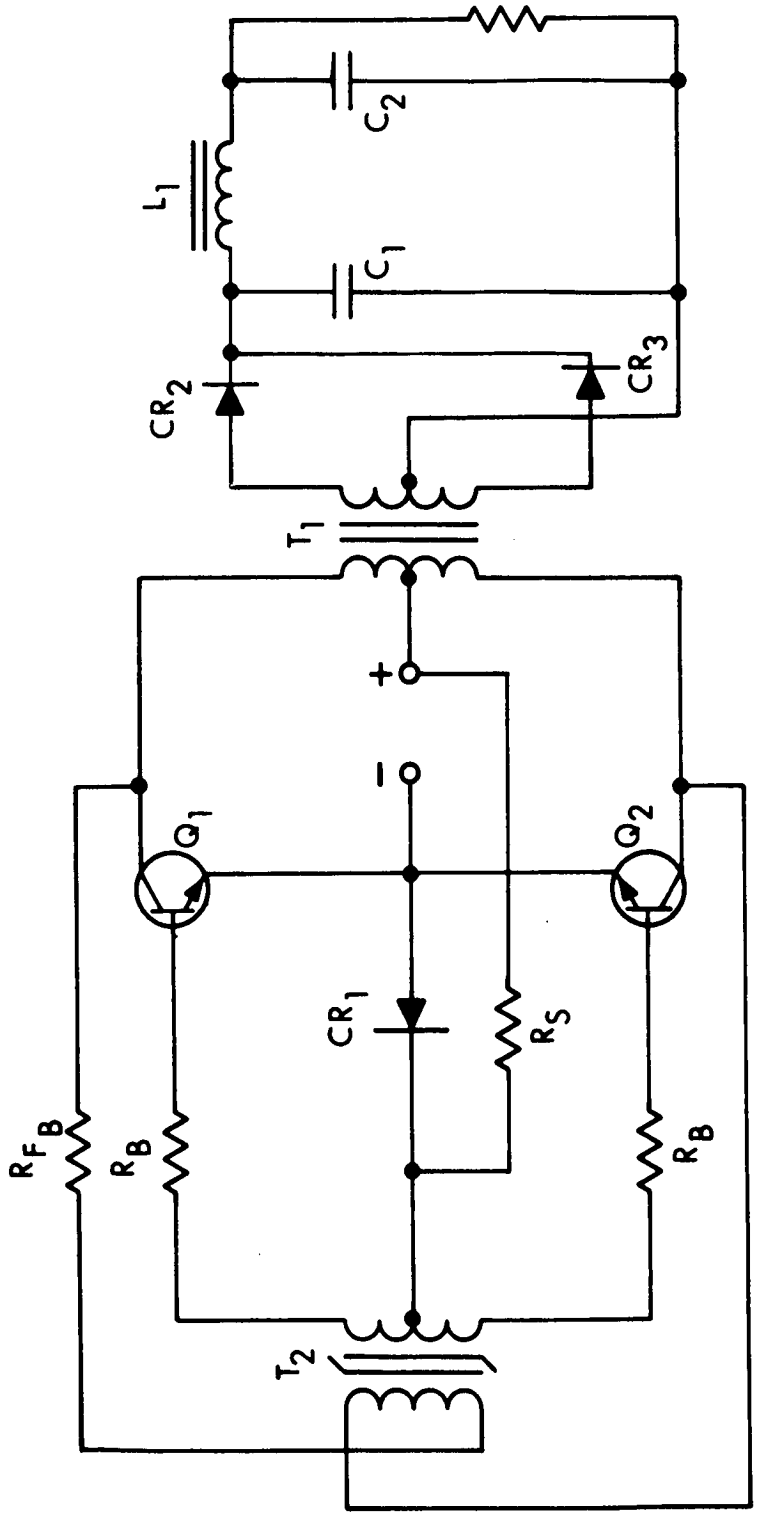

FIG. 18 MODULE NO. 2 - 50 kHz CIRCUIT

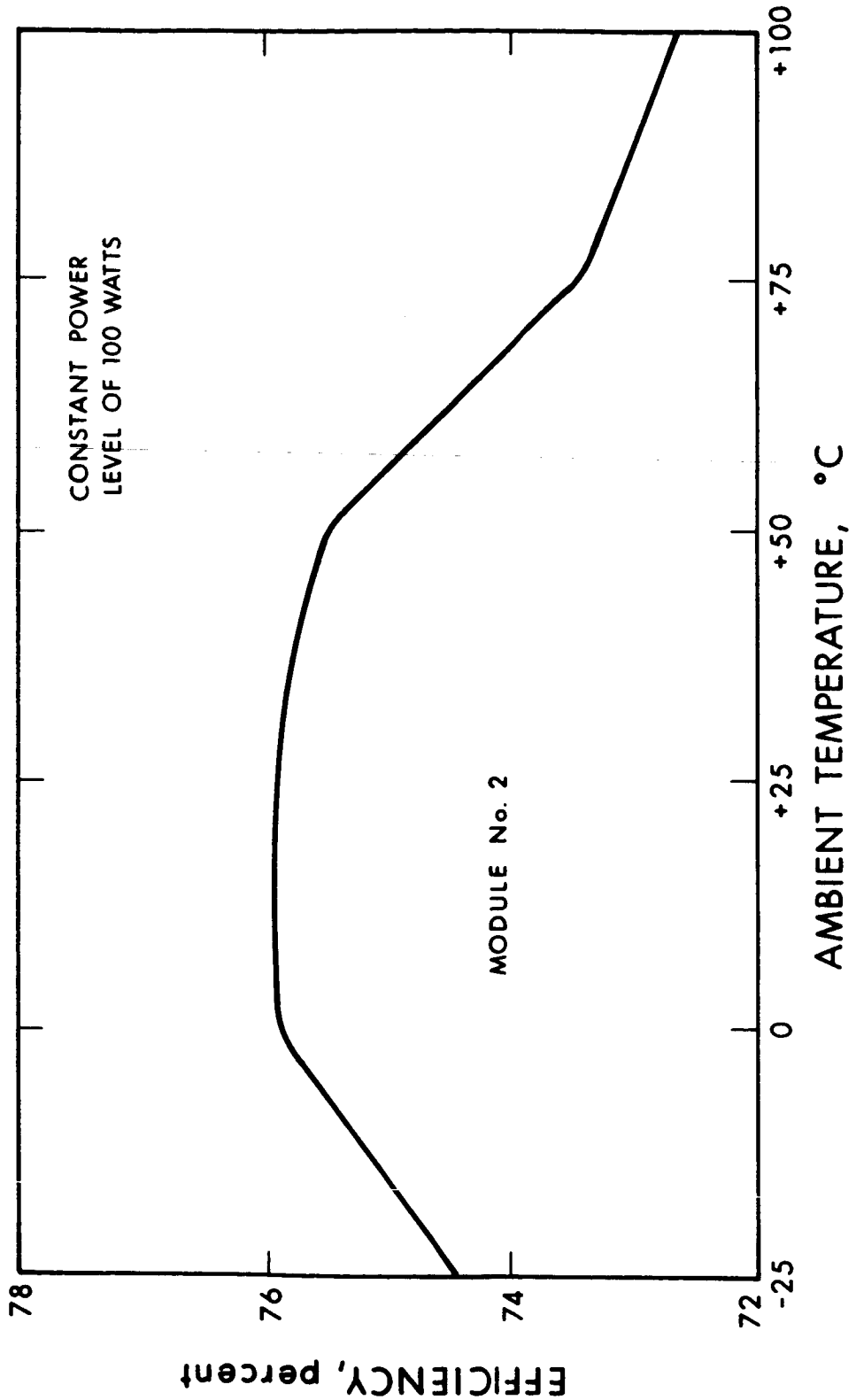

FIG. 19 EFFICIENCY VERSUS AMBIENT TEMPERATURE

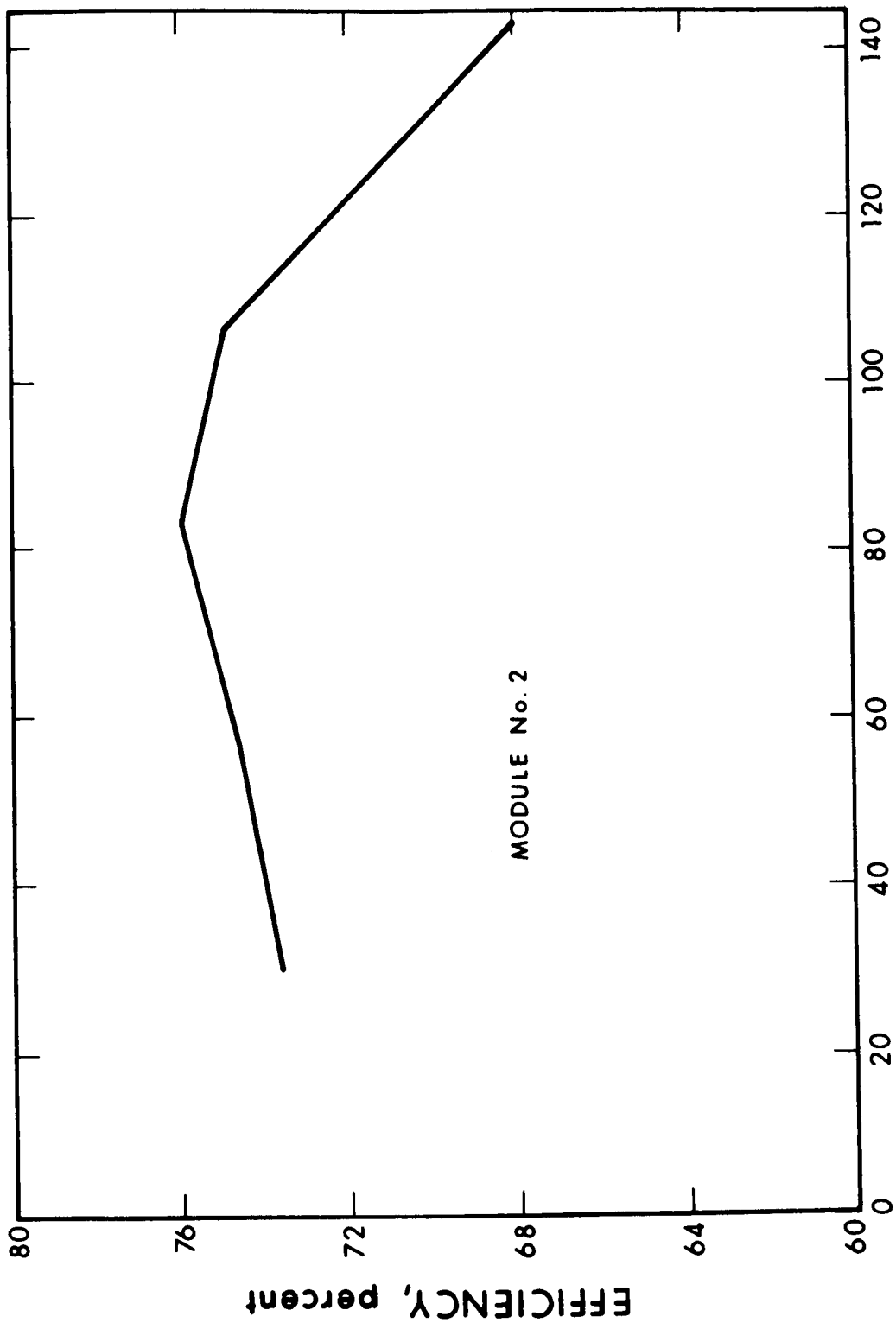

FIG. 20 EFFICIENCY VERSUS OUTPUT POWER

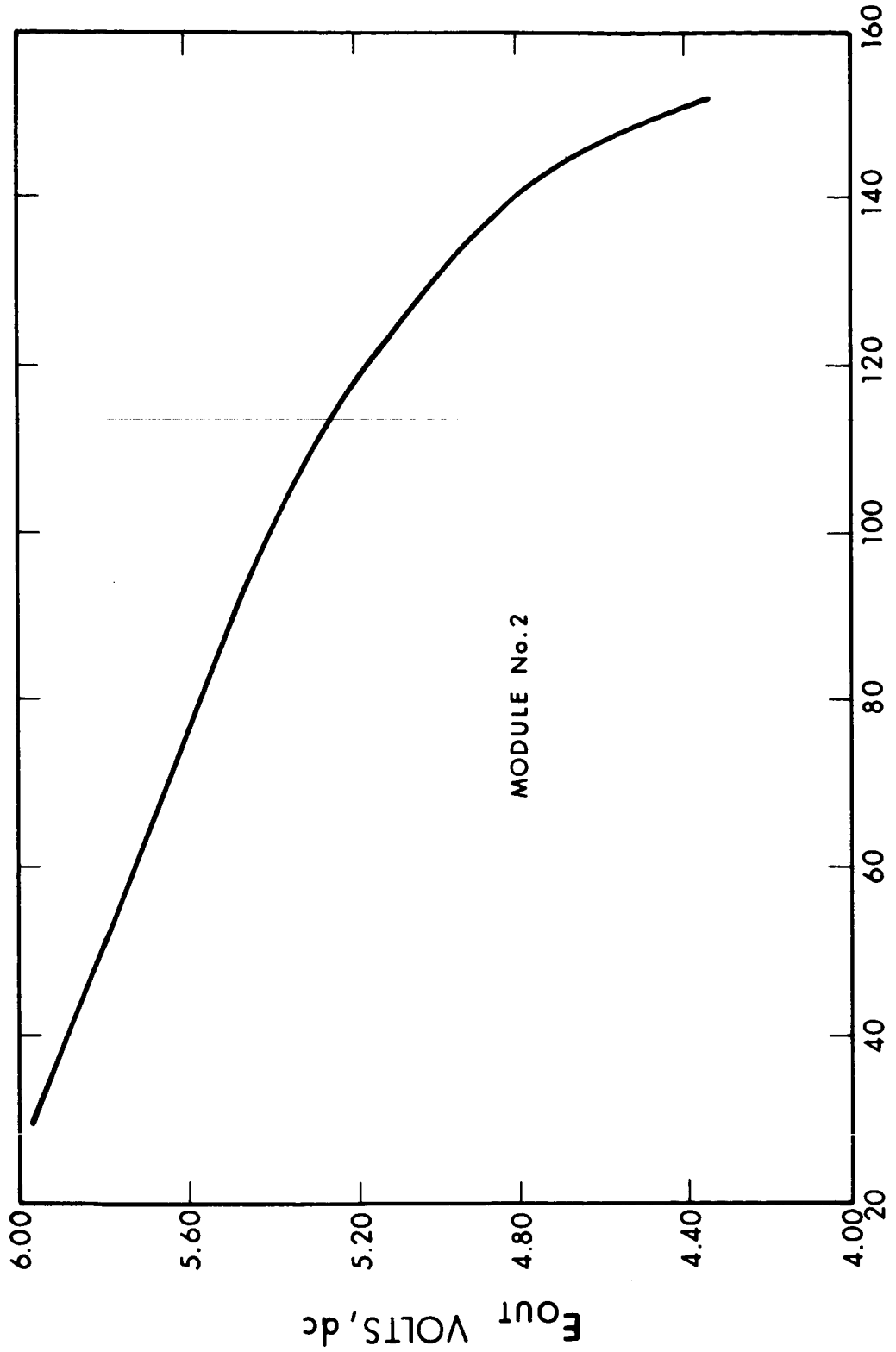

FIG. 21 OUTPUT VOLTAGE VERSUS OUTPUT POWER

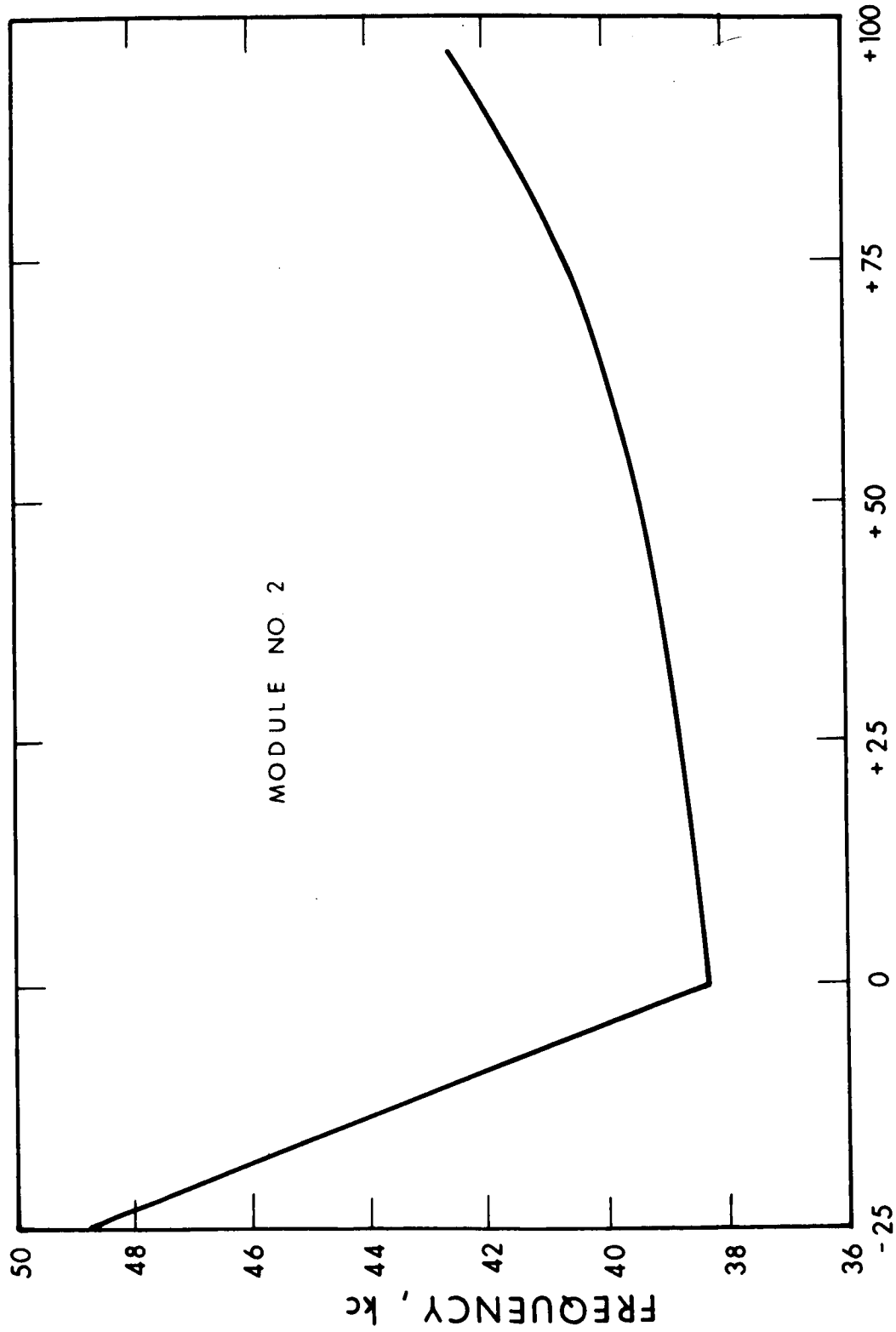

FIG. 22 SWITCHING FREQUENCY VERSUS AMBIENT TEMPERATURE

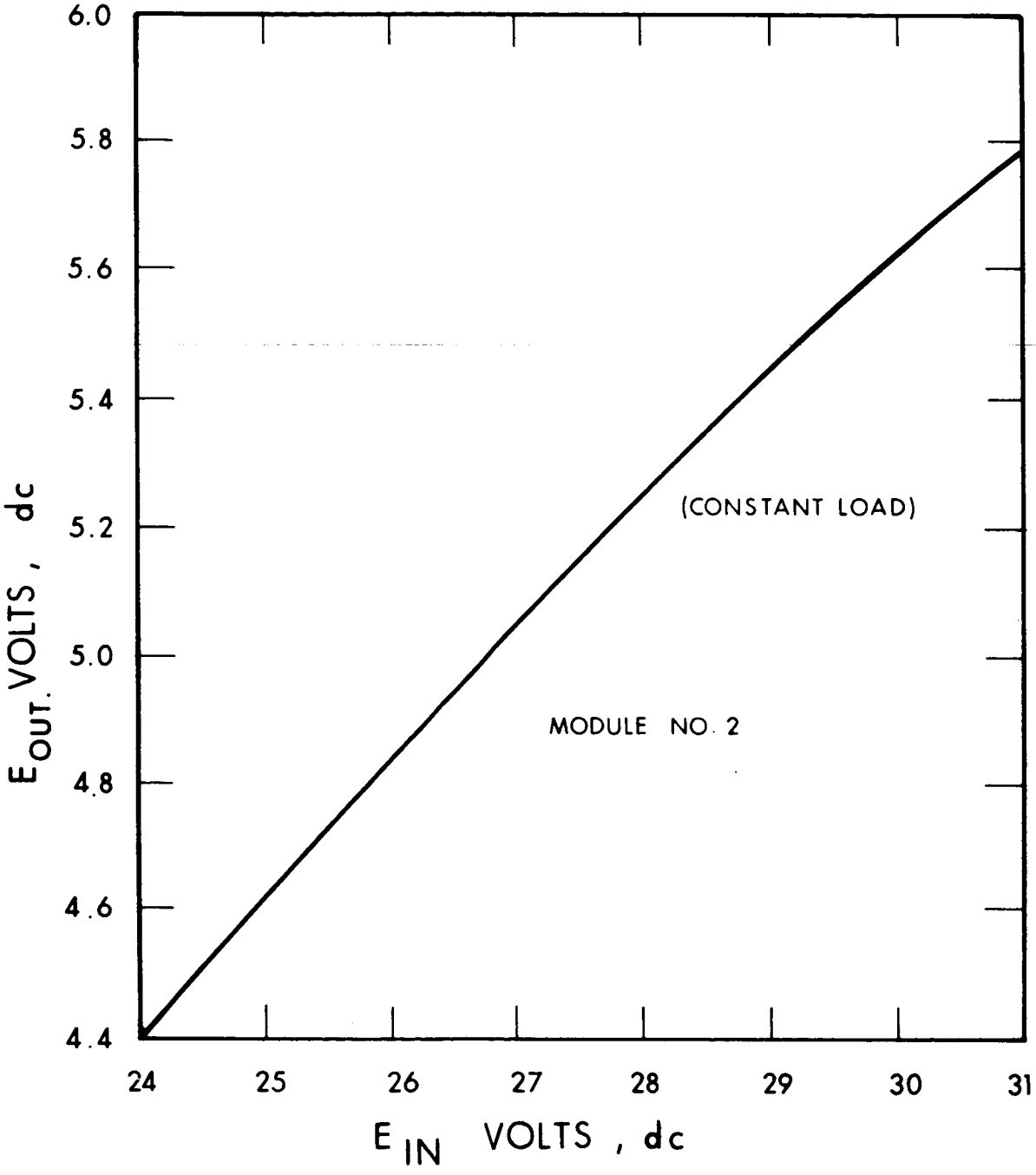

FIG. 23 OUTPUT VOLTAGE VERSUS INPUT VOLTAGE

TABLE VIII

MODULE NO. 2 — COMPONENT WEIGHTS

Significant Components	Weight (grams)
Output Transformer	40.10
Driver Transformer	2.75
Current Transformer	2.85
Filter Inductor	10.06
Output Capacitors (2)	16.00
Output Power Transistors (2)	8.45
Output Rectifiers (2)	37.00
Basic Dc-Dc Converter Circuit	
Total Components	123.81 (or 4.36 oz)
Complete Module No. 2 Circuit with Overload and Short Circuit Protection	
Total Components	141.41 (or 4.96 oz)

4.5.4 Module No. 3 (1000 Vdc)

Four circuits of Module No. 3 were designed, breadboarded, and tested. One output transformer was checked with two different types of power transistors. The resulting efficiency as a function of output power is shown in Fig. 24. The efficiencies obtained at the 100 watt level were 85.5 percent and 89 percent.

The component weights for the Module No. 3 circuits breadboarded and tested are shown below:

Circuit (No.)	Weight (grams)
1	169.2
2	139.4
3	136.3
4	169.2

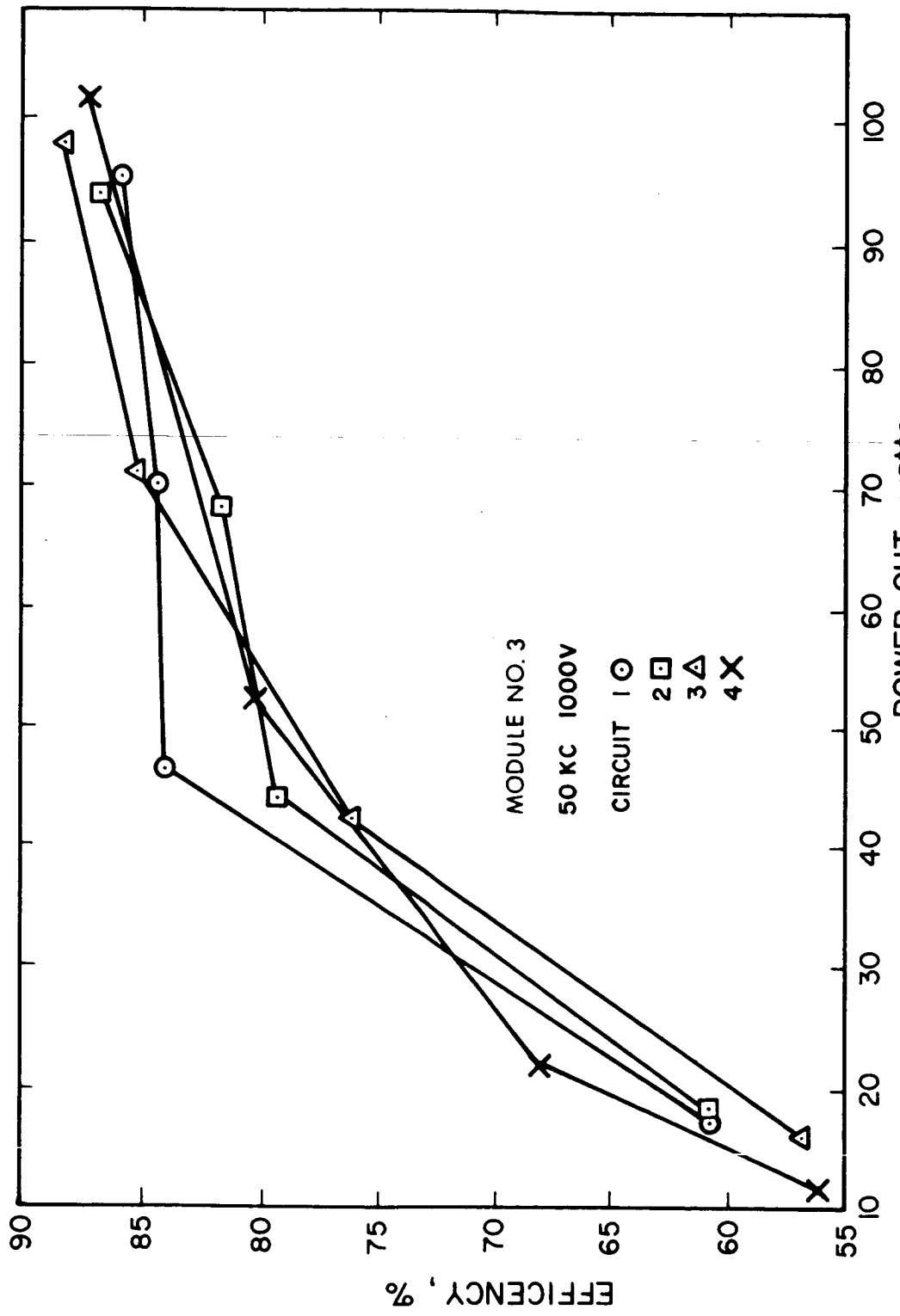

FIG. 24 EFFICIENCY VERSUS OUTPUT POWER, MODULE NO. 3 (50 kHz CIRCUIT)

A representative circuit of Module No. 3, shown in Fig. 25, was subjected to further performance tests.

Figure 26 shows the variation of module efficiency as a function of output power.

Figure 27 shows the variation of module efficiency as a function of ambient temperature.

Figure 28 shows the variation of output voltage as a function of input voltage.

Figure 29 shows the variation of output voltage as a function of output power.

Figure 30 shows the variation of switching frequency as a function of ambient temperature.

Table IX shows a breakdown of the components for Module No. 3.

TABLE IX

MODULE NO. 3 — COMPONENT WEIGHTS

Significant Components	Weight (grams)
Output Transformer	39.10
Driver Transformer	3.60
Current Transformer	3.10
Output Power Transistors (2)	8.45
Output Rectifier Bridge	8.50
Basic Dc-Dc Converter Circuit	
Total Components	83.6 (or 2.94 oz)
Complete Module No. 3 Circuit with Overload and Short Circuit Protection	
Total Components	100.6 (or 3.54 oz)

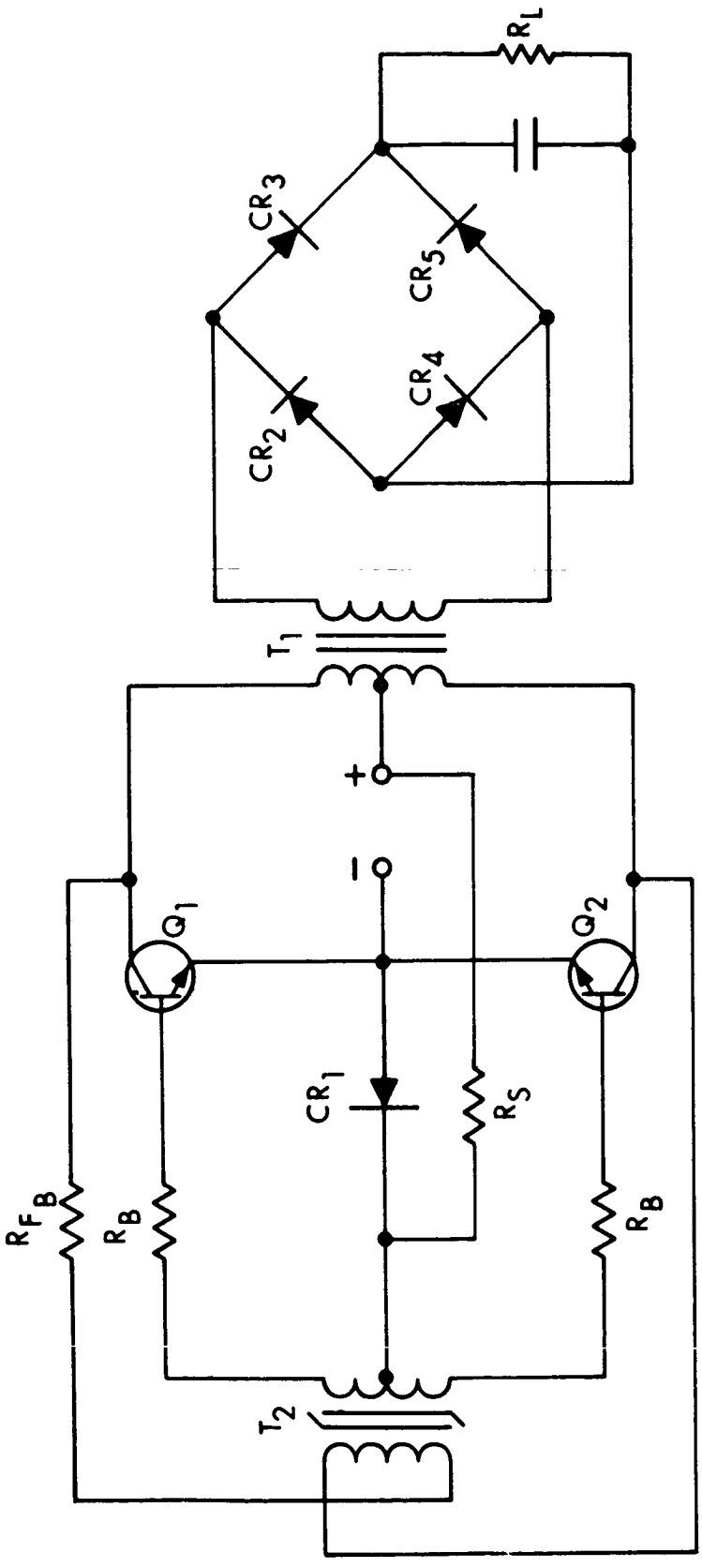

FIG. 25 MODULE NO. 3 - 50 kHz CIRCUIT

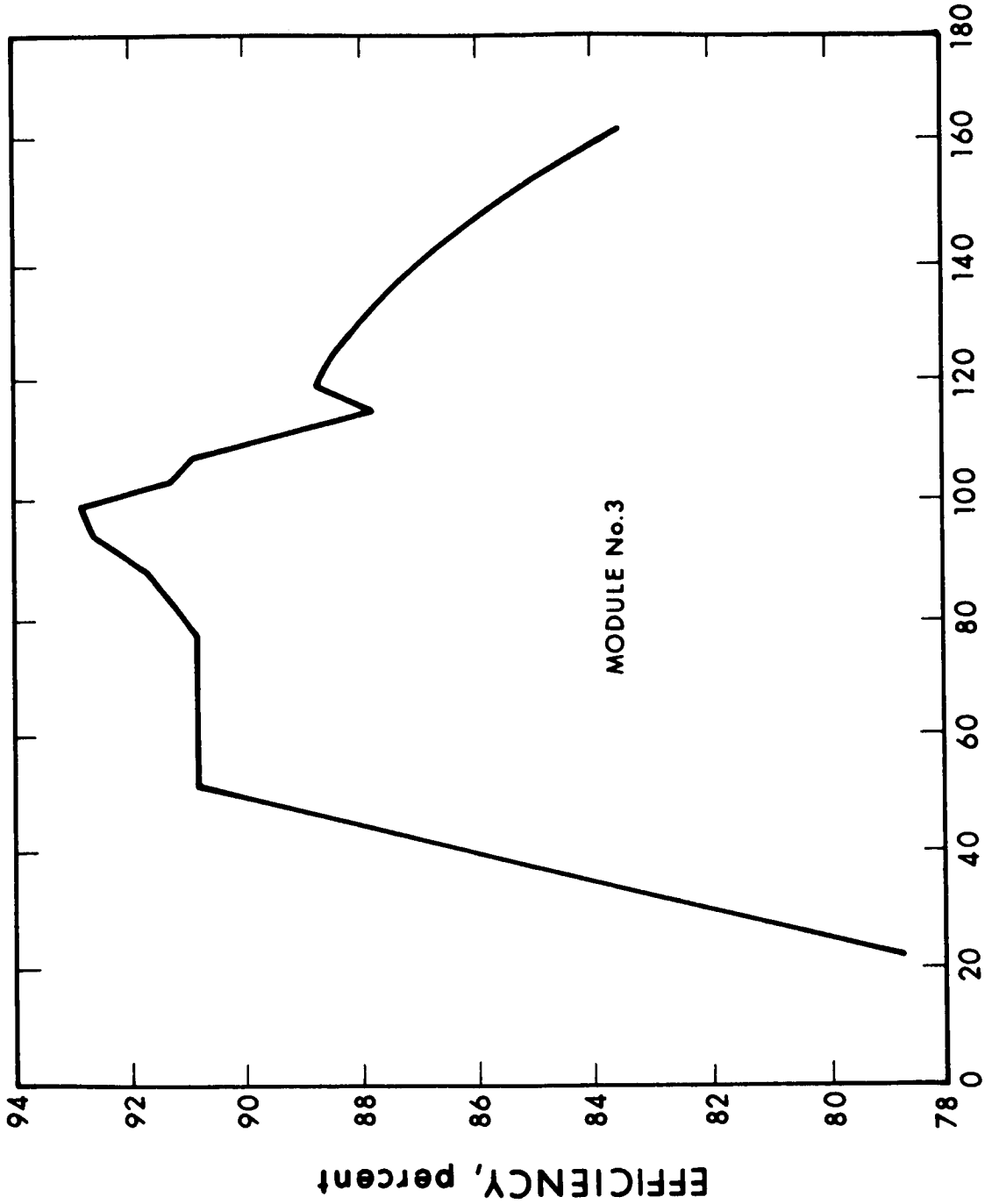

FIG. 26 EFFICIENCY VERSUS OUTPUT POWER, MODULE NO. 3 (50 kHz CIRCUITS)

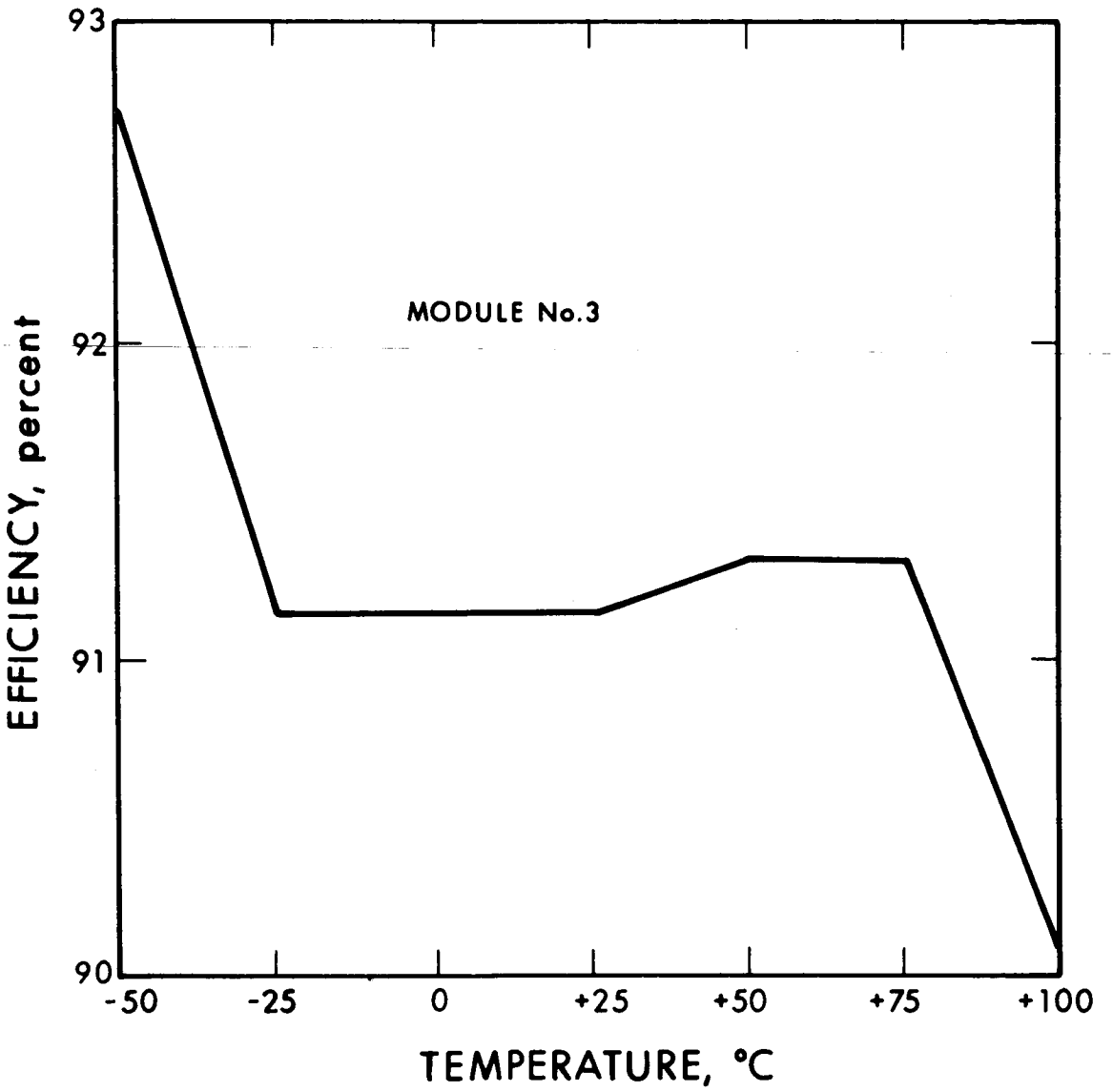

FIG. 27 EFFICIENCY VERSUS TEMPERATURE — MODULE NO. 3

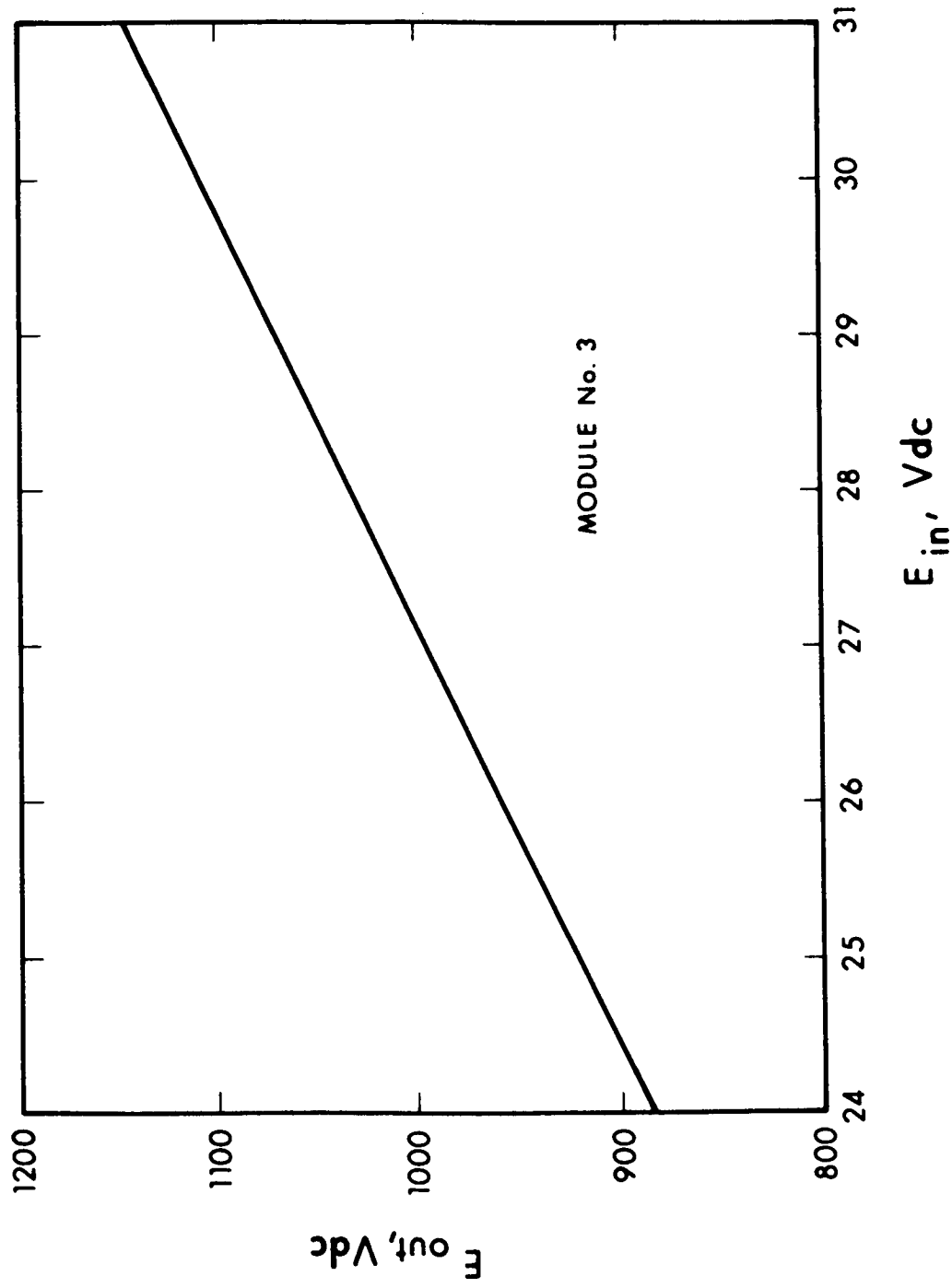

FIG. 28 E_{in} VERSUS E_o, MODULE NO. 3

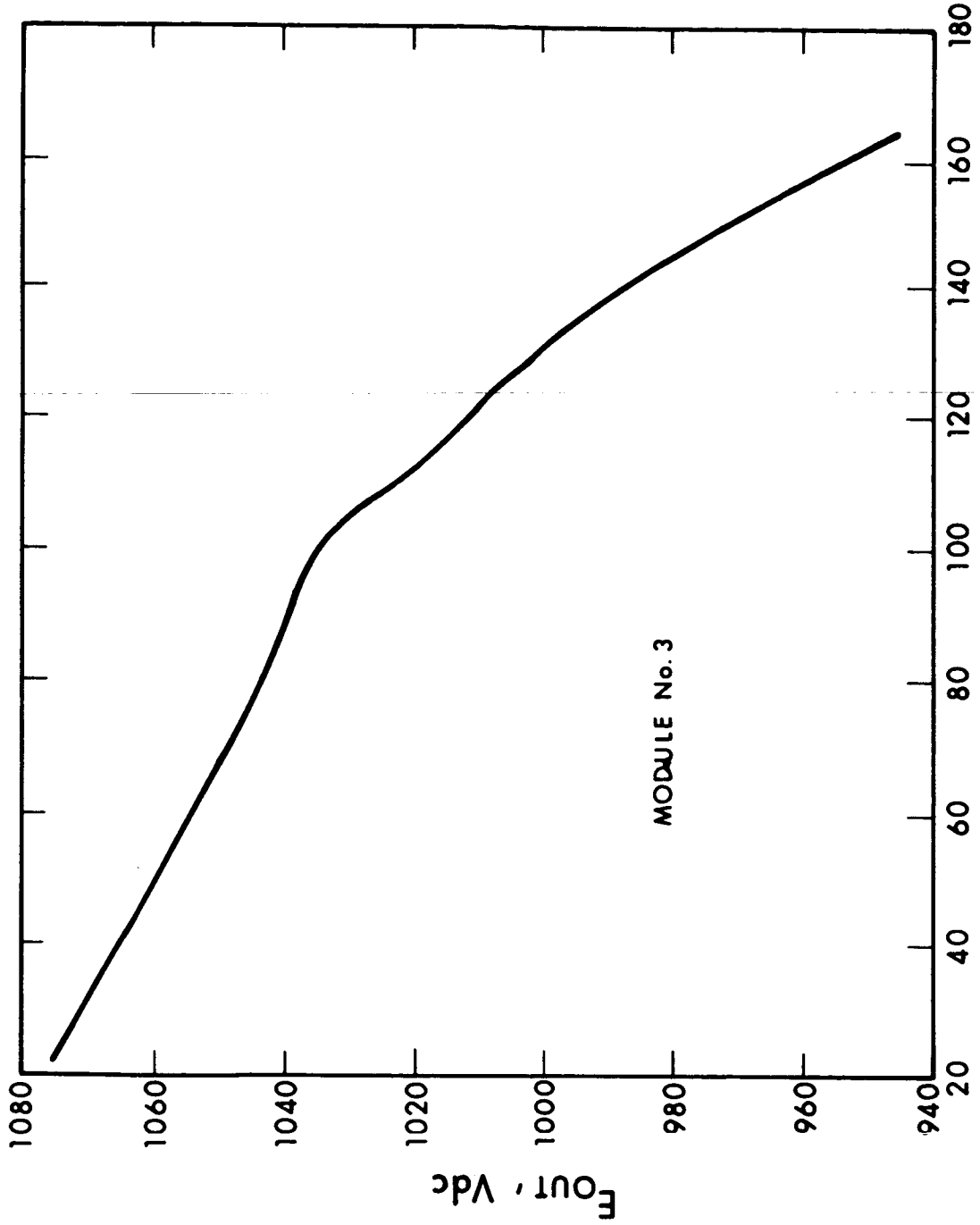

FIG. 29 OUTPUT VOLTAGE VERSUS OUTPUT POWER

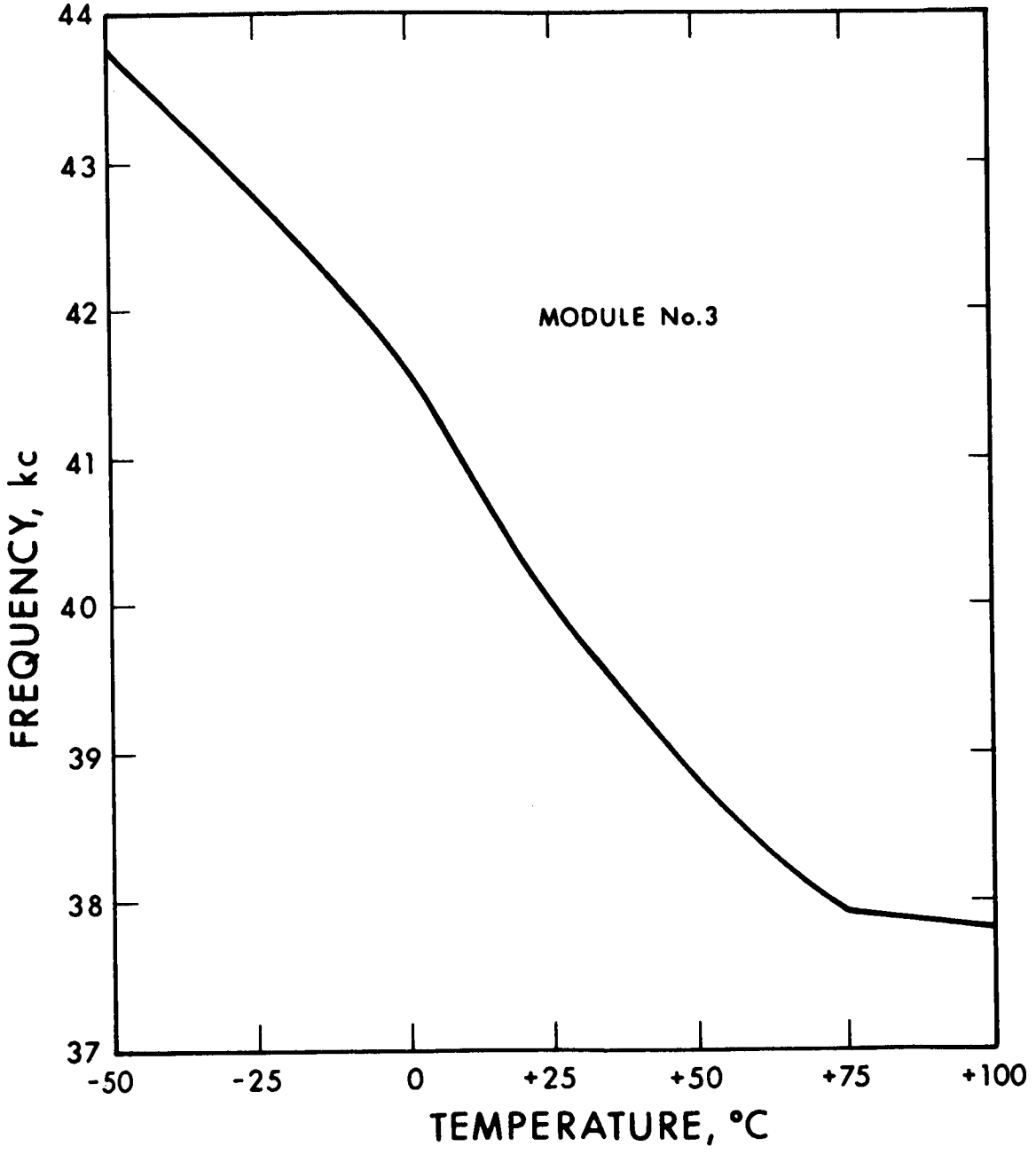

FIG. 30 FREQUENCY VERSUS TEMPERATURE — MODULE NO. 3

4.5.5 Overload and Short Circuit Protection

Ion engines are subject to arcing quite frequently and, if adequate protection is not provided, the power conditioning subsystem can easily be destroyed. It was for this reason that the basic module was provided with overload and short circuit protection. In the event of an overload or short circuit condition it was desirable to shut down the oscillator circuit for as long as the overload or arc persisted. Upon removal of the overload or short circuit, the converter circuit would automatically return to its normal mode of operation.

Figure 31 is a schematic diagram of the Module No. 1 converter circuit together with the overload and short circuit protection circuitry.

The current overloads are sensed by current transformer T3. The output voltage from the current transformer is proportional to the current flowing in the primary winding. This output voltage is rectified by the full-wave bridge circuit composed of CR5, CR6, CR7, and CR8. Filtering of the output voltage is provided by capacitor C10. A near constant impedance is provided by a resistor network composed of R15 and R17. A portion of the rectified voltage is then used to drive a level detector circuit (Schmitt trigger) composed of Q5 and Q6. The output from the level detector circuit is then coupled to an emitter following circuit (Q8), which in turn drives the output transistor (Q7). The output stage of the overload circuit provides sufficient drive to saturate transistors Q3 and Q4 which serve to short out the base drive to the power switching transistors Q1 and Q2. When the base drive to the oscillator transistors is removed, the oscillator ceases to function for a prescribed period of time (the off time is determined by the amount of overload).

After the predetermined off time, the oscillator circuit attempts to start again and if the overload or short circuit is still present the oscillator circuit shuts down again. The converter

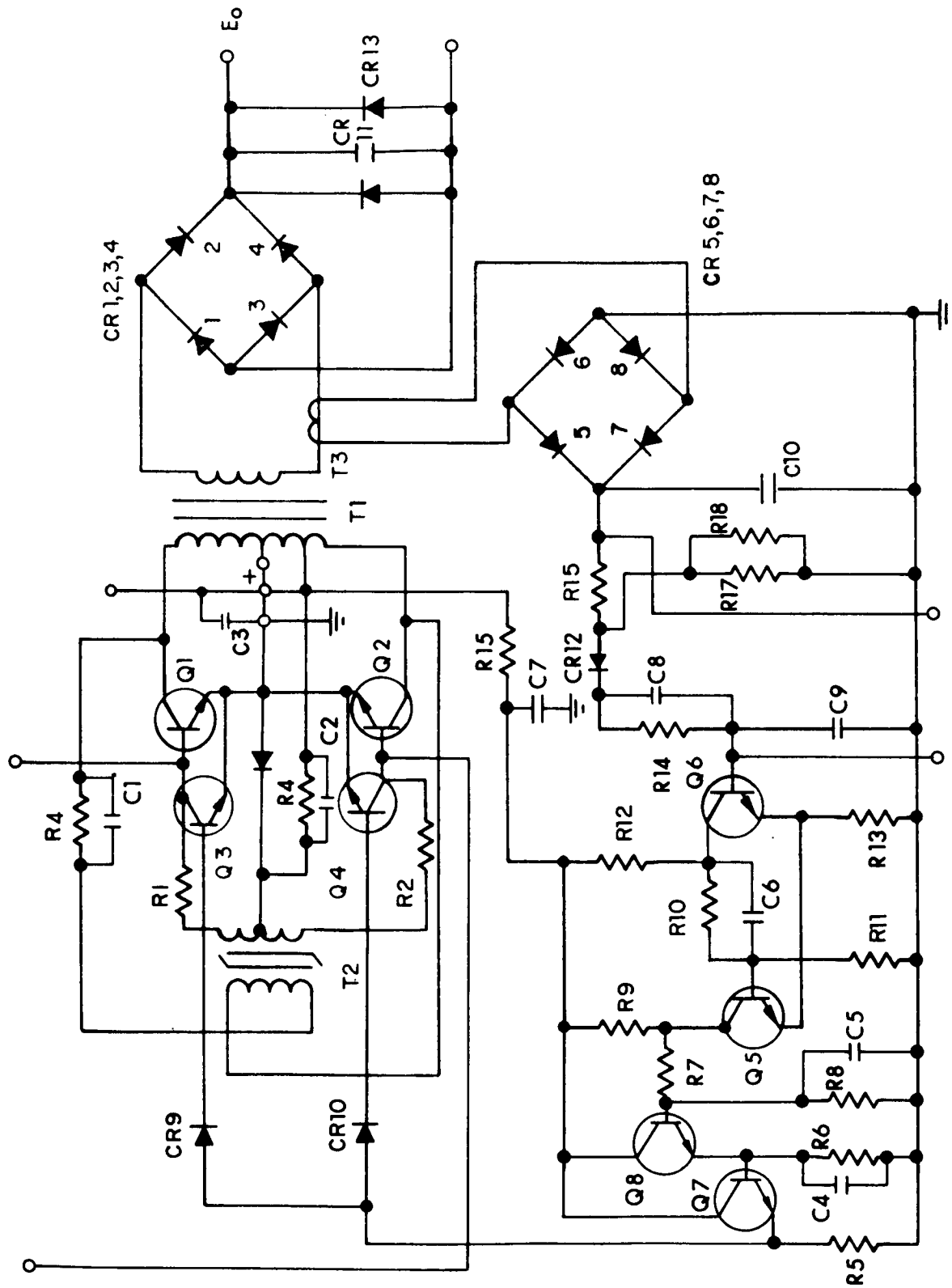

FIG. 31 DIAGRAM, MODULE NO. 1 WITH OVERLOAD CIRCUITRY

circuit will cycle on and off until the overload or short circuit is removed from the output terminals. Upon removal of the overload or short circuit, the converter will automatically return to its normal mode of operation.

The overload circuits for Modules No. 2 and No. 3 are identical to that described above. Only the current transformer is changed.

4.6 Other High Frequency Designs

During the program, work was initiated on the design of a 100 kHz, 100 watt circuit. The purpose of going beyond 50 kHz was to investigate further decreases in size and weight of the output transformer.

For the 100 kHz circuit the oscillator transformer was first designed. The size and weight of this transformer turned out to be approximately the same as the 50 kHz version. It measured 0.594 inch o.d. by 0.313 inch high and weighed 2.6 grams.

In the design of the 100 kHz output transformer, it was noted that approximately a 10 to 15 percent decrease in core size would result. The core required, however, is a nonstandard core and would have to be specially made.

Another problem was faced in the design of the output transformer. The required high voltage insulation dictated the size of the core. For example, the double E core used in Module No. 1 had practically no window area left. An attempt was made to increase the wire size in the transformer, but because of the high voltage insulation required, it was impossible to wind the heavier wire on the core.

It was concluded that the output transformers had been optimized for minimum size and weight at the 100 watt levels and concurrently meet the high voltage (10 kVdc) insulation requirements.

EOS submitted the proposed 50 kHz designs for approval of the NASA Project Manager.

4.7 Transformer Optimization

The transformer design for the high frequency modules was an important part of the overall converter design. Optimization of the output transformer contributed to high circuit efficiency and low circuit weight. In order to attain the goals of the program, a computer (CDC3100) was used to optimize the transformer design.

The basic approach to the design was to develop a mathematical model which would be expressed as a computer program. The design requirements, core material, wire gauge insulation, etc., constitute the necessary input conditions and are shown in Table X for each transformer. An example of how the computer was used to optimize the output transformer is shown below.

Step 1 Determine number of primary turns in first primary layer.

$$nl_{p_1} = \frac{2\pi\left[r_n + t_s + t_p + t_1 + (2\,S_p - 1)(d_p/2 + t_w)\right]}{(d_p + 2\,t_w)}$$

$$\text{with } S_p = 1$$

Step 2 Compare number of turns (nl_{p_1}) with total number of primary turns

a. If $\frac{2\,E_p}{(E_p/N_p)} \leq nl_{p_1}$, go on to Step 4.

b. If $\frac{2\,E_p}{(E_p/N_p)} > nl_{p_1}$, repeat Step 1 with

$S_p = 2$

Step 3 Compare number of turns

a. If $\frac{2\,E_p}{(E_p/N_p)} \leq nl_{p_1} + nl_{p_2}$, go on to Step 4.

TABLE X

INPUT CONDITIONS

1.	E_p	=	Primary Volts (rms)
2.	I_p	=	Primary Current (rms)
3.	E_s	=	Secondary Volts (rms)
4.	I_s	=	Secondary Current (rms)
5.	F	=	Frequency (Hz)
6.	B_n	=	Maximum Flux Density (guass)
7.	d_p	=	Primary Wire Diameter (inches)
8.	d_s	=	Secondary Wire Diameter (inches)
9.	r_n	=	Hole Radius (inches)
10.	t_s	=	Column Thickness (inches)
11.	t_p	=	Potting Thickness (inches)
12.	t_1	=	First Layer Insulation Thickness (inches)
13.	t_2	=	Second Layer Insulation Thickness (inches)
14.	t_3	=	Third Layer Insulation Thickness (inches)
15.	t_w	=	Wire Insulation Thickness (inches)
16.	E_p/N_p	=	Volts Per Turn Ratio
17.	W_m	=	Core Material Weight Constant ($lb/in.^3$)
18.	P_m	=	Core Material Loss Constant (watts/lb)
19.	K_s	=	Secondary Wire Resistance Constant (ohms/ft)
20.	K_p	=	Primary Wire Resistance Constant (ohms/ft)
21.	W_s	=	Secondary Wire Weight Constant (lb/ft)
22.	W_p	=	Primary Wire Weight Constant (lb/ft)
23.	C_{s1}	=	Secondary ac Resistance Factor No. 1
24.	C_{s2}	=	Secondary ac Resistance Factor No. 2
25.	C_{s3}	=	Secondary ac Resistance Factor No. 3
26.	C_{s4}	=	Secondary ac Resistance Factor No. 4

TABLE X

INPUT CONDITIONS (contd)

27. C_{s5} = Secondary ac Resistance Factor No. 5
28. C_{s6} = Secondary ac Resistance Factor No. 6
29. C_{s7} = Secondary ac Resistance Factor No. 7
30. C_{s8} = Secondary ac Resistance Factor No. 8
31. C_{p1} = Primary ac Resistance Factor No. 1
32. C_{p2} = Primary ac Resistance Factor No. 2
33. C_{p3} = Primary ac Resistance Factor No. 3
34. C_{p4} = Primary ac Resistance Factor No. 4
35. C_{p5} = Primary ac Resistance Factor No. 5
36. C_{p6} = Primary ac Resistance Factor No. 6
37. C_{p7} = Primary ac Resistance Factor No. 7
38. C_{p8} = Primary ac Resistance Factor No. 8

b. If $\frac{2\ E_p}{(E_p/N_p)} > nl_{p_2} + nl_{p_2}$, repeat Step 1 with

$S_p = 3$

NOTE: Repeat computation of Step 1 until

$$\frac{2\ E_p}{(E_p/N_p)} \leq nl_{p_1} + nl_{p_2} + nl_{p_3} \text{ ---- } + nl_{p_n}$$

Store each nl_p computation and also the number of times Step 1 is computed which is equal to the number of layers (S_p).

Step 4 Determine number of secondary turns in first secondary layer.

$$nl_{s_1} = \frac{2\pi\left[r_n + t_s + t_p + t_1 + S_p(d_p + 2\ t_w) + t_2 + (2\ S_s - 1)(d_s/2 + t_w)\right]}{(d_s + 2\ t_w)}$$

with $S_s = 1$

Step 5 Compare number of turns (nl_{s_1}) with total number of secondary turns.

a. If $\frac{E_s}{(E_p/N_p)} \leq nl_{s_1}$, go on to Step 7.

b. If $\frac{E_s}{(E_p/N_p)} > nl_{s_1}$, repeat Step 4 with

$S_s = 2$

Step 6 Compare number of turns

a. If $\frac{E_s}{(E_p/N_p)} \leq nl_{s_1} + nl_{s_2}$, go on to Step 7.

b. If $\frac{E_s}{(E_p/N_p)} > nl_{s_1} + nl_{s_2}$, repeat Step 4 with

$$S_s = 3$$

NOTE: Repeat computation of Step 4 until

$$\frac{E_s}{(E_p/N_p)} \leq nl_{s_1} + nl_{s_2} + nl_{s_3} + \text{---} + nl_{s_n}$$

Store each nl_s computation and also the number of times Step 4 is computed which is equal to the number of secondary layers (S_s).

Step 7 Compute inner radius of core

$$R_i = r_n + t_s + t_p + t_1 + S_p(d_p + 2\ t_w) + t_2 + S_s(d_s + 2\ t_w) + t_3$$

Step 8 Compute core cross sectional area

$$A_c = \left[\frac{E_p}{N_p}\right]\left[\frac{1}{B_m F\ 4 \times 10^{-8}}\right]$$

Step 9 Determine length of one side of core

$$a = \frac{\sqrt{A_c}}{2.54}$$

Step 10 Compute volume of core

$$V_c = \pi a^2 (2 R_i + a)$$

Step 11 Compute weight of core in pounds

$$W_c = W_m V_c$$

Step 12 Compute core loss in watts

$$P_c = W_c P_m$$

Step 13 Compute length of first secondary winding.

$$L_{s_1} = 4\, nl_{s_n} \left[a + d_s + 2(t_3 + t_w) + 2(S_s - K_1)(d_s + 2\, t_w)\right]$$

$$\text{with } K_1 = S_s$$

Step 14 Compute length of second secondary winding.

$$L_{s_2} = 4\, nl_{s_{n-1}} \left[a + d_s + 2(t_3 + t_w) + 2(S_s - K_1)(d_s + 2\, t_w)\right]$$

$$\text{with } K_1 = S_s - 1$$

Step 15 Compute length of third secondary winding.

$$L_{s_3} = 4\, nl_{s_{n-2}} \left[a + d_s + 2(t_3 + t_w) + 2(S_s - K_1)(d_s + 2\, t_w)\right]$$

$$\text{with } K_1 = S_s - 2$$

NOTE: Store each L_{s_n} computation and continue to compute until $K_1 = 0$, i.e., subtracting an additional quantity from S_s until $K_1 = S_s - S_s = 0$. Note that the nl_{s_n} quantities used are in the reverse order to those computed in Step 4, i.e., use last nl_{s_n} first in Step 13.

Step 16 Compute total secondary wire length.

$$L_s = L_{s_1} + L_{s_2} + L_{s_3} + \text{---} + L_{s_n}$$

Step 17 Compute length of first primary winding.

$$L_{p_1} = 4\ nl_{p_n}\left[a + 2(t_2 + t_3) + 2\ S_s(d_s + 2\ t_w) + d_p + 2\ t_w + 2(S_p - K_2)(d_s + 2\ t_w)\right]$$

$$\text{with } K_2 = S_p$$

Step 18 Compute length of second primary winding.

$$L_{p_2} = 4\ nl_{p_{n-1}}\left[a + 2(t_2 + t_3) + 2\ S_s(d_s + 2\ t_w) + d_p + 2\ t_w + 2(S_p - K_2)(d_s + 2\ t_w)\right]$$

$$\text{with } K_2 = S_p - 1$$

Step 19 Compute length of third primary winding.

$$L_{p_3} = 4\ nl_{p_{n-2}}\left[a + 2(t_2 + t_3) + 2\ S_s(d_s + 2\ t_w) + d_p + 2\ t_w + 2(S_p - K_2)(d_s + 2\ t_w)\right]$$

$$\text{with } K_2 = S_p - 2$$

NOTE: Store each L_{p_n} computation and continue to compute until $K_2 = 0$, i.e., subtracting an additional quantity from S_p until $K_2 = S_p - S_p = 0$. Note that the nl_{p_n} quantities used are in the reverse order to those computed in Step 1, i.e., use last nl_{p_n} first in Step 17.

Step 20 Compute total primary wire length

$$L_p = L_{p_1} + L_{p_2} + \text{---} + L_{p_n}$$

Step 21 Compute ac resistance of first secondary winding.

$$R_{sac_1} = \left(\frac{L_{s_1} K_s}{12}\right) C_{s_1}$$

Step 22 Compute ac resistance of second secondary winding.

$$R_{sac_2} = \left(\frac{L_{s_2} K_s}{12}\right) C_{s_2}$$

Step 23 Compute ac resistance of third secondary winding.

$$R_{sac_3} = \left(\frac{L_{s_3} K_s}{12}\right) C_{s_3}$$

NOTE: Continue to compute all secondary ac resistances from supplied constants C_{s_n} and K_s and computed winding lengths L_{s_n}.

Step 24 Compute total secondary resistance.

$$R_s = R_{sac_1} + R_{sac_2} + R_{sac_3} + \text{---} + R_{sac_n}$$

Step 25 Compute secondary power loss.

$$P_s = (I_s)^2 R_s$$

Step 26 Compute ac resistance of last primary winding. Note that the L_{p_n} quantities used are in the reverse order to those computed in Step 17.

$$R_{pac_n} = \left(\frac{L_{p_n} K_p}{12}\right) C_{p_1}$$

Step 27 Compute ac resistance of next to last primary winding.

$$R_{pac_{n-1}} = \left(\frac{L_{p_{n-1}} K_p}{12}\right) C_{p_2}$$

NOTE: Continue to compute all primary ac resistances in reverse order using supplied constants K_p and C_{p_n} and computed winding lengths L_{p_n}.

Step 28 Compute total primary resistance.

$$R_P = R_{pac_1} + R_{pac_2} + R_{pac_3} + \text{---} + R_{pac_n}$$

Step 29 Compute primary power loss.

$$P_p = (I_p)^2 R_p$$

Step 30 Compute voltage regulation.

$$\upsilon_r = \left[\frac{I_s}{E_s}\right]\left[R_s + (E_s/E_p)^2 R_p\right] \times 100$$

Step 31 Compute efficiency.

$$z = \left[\frac{E_s I_s}{E_s I_s + P_c + P_p + P_s}\right] \times 100$$

Step 32 Compute weight of primary winding.

$$W_p = \frac{L_p W_p}{12}$$

Step 33 Compute weight of secondary winding.

$$W_s = \frac{L_s W_s}{12}$$

Step 34 Compute total transformer weight.

$$W_T = W_p + W_s + W_c$$

The input conditions are fed into the computer for a particular transformer design and the computer prints out the values as shown below:

TRANSFORMER CHARACTERISTICS

Transformer Weight _____.
Efficiency _____%
Voltage Regulation _____%

	Primary	Secondary	
Power Loss	_____	_____	(watts)
Ac Resistance	_____	_____	(ohms)
Wire Length	_____	_____	(inches)

Core Loss _____ watts Core Side Length _____ inch
Core Weight _____ lb Core Inner Radius _____ inch
Number of Primary Layers = _____.

Layer	Number of Turns
1	_____
2	_____
N	_____

Number of Secondary Layers = _____.

Layer	Number of Turns
1	_____
2	_____
N	_____

The variation of transformer losses as a function of volts per turn ratio for a rectified output of 250 Vdc, 5 Vdc, and 1000 Vdc are shown in Figs. 32, 33, and 34, respectively. The curves present transformer losses using a 50 kHz square wave drive and Allen Bradley

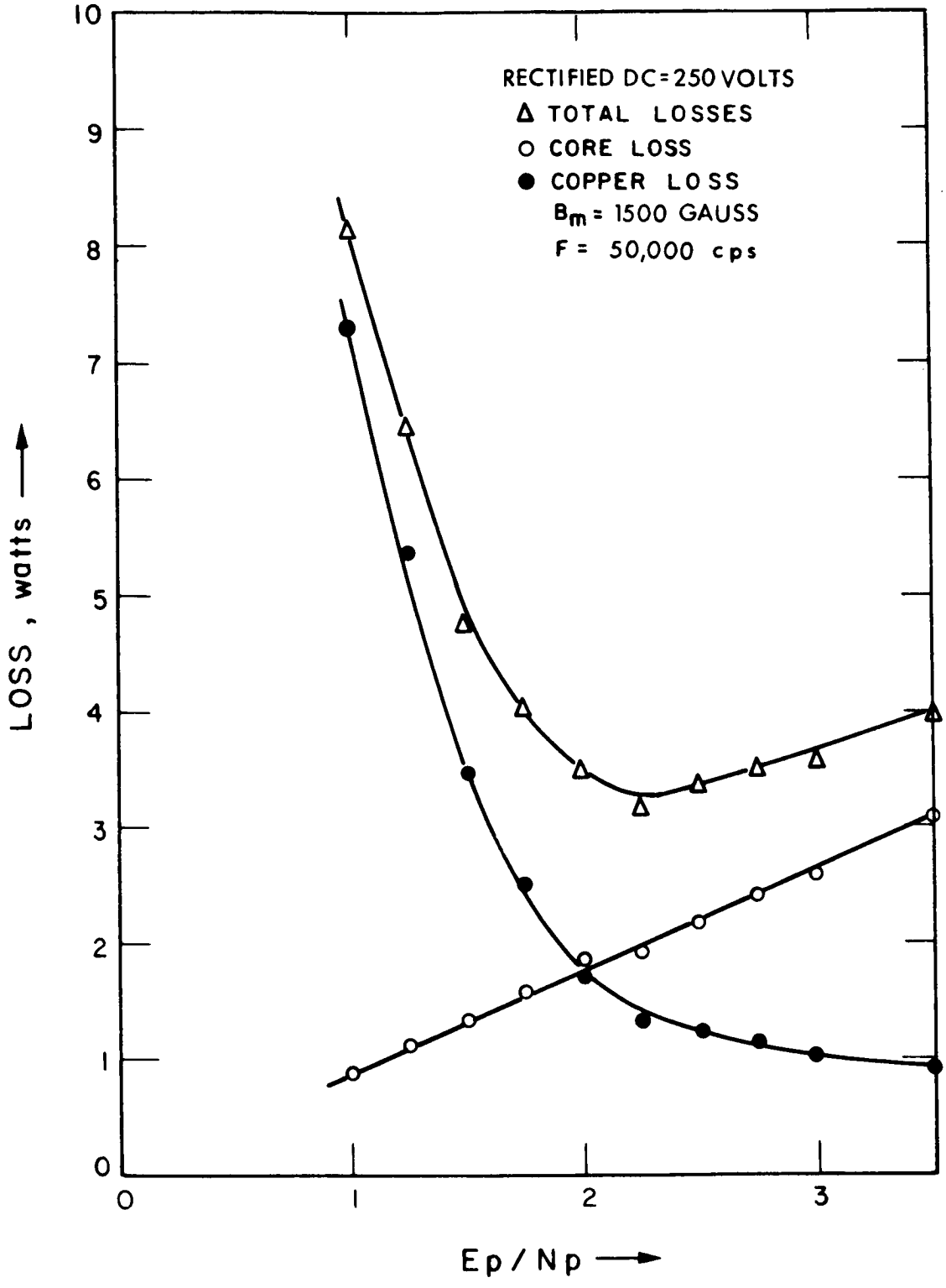

FIG. 32 TRANSFORMER LOSS VERSUS VOLT PER TURN RATIO

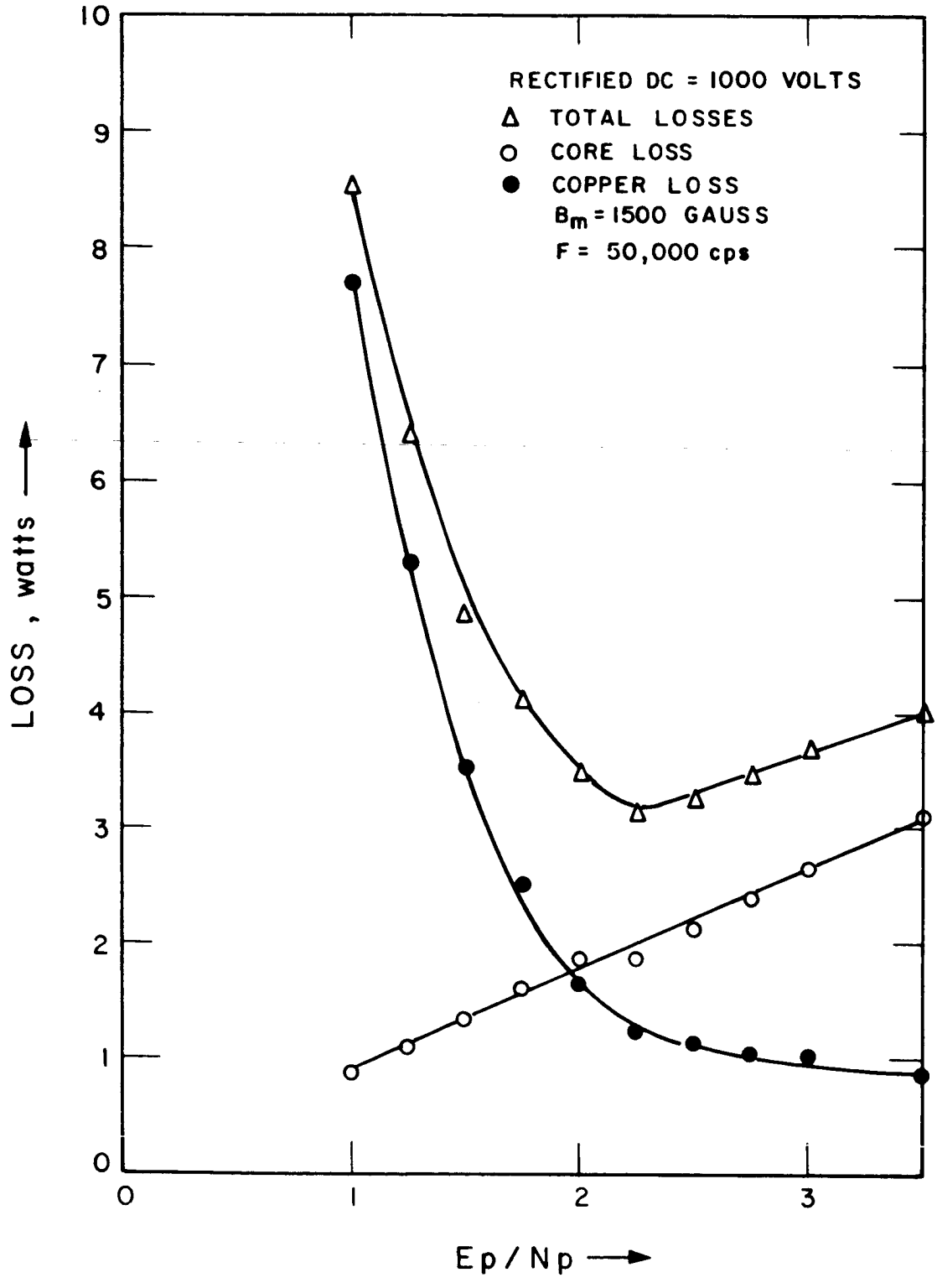

FIG. 33 TRANSFORMER LOSS VERSUS VOLT PER TURN RATIO

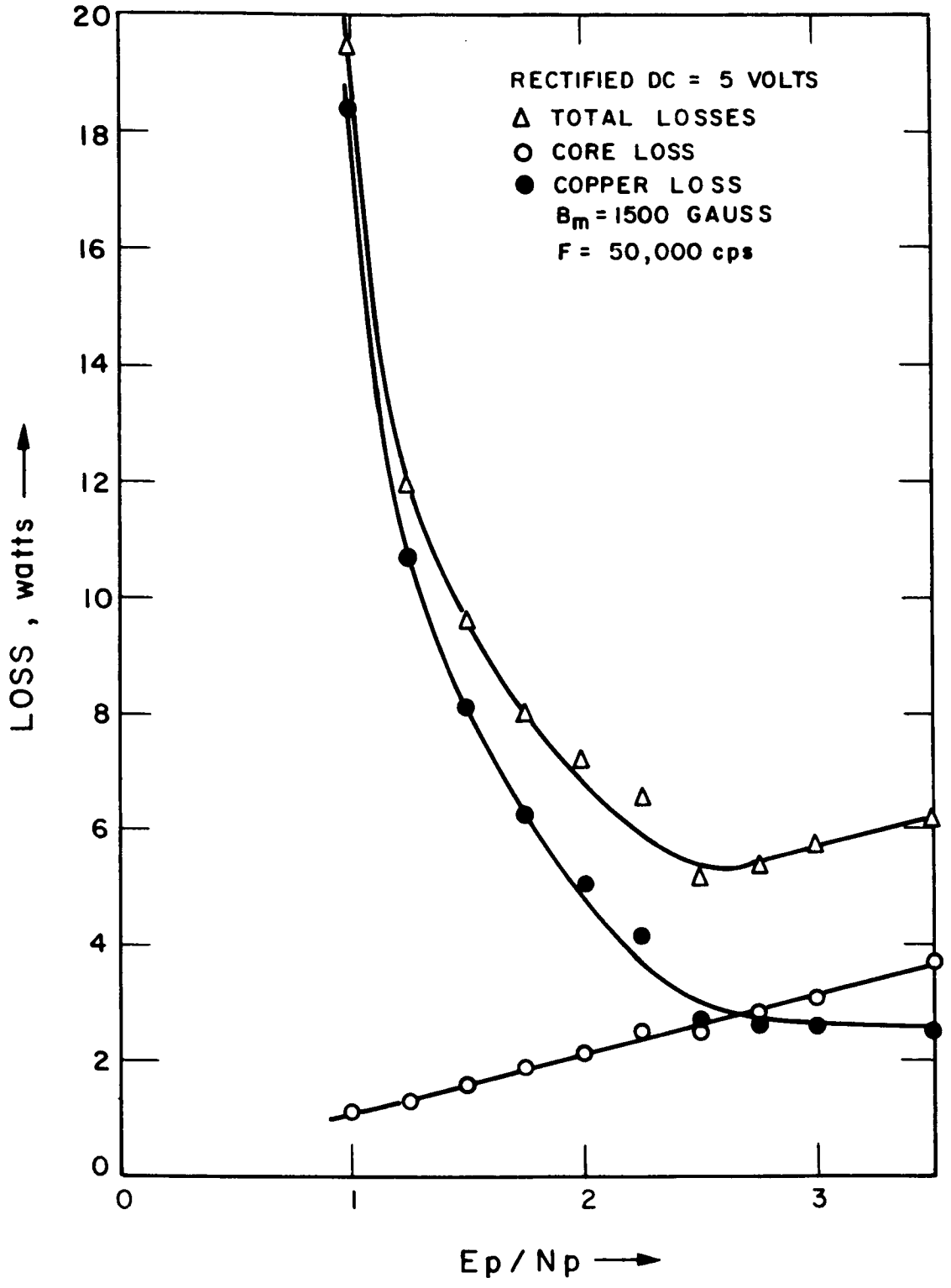

FIG. 34 TRANSFORMER LOSS VERSUS VOLT PER TURN RATIO

W-03 ferrite core material. Tables XI, XII, and XIII include additional weight, voltage regulation, and efficiency information - also as a function of the volts per turn ratio. The data is useful in selecting original design parameters as the first step toward transformer optimization.

As the drive frequency is increased, additional wire loss can occur, due to skin effect and proximity factor. Table XIV is a comparison of effective coil resistance using various wire gauges, coil configurations (1 or 2 layers), and frequencies (10 kHz and 50 kHz). It should be noted that coil losses can be minimized by incorporating small diameter wire in minimum layer winding configurations. Since a relative flat area of transformer loss exists around an optimum volt per turn ratio, some degree of freedom is left to the designer in the initial design considerations. As an example, consider the 5 volt transformer. A variation of 0.6 watt occurs between volt per turn ratios of 2.5 and 3 with voltage regulation steadily decreasing and weight steadily increasing (Table XI). Using 500 circular mils per amp to size and wires, a No. 16 gauge wire is selected for the primary winding and a No. 10 gauge wire is selected for the secondary winding. In light of the data presented in Table XIV, parallel connections of smaller diameter wire were made to optimize the 5 Vdc transformer about a volt per turn ratio of 3, as demonstrated in Table XV. The net effect was to reduce the effective coil resistance and inner diameter requirement of the core with an overall increase in efficiency and reduction in transformer weight.

A 5 Vdc output (rectified) transformer was fabricated per the improved transformer specifications listed in Table XV, with the following changes:

1. The primary winding was adjusted to a 36 turn total in two parallels to eliminate the half-turn relationship either side of center tap.
2. Number 20 gauge wire was used in place of number 19 gauge wire.

TABLE XI

TRANSFORMER DATA

E_p = 28 V E_s = 6 V F = 50 kc

E_p/N_p	Core Loss (w)	Copper Loss (w)	Transformer Loss (w)	z (%)	γ_r (%)	Weight (lb)
0.50	0.553	88.4347	88.9877	57.4	71.50	0.3206
1.00	1.067	20.9068	21.9738	84.5	15.60	0.2005
1.25	1.241	12.8699	14.1109	89.4	9.01	0.1586
1.50	1.522	9.9581	11.5801	91.25	6.82	0.1523
1.75	1.811	7.7060	9.5170	92.60	5.25	0.1488
2.00	2.107	6.5993	8.7063	93.30	4.25	0.1547
2.25	2.410	5.7483	8.1583	93.60	3.47	0.1619
2.50	2.473	3.7716	6.2446	94.10	2.23	0.1377
2.75	2.764	3.7512	6.5152	94.50	2.17	0.1451
3.00	3.060	3.7912	6.8512	94.50	2.17	0.1544
3.50	3.669	3.7717	7.4407	94.20	2.09	0.1710
4.00	4.299	3.7987	8.0977	93.75	2.06	0.1897

TABLE XII

TRANSFORMER DATA

E_p = 28 V E_s = 260 V F = 50 kc

E_p/N_p	Core Loss (w)	Copper Loss (w)	Transformer Loss (w)	z (%)	γ_r (%)	Weight (lb)
0.50	0.520	45.0157	45.5357	69.55	43.15	0.1588
1.00	0.857	7.3086	8.1656	92.72	7.01	0.0945
1.25	1.102	5.3588	6.4608	94.15	5.14	0.0927
1.50	1.305	3.4455	4.7505	95.63	3.30	0.0892
1.75	1.558	2.4960	4.0540	96.25	2.39	0.0932
2.00	1.818	1.6680	3.4860	96.76	1.60	0.0980
2.25	1.885	1.3023	3.1873	97.03	1.25	0.0955
2.50	2.136	1.1963	3.3296	96.90	1.15	0.1006
2.75	2.393	1.1292	3.5222	96.72	1.08	0.1069
3.00	2.558	1.0020	3.5600	96.69	0.96	0.1099
3.50	3.083	0.8977	3.9807	96.31	0.86	0.1239
4.00	3.629	0.8290	4.4580	95.89	0.80	0.1394

TABLE XIII

TRANSFORMER DATA

E_p = 28 V E_s = 1020 V F = 50 kc

E_p/N_p	Core Loss (w)	Copper Loss (w)	Transformer Loss (w)	z (%)	γ_r (%)	Weight (lb)
0.50	0.535	46.6495	47.1845	68.37	43.88	0.1725
1.00	0.888	7.7003	8.5883	92.23	7.25	0.1036
1.25	1.114	5.2922	6.4062	94.09	4.98	0.0973
1.50	1.337	3.5128	4.8498	95.46	3.31	0.0946
1.75	1.595	2.5094	4.1044	96.13	2.37	0.0980
2.00	1.860	1.6395	3.4995	96.68	1.55	0.1025
2.25	1.884	1.2286	3.1126	97.04	1.16	0.0977
2.50	2.135	1.1248	3.2598	96.90	1.06	0.1027
2.75	2.391	1.0578	3.4488	96.73	1.00	0.1088
3.00	2.654	1.0328	3.6868	96.51	0.98	0.1163
3.50	3.120	0.8839	4.0039	96.22	0.83	0.1271
4.00	3.671	0.8147	4.4857	95.79	0.77	0.1426

TABLE XIV

COMPARISON OF EFFECTIVE RESISTANCE

Wire Gauge	Frequency	Effective Resistance 1st Layer (R_{dl})*	Effective Resistance 2nd Layer (R_{dl})
#10	10 kc	2.95	15.75
#10	50 kc	6.64	33.50
#16	10 kc	1.35	3.86
#16	50 kc	3.27	17.50
#17	10 kc	1.22	2.85
#17	50 kc	2.85	15.40
#19	10 kc	1.09	1.82
#19	50 kc	2.25	10.80
#27	10 kc	1.00	1.01
#27	50 kc	1.05	1.35
#32	10 kc	1.00	1.00
#32	50 kc	1.00	1.03

*R_{dl} = f (gauge, length, temperature)

Note: The constants above were computed at a temperature of 105°C.

Reference: High Power, High Voltage, Audio Frequency, Transformer Design Manual, Navy Department Bureau of Ships, AD 60774, p. 323.

TABLE XV

SAMPLE OPTIMIZATION

Original Transformer		Improved Transformer	
Frequency	= 50 kHz	Frequency	= 50 kHz
Volts Per Turn	= 3	Volts Per Turn	= 3
Primary Winding		Primary Winding	
Voltage	= 28V peak	Voltage	= 28V peak
Current	= 4.25A	Current	= 4.25A
19 Turn Total #16 gage wire		38 Turn Total (2 parallels) #19 gage wire	
Resistance	= 0.0764 ohms	Resistance	= 0.0354 ohms
Secondary Winding		Secondary Winding	
Voltage	= 5.9V peak	Voltage	= 5.9V peak
Current	= 20A	Current	= 20A
4 Turn Total #10 gage wire		32 Turn Total (8 parallels) #19 gage wire	
Resistance	= 0.0060 ohms	Resistance	= 0.0023 ohms
Core		Core	
Material	= W-03 ferrite	Material	= W-03 ferrite
I.D.	= 0.7924 inch	I.D.	= 0.5810 inch
O.D.	= 1.5298 inch	O.D.	= 1.3784 inch
Height	= 0.3937 inch	Height	= 0.3937 inch
Losses		Losses	
Primary	= 1.3806 watts	Primary	= 0.6394 watts
Secondary	= 2.4106 watts	Secondary	= 0.9200 watts
Core	= 3.0600 watts	Core	= 2.6313 watts
Total	= 6.8512 watts	Total	= 4.1907 watts
Efficiency	= 94.5 percent	Efficiency	= 96.4 percent
Weight		Weight	
Wire	= 0.0455 lb	Wire	= 0.0455 lb
Core	= 0.0980 lb	Core	= 0.0842 lb
Total	= 0.1436 lb	Total	= 0.1297 lb

3. Ferroxcube 3E2A ferrite core material was used in place of Allen Bradley W-03 ferrite material.

Table XVI shows the basic characteristics of several ferroxcube materials.

Figure 35 shows the initial permeability (μ_o) versus frequency.

Figure 36 shows the loss factor $\left(\frac{\tan\delta}{\mu_o}\right)$ versus frequency.

Figure 37 shows the temperature effects on the initial permeability (μ_o).

Figure 38 shows the performance of Module No. 2 using the above transformer (T5-800) at approximately 50 and 90 kHz. The rectified voltages at the 100 watt level were 4.79 Vdc at 50 kHz and 4.37 Vdc at 90 kHz.

A second transformer (T4-900A) was fabricated in an attempt to raise the dc rectified voltage. The transformer used number 22 gauge wire throughout with 16 parallels on the secondary and 4 parallels on the primary. A volt per turn ratio of 2.33 was selected with a primary to secondary turns ratio of 4 to 1. Figure 39 shows the performance of Module No. 2 using the T5-900A transformer at square wave drive frequencies of approximately 50 to 90 kHz. The rectified voltages at the 100 watt level were 5.61 Vdc for 60 kHz and 5.27 Vdc for 90 kHz.

4.8 Prototype Modules

Upon completion of fabrication, the modules were subjected to operational tests in the laboratory. The following data was tabulated.

1. Prototype Module Efficiencies

Module	Efficiency at 100 Watts Output
No. 1	88.7 percent
No. 2	72.0 percent
No. 3	91.3 percent

2. Prototype Module Weights

Module	Weight (ounces)
No. 1	12.0
No. 2	25.6
No. 3	12.0

TABLE XVI

BASIC CHARACTERISTICS OF FERROXCUBE MATERIALS

Parameter	Material			
	3E2A	3E	3C5	4C4
μ_o minimum μ_o typical range	3500 4000-6000	2000 2200-3300	650 700-1400	100 100-125
B max, Gauss, typical	3600 at H = 2 Oers.	3000 at H = 2 Oers.	3600 at H = 2 Oers.	3000 at H = 10 Oers.
DC H_o Oersteds, typical	0.08	0.1	0.2	3.0
Curie Temperature, ^oC	$\geq$ 170	$\geq$ 125	$\geq$ 200	$\geq$ 300
Temperature Factor of μ_o	$+2 \times 10^{-6}$	$+4 \times 10^{-6}$	$+2 \times 10^{-6}$	0 to -10×10^{-6}
Temperature Range ^oC	$+20^o$ to $+70^oC$	$+20^o$ to $+50^oC$	$+20^o$ to $+50^oC$	$+20^o$ to $+55^oC$

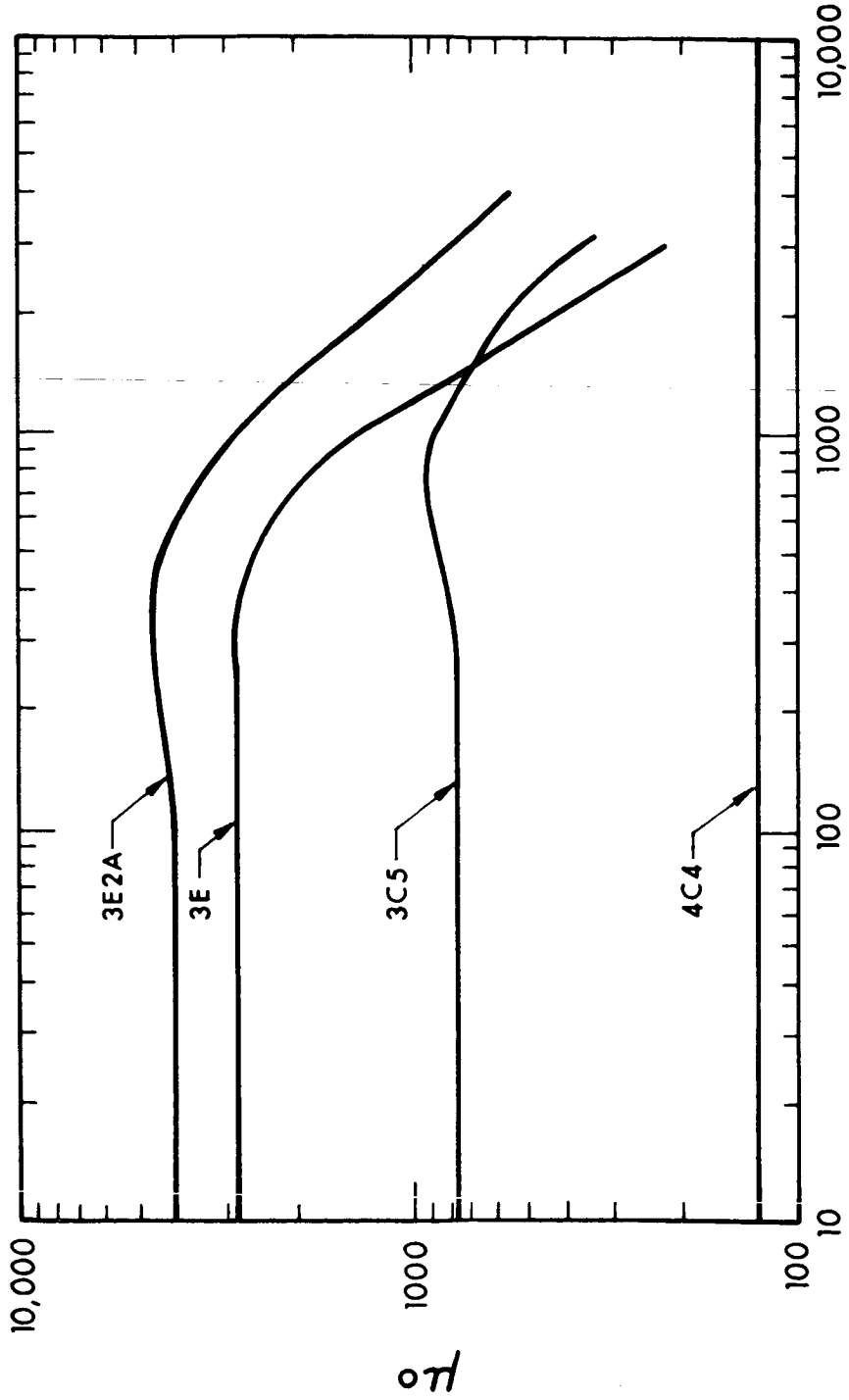

FIG. 35 INITIAL PERMEABILITY (μo) VERSUS FREQUENCY

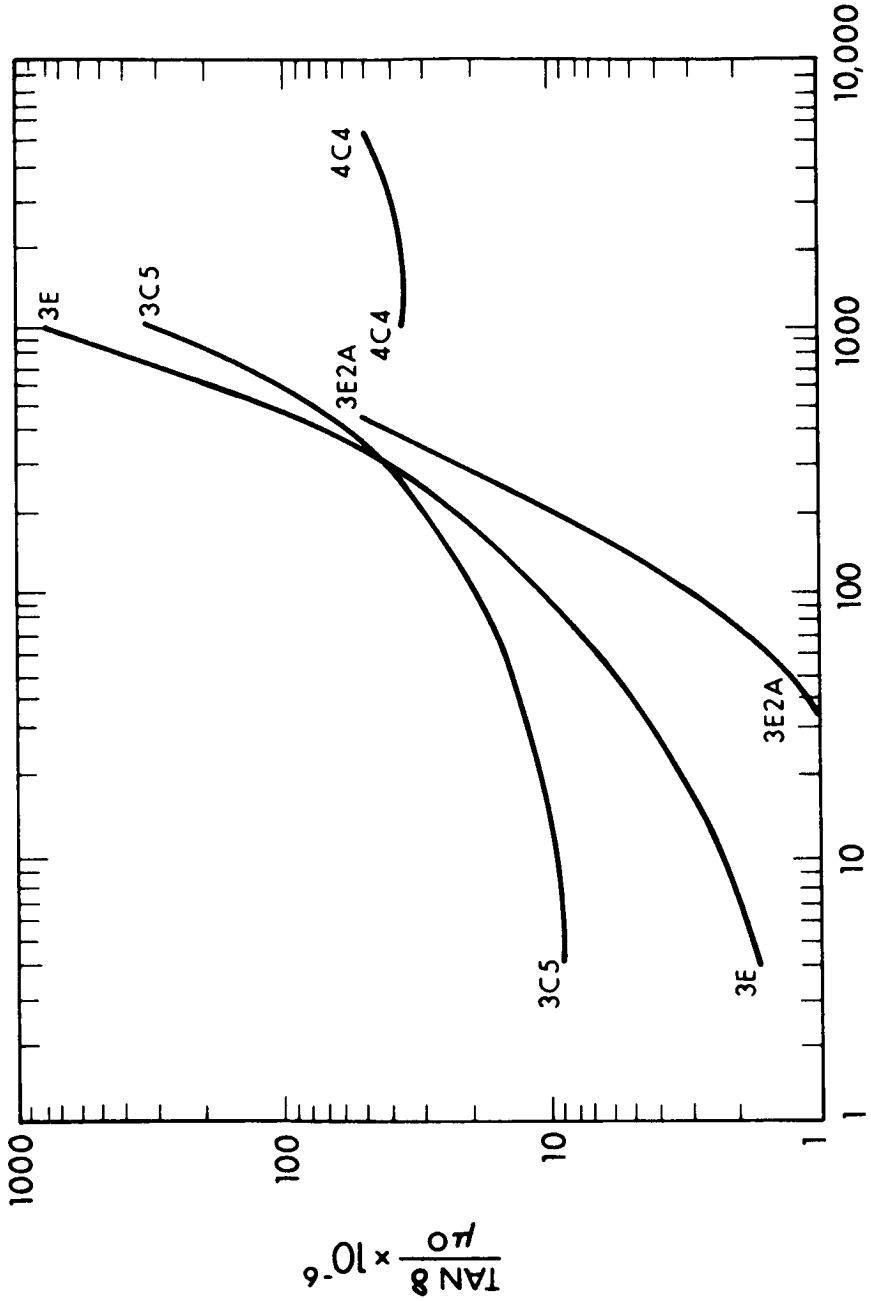

FIG. 36 LOSS FACTOR (tanδ/μo) VERSUS FREQUENCY

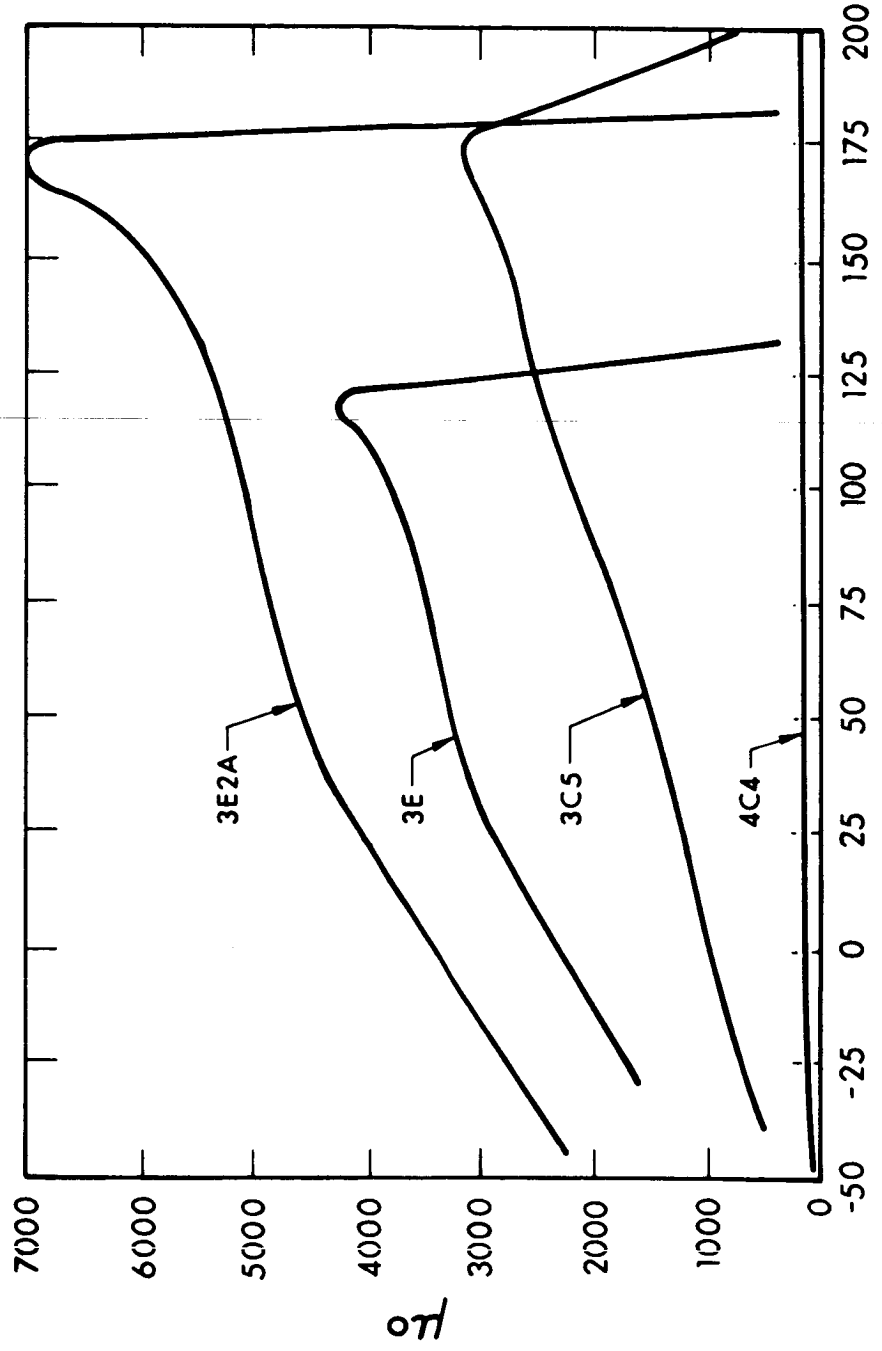

FIG. 37 INITIAL PERMEABILITY (μo) VERSUS TEMPERATURE

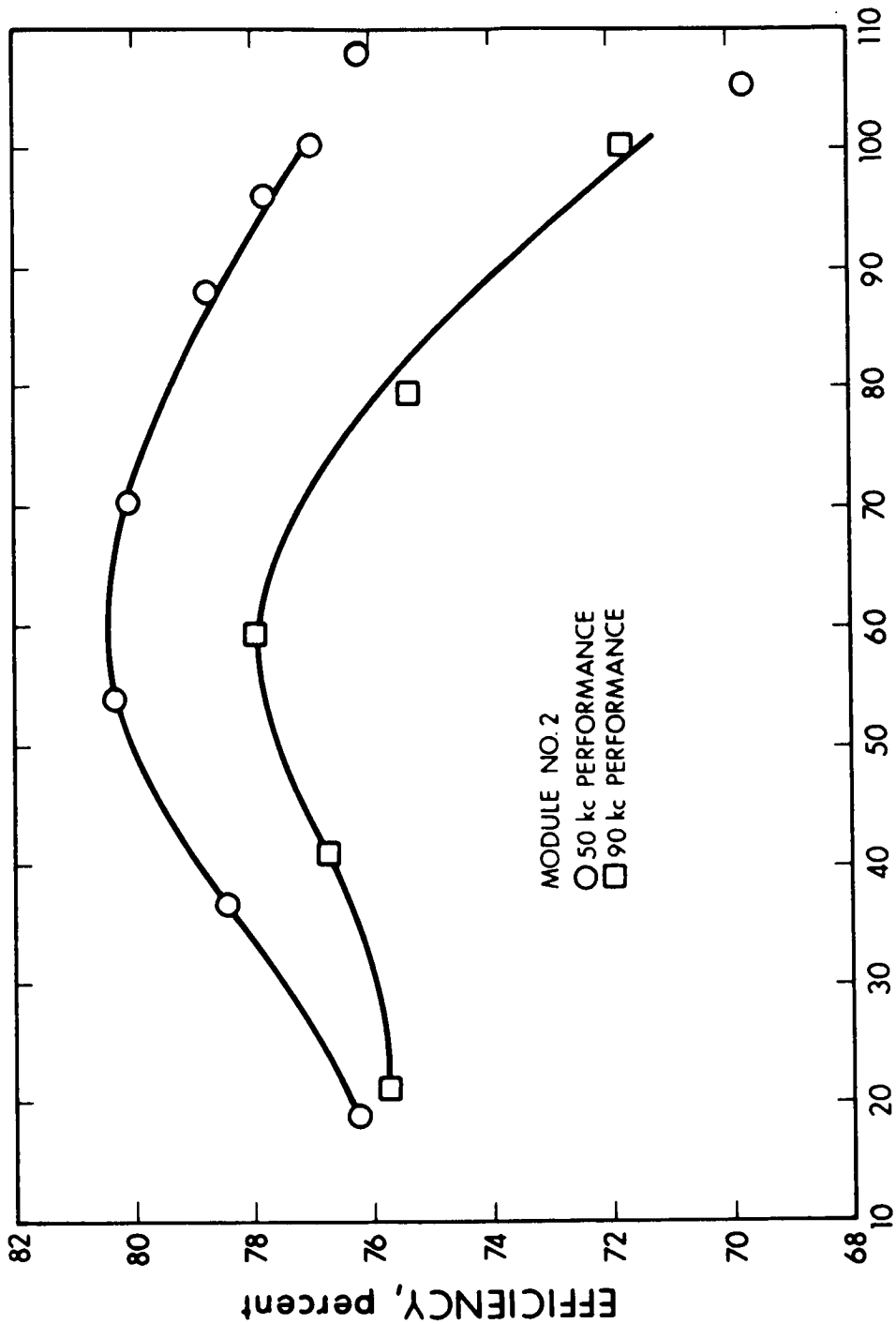

FIG. 38 MODULE NO. 2 PERFORMANCE

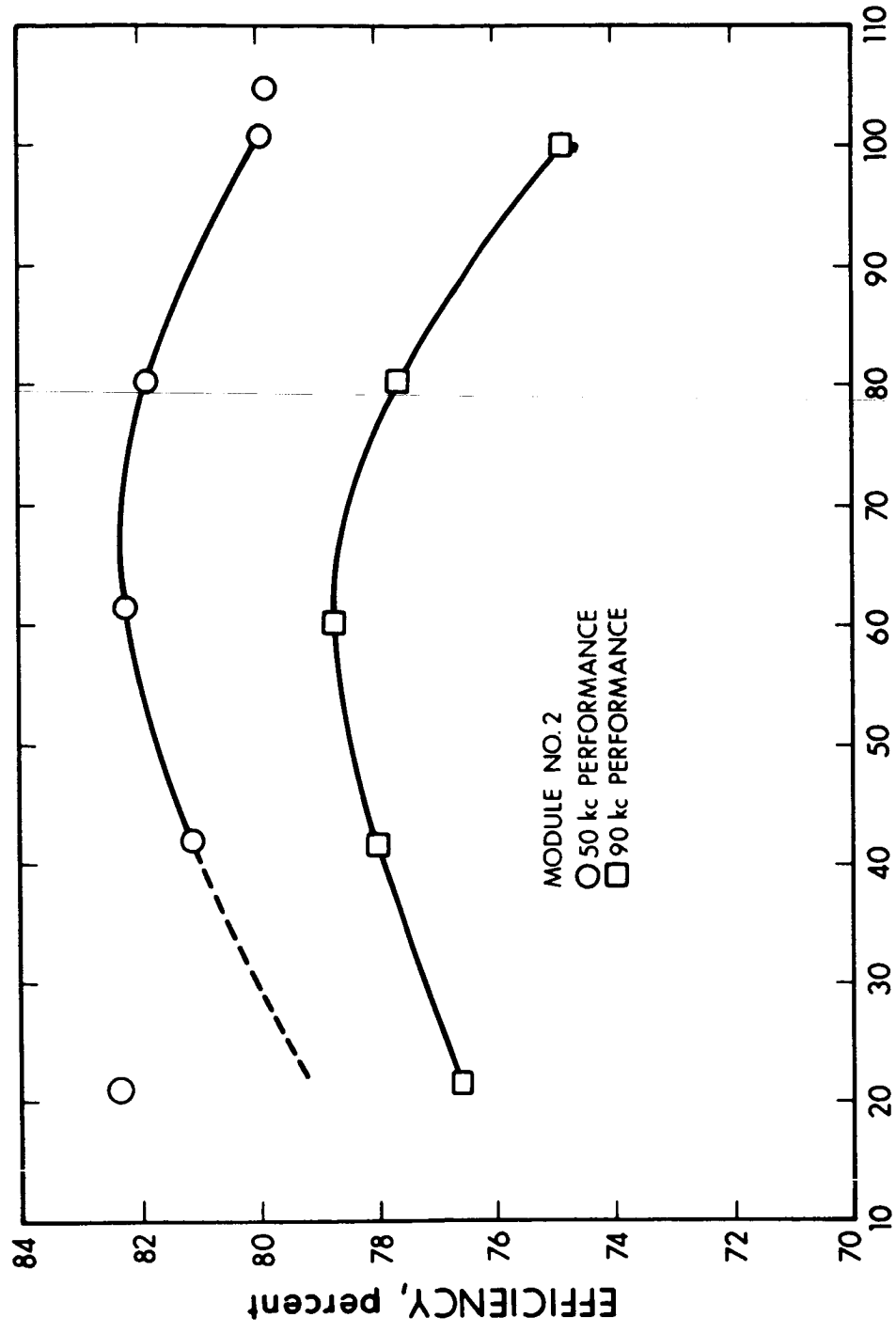

FIG. 39 MODULE NO. 2 IMPROVED PERFORMANCE

3. Prototype Module Sizes

Module	Size (L x W x H)
No. 1	4.75 x 5.25 x 1.50 inch
No. 2	11.83 x 5.25 x 1.50 inch
No. 3	4.75 x 5.25 x 1.50 inch

4.9 Prototype Final Test Data

Prototype Modules No. 1, No. 2 and No. 3 were subjected to the performance tests as outlined in paragraph 2 (testing specifications) of Appendix A (Design Objectives and Test Specifications) for the power conditioning modules) of the Work Authorization. These tests were conducted first at room pressure (760 torr) then in a vacuum of 10^{-4} torr or less.

Test No. 1

With the unit operating normally, but with no load, a dummy load of resistors and capacitors were connected to the output terminals of the module by means of a relay closure. Peak and average currents and voltage were measured on the switching transistors by means of oscilloscope photographs and meters to record the steady state and transient data. This test was conducted at a repetition rate of five times per minute for 1 hour without failure or measurable degradation in performance of the module.

Test No. 2

With the module operating at rated load, Test No. 1 was repeated in its entirety.

Test No. 3

With the module operating normally, but with no load, a potential of 10,000 Vdc was applied between input and output terminals and heat sinks for 10 minutes. The leakage currents with the dc potential of either polarity were recorded. There was no measurable degradation or failure due to this test.

Test No. 4

With the module operating into its rated load, Test No. 3 was repeated in its entirety.

4.9.1 Module No. 1

Module No. 1 was subjected to the tests described above and the results are tabulated in the following tables.

1. Room Temperature and Pressure Tests

Test No. 1 _____ Table XVII

Test No. 2 _____ Table XVIII

Test No. 3 _____ Table XIX

Test No. 4 _____ Table XX

2. Vacuum Tests

Test No. 1 _____ Table XXI

Test No. 2 _____ Table XXII

Test No. 3 _____ Table XXIII

Test No. 4 _____ Table XXIV

4.9.2 Module No. 2

Module No. 2 was subjected to the tests previously described and the results are tabulated below.

1. Room Temperature and Pressure Tests

Test No. 1 _____ Table XXV

Test No. 2 _____ Table XXVI

Test No. 3 _____ Table XXVII

Test No. 4 _____ Table XXVIII

2. Vacuum Tests

Test No. 1 _____ Table XXIX

Test No. 2 _____ Table XXX

Test No. 3 _____ Table XXXI

Test No. 4 _____ Table XXXII

4.9.3 Module No. 3

Module was subjected to the performance tests and the results are tabulated in the tables indicated below:

1. Room Temperature and Pressure Tests

   Test No. 1 _____ Table XXXIII

   Test No. 2 _____ Table XXXIV

   Test No. 3 _____ Table XXXV

   Test No. 4 _____ Table XXXVI

2. Vacuum Tests

   Test No. 1 _____ Table XXXVII

   Test No. 2 _____ Table XXXVIII

   Test No. 3 _____ Table XXXIX

   Test No. 4 _____ Table XL

4.10 Packaging and Thermal Design

4.10.1 Thermal Design Philosophy

The modules are designed to operate on the exterior of a spacecraft without protection from sunlight and without internal pressurization. They must also be thermally isolated from the spacecraft interior. To meet these design requirements, all three modules have followed the same basic configuration: a flat base plate with a white painted exterior surface which acts as a radiator, and to which all heat producing components are mounted, and a polished, double walled deep drawn aluminum cover plate. A discussion of package sizing and other thermal and mechanical design considerations is given below.

Module dimensions are governed by the area required for effective heat dissipation and by the space required inside the package to eliminate high voltage arcing. The overall package size is 4.75 x 5.25 x 1.50 inches for Modules No. 1 and No. 3 and 5.25 x 11.83 x 1.50 inches for Module No. 2. A picture of Modules 1 and 3 is shown in Fig. 40.

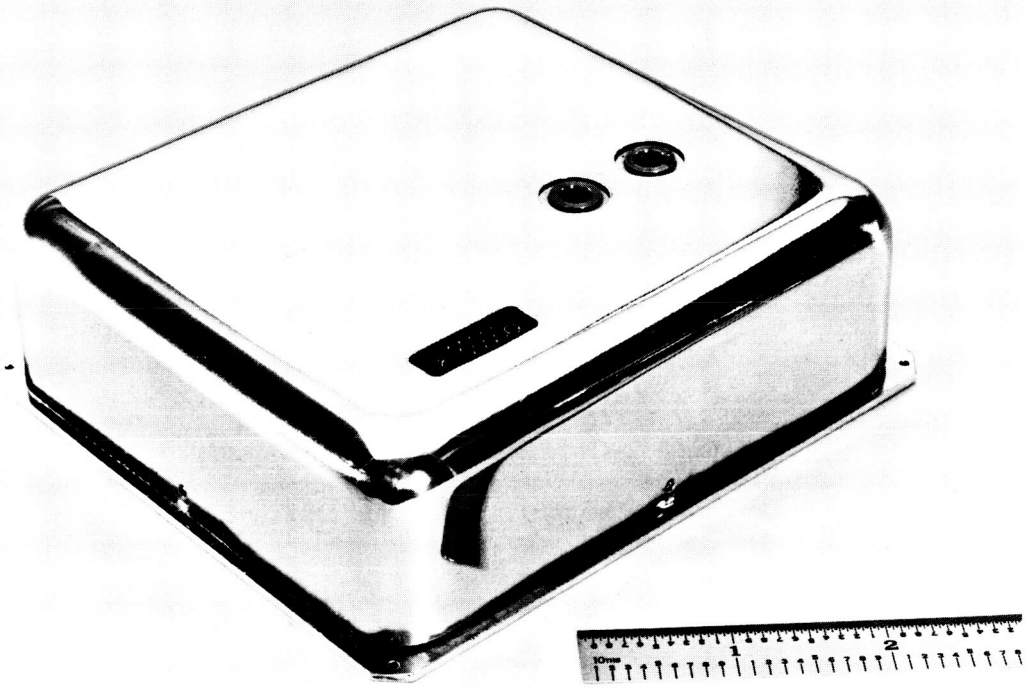

FIG. 40 MODULE NO. 1

DATE 7-13-66

TECH. O. DIVERS

ENGR. P. RAMIREZ

Q.C. E. SHOCKLEY

TABLE XVII

MODULE # 1 TEST DATA SHEET (NAS-37926)

1. Test Conditions: NORMAL TEMPERATURE AND PRESSURE (760 mm Hg)
2. Test No. 1 (No Load)

Test Data (Beginning of Test)

Load Condition	INPUT			OUTPUT		
	Voltage	Current	Ripple	Voltage	Current	Ripple
	VDC	AMPS	VPP	VDC	AMPS	VPP
NL	28.02	0.215	0.7	358.0	0.0	0.1
50%	28.02	2.0	0.8	263.9	0.185	5.0
100%	27.99	3.92	1.2	254.6	0.380	10.0
125%	28.04	5.15	1.0	250.8	0.500	12.0
Short Circuit	28.02	0.420	0.3	0.0	0.0	0.0

Test Data (End of 1 Hour Test)

Load Condition		INPUT		OUTPUT		
	Voltage	Current	Ripple	Voltage	Current	Ripple
	VDC	AMPS	VPP	VDC	AMPS	VPP
NL	28.00	0.205	0.7	342.7	0.0	0.1
50%	28.02	2.0	0.8	263.7	0.184	7.0
100%	28.02	3.92	.2	255.0	0.380	10.0
125%	28.00	5.15	1.3	250.4	0.500	14.0
Short Circuit	28.02	0.54	0.3	0.0	0.0	0.0

DATE 7-13-66

TECH. O. DIVERS

ENGR. P. RAMIREZ

Q.C. E. SHOCKLEY

TABLE XVIII

MODULE # 1 TEST DATA SHEET (NAS-37926)

1. Test Conditions: NORMAL TEMPERATURE AND PRESSURE (760 mm Hg)
2. Test No. 2 (Rated Load)

Test Data (Beginning of Test)

Load Condition	INPUT			OUTPUT		
	Voltage	Current	Ripple	Voltage	Current	Ripple
	VDC	AMPS	VPP	VDC	AMPS	VPP
100%	28.04	3.92	1.20	255.0	0.380	10.0
110%	28.01	4.39	1.35	253.0	0.425	12.0
115%	28.02	4.68	1.35	251.2	0.452	13.0
125%	27.98	5.10	1.40	250.0	0.492	13.0
Short Circuit	27.97	0.58	0.30	0.0	0.0	0.0

Test Data (End of 1 Hour Test)

Load Condition	INPUT			OUTPUT		
	Voltage	Current	Ripple	Voltage	Current	Ripple
	VDC	AMPS	VPP	VDC	AMPS	VPP
100%	28.03	3.85	1.25	254.4	0.375	10.0
110%	28.01	4.33	1.30	251.5	0.420	12.0
115%	27.97	4.68	1.35	249.8	0.450	14.0
125%	28.00	5.10	1.35	249.0	0.492	12.0
Short Circuit	27.96	0.65	0.3	0.0	0.0	0.0

DATE 7-13-66

TECH. O. DIVERS

ENGR. P. RAMIREZ

Q.A. E. SHOCKLEY

TABLE XIX

MODULE # 1 TEST DATA SHEET (NAS-37926)

1. Test Condition: NORMAL TEMPERATURE AND PRESSURE (760 mm Hg)

2. Test No. 3 (No Load and 10,000 Vdc)

HI-POT TEST

Circuit and Polarity	Leakage Current μ Amps
+ - Input to Output	0.5
+ - Output to Heat Sink	0.0
- + Input to Output	0.0
- + Output to Hink Sink	0.5

DATE 7-13-66

TECH. O. DIVERS

ENGR. P. RAMIREZ

Q.A. E. SHOCKLEY

TABLE XX

MODULE # 1 TEST DATA SHEET (NAS 3-7926)

1. Test Condition: NORMAL TEMPERATURE AND PRESSURE (760 mm Hg)
2. Test No. 4 (Rated Load and 10,000 Vdc)

HI-POT TEST

Circuit and Polarity	Leakage Current μ Amps
+ - Input to Output	2.5
+ - Output to Heat Sink	0.0
- + Input to Output	0.0
- + Output to Heat Sink	2.5

DATE 7-20-66

TECH. O. DIVERS

ENGR. P. RAMIREZ

Q.C. E. SHOCKLEY

TABLE XXI

MODULE # 1 TEST DATA SHEET (NAS-37926)

1. Test Conditions: VACUUM (10^{-4} TORR OR LESS)
2. Test No. 1 (No Load)

Test Data (Beginning of Test)

Load Condition	INPUT			OUTPUT		
	Voltage	Current	Ripple	Voltage	Current	Ripple
	VDC	AMPS	VPP	VDC	AMPS	VPP
NL	28.05	0.22	0.20	369.8	0	0.05
50%	28.05	2.00	0.30	262.3	0.184	2.20
100%	28.04	3.92	0.80	253.2	0.370	10.0
125%	28.03	5.20	0.90	250.0	0.485	13.0
Short Circuit	28.57	0.46	0.30	0	0	0

Test Data (End of 1 Hour Test)

Load Condition		INPUT			OUTPUT	
	Voltage	Current	Ripple	Voltage	Current	Ripple
	VDC	AMPS	VPP	VDC	AMPS	VPP
NL	28.60	0.228	0.50	378.6	0	0.05
50%	28.01	2.00	0.25	262.9	0.186	2.00
100%	28.00	3.90	0.50	252.6	0.380	6.00
125%	28.00	5.00	0.60	244.2	0.485	10.00
Short Circuit	28.50	0.410	0.20	0	0.015	0

DATE 8-3-66

TECH. O. DIVERS

ENGR. P. RAMIREZ

Q.C. J. LEE

TABLE XXII

MODULE #1 TEST DATA SHEET (NAS-37926)

1. Test Conditions: VACUUM (10⁻⁴ TORR OR LESS)
2. Test No. 2 (Rated Load)

Test Data (Beginning of Test)

Load Condition	INPUT			OUTPUT		
	Voltage	Current	Ripple	Voltage	Current	Ripple
	VDC	AMPS	VPP	VDC	AMPS	VPP
100%	28.01	3.90	0.80	255.3	0.385	10.0
110%	27.93	4.30	0.90	253.0	0.422	10.0
115%	28.11	4.65	1.00	253.8	0.458	11.0
125%	28.06	5.05	1.00	251.8	0.500	11.0
Short Circuit	28.71	0.49	0.30	0.90	0	0

Test Data (End of 1 Hour Test)

Load Condition	INPUT			OUTPUT		
	Voltage	Current	Ripple	Voltage	Current	Ripple
	VDC	AMPS	VPP	VDC	AMPS	VPP
100%	28.00	3.90	0.80	254.2	0.380	8.0
110%	27.94	4.35	0.80	252.4	0.425	10.0
115%	28.08	4.70	1.00	252.8	0.460	11.0
125%	28.04	5.08	1.10	250.2	0.495	11.5
Short Circuit	28.65	0.58	0.30	0.70	0	0

DATE 8-4-66

TECH. O. DIVERS

ENGR. D. RAMIREZ

Q.A. J. LEE

TABLE XXIII

MODULE # 1 TEST DATA SHEET (NAS-37926)

1. Test Condition: VACUUM (10^{-4} TORR OR LESS)

2. Test No. 3 (No Load and 10,000 Vdc)

HI-POT TEST

Circuit and Polarity	Leakage Current μ Amps
+ - Input to Output	8.0
+ - Output to Heat Sink	0.5
- + Input to Output	0.5
- + Output to Hink Sink	8.0

DATE 8-15-66
TECH. O. DIVERS
ENGR. D. RAMIREZ
Q.A. J. LEE

TABLE XXIV

MODULE # 1 TEST DATA SHEET (NAS 3-7926)

1. Test Condition: VACUUM (10^{-4} TORR OR LESS)
2. Test No. 4 (Rated Load and 10,000 Vdc)

HI-POT TEST

Circuit and Polarity	Leakage Current μ Amps
+ Input to Output -	8.0
+ Output to Heat Sink -	0.5
- Input to Output +	0.5
- Output to Heat Sink +	8.0

DATE 6-28-66

TECH. O. DIVERS

ENGR. D. RAMIKER

Q.C. S. LEE

TABLE XXV

MODULE #2 TEST DATA SHEET (NAS-37926)

1. Test Conditions: NORMAL TEMPERATURE AND PRESSURE (760 mm Hg)
2. Test No. 1 (No Load)

Test Data (Beginning of Test)

Load Condition	INPUT			OUTPUT		
	Voltage	Current	Ripple	Voltage	Current	Ripple
	VDC	AMPS	VPP	VDC	AMPS	VPP
NL	27.99	0.194	0.50	8.85	0.	0.004
50%	28.00	2.16	0.50	5.80	8.0	0.40
100%	28.02	5.05	0.70	5.156	19.7	1.00
125%	28.02	6.30	0.70	4.88	24.2	1.30
Short Circuit	28.01	0.21	0.40	0	0	0

Test Data (End of 1 Hour Test)

Load Condition		INPUT		OUTPUT		
	Voltage	Current	Ripple	Voltage	Current	Ripple
	VDC	AMPS	VPP	VDC	AMPS	VPP
NL	28.01	0.193	0.50	8.805	0	0.004
50%	28.00	2.24	0.60	5.774	8.10	0.30
100%	28.00	5.00	0.60	5.159	19.4	1.00
125%	28.00	6.15	0.70	4.97	23.5	1.20
Short Circuit	28.01	0.22	0.4	0	0	0

DATE 6-[illegible]-[illegible]

TECH. O. DIXELS

ENGR. D. RAMIREZ

Q.C. J. LEE

TABLE XXVI

MODULE # 2 TEST DATA SHEET (NAS-37926)

1. Test Conditions: NORMAL TEMPERATURE AND PRESSURE (760 mm Hg)
2. Test No. 2 (Rated Load)

Test Data (Beginning of Test)

Load Condition	INPUT			OUTPUT		
	Voltage	Current	Ripple	Voltage	Current	Ripple
	VDC	AMPS	VPP	VDC	AMPS	VPP
100%	28.00	5.20	0.60	5.13	20.2	0.50
110%	28.00	5.90	0.65	4.84	22.5	0.75
115%	28.00	6.15	0.70	4.86	23.6	0.75
125%	28.00	6.65	0.75	4.63	26.0	0.75
Short Circuit	28.00	0.22	0.20	0	0	0

Test Data (End of 1 Hour Test)

Load Condition	INPUT			OUTPUT		
	Voltage	Current	Ripple	Voltage	Current	Ripple
	VDC	AMPS	VPP	VDC	AMPS	VPP
100%	28.00	5.20	0.60	5.135	20.0	0.50
110%	28.00	5.90	0.65	4.895	22.4	1.5
115%	28.00	6.05	0.70	4.755	23.2	1.0
125%	28.00	6.90	0.70	4.52	26.0	1.2
Short Circuit	28.00	0.23	0.30	0	0	0

DATE 6-27-66

TECH. O. DIVERS

ENGR. D. RAMIREZ

Q.A. J. LEE

TABLE XXVII

MODULE # 2 TEST DATA SHEET (NAS-37926)

1. Test Condition: NORMAL TEMPERATURE AND PRESSURE (760 mm Hg)

2. Test No. 3 (No Load and 10,000 Vdc)

HI-POT TEST

Circuit and Polarity	Leakage Current μ Amps
+ - Input to Output	0
+ - Output to Heat Sink	0
- + Input to Output	0
- + Output to Hink Sink	0

DATE 6-27-66

TECH. G. DIVERS

ENGR. D. RAMIREZ

Q.A. J. LEE

TABLE XXVIII

MODULE # 2 TEST DATA SHEET (NAS 3-7926)

1. Test Condition: NORMAL TEMPERATURE AND PRESSURE (760 mm Hg)
2. Test No. 4 (Rated Load and 10,000 Vdc)

HI-POT TEST

Circuit and Polarity	Leakage Current μ Amps
+ - Input to Output	0
+ - Output to Heat Sink	0
- + Input to Output	0
- + Output to Heat Sink	0

DATE 7-18-66

TECH. O. DIVERS

ENGR. P. RAMIREZ

Q.C. J. LEE

TABLE XXIX

MODULE # 2 TEST DATA SHEET (NAS-37926)

1. Test Conditions: VACUUM (10^{-4} TORR OR LESS)
2. Test No. 1 (No Load)

Test Data (Beginning of Test)

Load Condition	INPUT			OUTPUT		
	Voltage	Current	Ripple	Voltage	Current	Ripple
	VDC	AMPS	VPP	VDC	AMPS	VPP
NL	28.10	0.23	0.40	8.80	0	0
50%	28.03	2.10	0.50	5.77	8.0	0.20
100%	28.06	4.50	0.60	5.24	17.5	0.60
125%	27.97	5.80	0.70	4.99	22.5	0.60
Short Circuit	28.40	0.32	0.30	0	0	0

Test Data (End of 1 Hour Test)

Load Condition		INPUT			OUTPUT	
	Voltage	Current	Ripple	Voltage	Current	Ripple
	VDC	AMPS	VPP	VDC	AMPS	VPP
NL	28.09	0.19	0.40	8.62	0	0
50%	28.09	2.18	0.60	5.77	8.2	0.15
100%	27.99	4.72	0.70	5.11	18.9	0.80
125%	28.02	5.50	0.70	4.94	22.0	0.70
Short Circuit	28.08	0.30	0.30	0	0	0

DATE 7-29-66

TECH. D. DIVERS

ENGR. P. RAMIREZ

Q.C. E. SHOCKLEY

TABLE XXX

MODULE #2 TEST DATA SHEET (NAS-37926)

1. Test Conditions: VACUUM (10^{-4} TORR OR LESS)
2. Test No. 2 (Rated Load)

Test Data (Beginning of Test)

Load Condition	INPUT			OUTPUT		
	Voltage	Current	Ripple	Voltage	Current	Ripple
	VDC	AMPS	VPP	VDC	AMPS	VPP
100%	29.08	4.95	0.30	5.24	19.3	0.50
110%	29.04	5.60	0.30	5.09	22.2	0.60
115%	28.97	6.10	0.30	4.96	24.0	0.70
125%	28.90	6.55	0.40	4.82	26.0	0.60
Short Circuit	29.50	0.32	0.50	0.06	0	0

Test Data (End of 1 Hour Test)

Load Condition	INPUT			OUTPUT		
	Voltage	Current	Ripple	Voltage	Current	Ripple
	VDC	AMPS	VPP	VDC	AMPS	VPP
100%	29.10	5.10	0.30	5.20	19.6	0.60
110%	29.05	5.75	0.30	5.03	22.3	0.60
115%	29.00	6.20	0.30	4.90	24.0	0.70
125%	28.96	6.60	0.30	4.74	26.3	0.51
Short Circuit	29.50	0.40	0.50	0.04	0	0

DATE 7-28-66

TECH. O. DIVERS

ENGR. D. RAMIREZ

Q.A. J. LEE

TABLE XXXI

MODULE # 2 TEST DATA SHEET (NAS-37926)

1. Test Condition: VACUUM (10^{-4} TORR OR LESS)

2. Test No. 3 (No Load and 10,000 Vdc)

HI-POT TEST

Circuit and Polarity	Leakage Current μ Amps
+ - Input to Output	1.4
+ - Output to Heat Sink	0.2
- + Input to Output	0.2
- + Output to Hink Sink	1.4

DATE 7-28-66

TECH. O. DIVERS

ENGR. P. RAMIREZ

Q.A. J. LEE

TABLE XXXII

MODULE # 2 TEST DATA SHEET (NAS 3-7926)

1. Test Condition: VACUUM (10^{-4} TORR OR LESS)
2. Test No. 4 (Rated Load and 10,000 Vdc)

HI-POT TEST

Circuit and Polarity	Leakage Current μ Amps
+ - Input to Output	2.0
+ - Output to Heat Sink	2.0
- + Input to Output	2.0
- + Output to Heat Sink	2.0

DATE 7-12-66

TECH. O. DIVERS

ENGR. D. RAMIREZ

Q.C. J. LEE

TABLE XXXIII

MODULE #3 TEST DATA SHEET (NAS-37926)

1. Test Conditions: NORMAL TEMPERATURE AND PRESSURE (160 mm Hg)
2. Test No. 1 (No Load)

Test Data (Beginning of Test)

Load Condition	INPUT			OUTPUT		
	Voltage	Current	Ripple	Voltage	Current	Ripple
	VDC	AMPS	VPP	VDC	AMPS	VPP
NL	28.02	0.345	0.80	2200.0	0	4.00
50%	28.00	2.01	0.70	1080.0	0.0469	50.0
100%	28.02	3.92	0.80	1045.0	0.0972	60.0
125%	28.04	5.09	0.90	1015.0	0.126	85.0
Short Circuit	28.02	0.274	0.30	0	0	0

Test Data (End of 1 Hour Test)

Load Condition		INPUT		OUTPUT		
	Voltage	Current	Ripple	Voltage	Current	Ripple
	VDC	AMPS	VPP	VDC	AMPS	VPP
NL	28.01	0.342	0.80	2165.0	0	4.0
50%	28.01	2.01	0.70	1065.0	0.0465	50.0
100%	27.97	3.92	0.80	1040.0	0.0972	60.0
125%	27.96	5.06	0.90	1020.0	0.126	85.0
Short Circuit	28.00	0.282	0.30	0	0	0

DATE 7-13-66

TECH. C. [illegible]

ENGR. P. RAMIREZ

Q.C. J. LEE

TABLE XXXIV

MODULE #3 TEST DATA SHEET (NAS-37926)

1. Test Conditions: NORMAL TEMPERATURE AND PRESSURE (760 mm Hg)
2. Test No. 2 (Rated Load)

Test Data (Beginning of Test)

Load Condition	INPUT			OUTPUT		
	Voltage	Current	Ripple	Voltage	Current	Ripple
	VDC	AMPS	VPP	VDC	AMPS	VPP
100%	28.02	3.90	0.70	1035.0	0.097	80.0
110%	27.98	4.35	0.90	1025.0	0.106	50.0
115%	27.97	4.50	0.90	1020.0	0.111	60.0
125%	28.00	5.05	1.0	1015.0	0.124	85.0
Short Circuit	28.03	0.277	0.30	0	0	0

Test Data (End of 1 Hour Test)

Load Condition	INPUT			OUTPUT		
	Voltage	Current	Ripple	Voltage	Current	Ripple
	VDC	AMPS	VPP	VDC	AMPS	VPP
100%	28.03	3.90	0.70	1035.0	0.0965	80.0
110%	27.99	4.32	0.80	1025.0	0.107	55.0
115%	27.98	4.52	0.80	1020.0	0.112	60.0
125%	28.01	5.05	0.90	1015.0	0.125	85.0
Short Circuit	28.04	0.285	0.30	0	0	0

DATE 7-13-66

TECH. O. DIVERS

ENGR. D. RAMIREZ

Q.A. J. LEE

TABLE XXXV

MODULE # 3 TEST DATA SHEET (NAS-37926)

1. Test Condition: NORMAL TEMPERATURE AND PRESSURE (760 mm Hg)

2. Test No. 3 (No Load and 10,000 Vdc)

HI-POT TEST

Circuit and Polarity	Leakage Current μ Amps
+ - Input to Output	1.0
+ - Output to Heat Sink	0
- + Input to Output	0
- + Output to Hink Sink	1.0

DATE 7-13-66

TECH. O. DIVERS

ENGR. D. RAMIREZ

Q.A. J. LEE

TABLE XXXVI

MODULE # 3 TEST DATA SHEET (NAS 3-7926)

1. Test Condition: NORMAL TEMPERATURE AND PRESSURE (760 mm Hg)
2. Test No. 4 (Rated Load and 10,000 Vdc)

HI-POT TEST

Circuit and Polarity	Leakage Current μ Amps
+ - Input to Output	1.0
+ - Output to Heat Sink	0
- + Input to Output	0
- + Output to Heat Sink	1.0

DATE 8-8-66

TECH. O. DIVELS

ENGR. P. RAMIREZ

Q.C. N. GOOD

TABLE XXXVII

MODULE #3 TEST DATA SHEET (NAS-37926)

1. Test Conditions: VACUUM (10^{-4} TORR OR LESS)
2. Test No. 1 (No Load)

Test Data (Beginning of Test)

Load Condition	INPUT			OUTPUT		
	Voltage	Current	Ripple	Voltage	Current	Ripple
	VDC	AMPS	VPP	VDC	AMPS	VPP
NL	28.65	0.365	0.40	2160.0	0	8.00
50%	28.38	2.02	0.40	1075.0	0.046	50.0
100%	28.10	3.82	0.50	1040.0	0.097	60.0
125%	27.94	4.94	0.60	1010.0	0.124	100.0
Short Circuit	28.68	0.145	0.30	0	0	0

Test Data (End of 1 Hour Test)

Load Condition	INPUT			OUTPUT		
	Voltage	Current	Ripple	Voltage	Current	Ripple
	VDC	AMPS	VPP	VDC	AMPS	VPP
NL	28.63	0.39	0.40	2170.0	0	10.0
50%	28.36	2.02	0.40	1075.0	0.0465	40.0
100%	28.10	3.90	0.50	1040.0	0.096	70.0
125%	27.92	4.95	0.60	1010.0	0.124	100.0
Short Circuit	28.66	0.154	0.30	0	0	0

DATE 8-8-66

TECH. C. DIAZ

ENGR. P. RAMIREZ

Q.C. N. GOOD

TABLE XXXVIII

MODULE #3 TEST DATA SHEET (NAS-37926)

1. Test Conditions: VACUUM (10^{-4} TORR OR LESS)
2. Test No. 2 (Rated Load)

Test Data (Beginning of Test)

Load Condition	INPUT			OUTPUT		
	Voltage	Current	Ripple	Voltage	Current	Ripple
	VDC	AMPS	VPP	VDC	AMPS	VPP
100%	28.16	3.92	0.60	1040.0	0.096	70.0
110%	28.12	4.30	0.50	1035.0	0.105	80.0
115%	28.09	4.40	0.60	1028.0	0.112	86.0
125%	28.02	4.70	0.60	1010.0	0.123	100.0
Short Circuit	28.70	0.140	0.30	0	0	0

Test Data (End of 1 Hour Test)

Load Condition	INPUT			OUTPUT		
	Voltage	Current	Ripple	Voltage	Current	Ripple
	VDC	AMPS	VPP	VDC	AMPS	VPP
100%	28.11	3.80	0.60	1040.0	0.096	70.0
110%	28.04	4.25	0.50	1025.0	0.108	80.0
115%	28.01	4.40	0.50	1022.0	0.112	84.0
125%	27.94	4.98	0.60	1010.0	0.124	100.0
Short Circuit	28.68	0.165	0.30	0	0	0

DATE 8-9-66

TECH. O. DIVERS

ENGR. D. RAMIREZ

Q.A. N. GOOD

TABLE XXXIX

MODULE # 3 TEST DATA SHEET (NAS-37926)

1. Test Condition: VACUUM (10-4 TORR OR LESS)

2. Test No. 3 (No Load and 10,000 Vdc)

HI-POT TEST

Circuit and Polarity	Leakage Current μ Amps
+ - Input to Output	1.0
+ - Output to Heat Sink	0.5
- + Input to Output	1.0
- + Output to Hink Sink	0.5

DATE 8-9-66

TECH. O. DIVERS

ENGR. D. RAMIREZ

Q.A. M. GOOD

TABLE XL

MODULE # 3 TEST DATA SHEET (NAS 3-7926)

1. Test Condition: VACUUM (10^{-4} TORR OR LESS)
2. Test No. 4 (Rated Load and 10,000 Vdc)

HI-POT TEST

Circuit and Polarity	Leakage Current μ Amps
+ - Input to Output	1.0
+ - Output to Heat Sink	0.5
- + Input to Output	0.5
- + Output to Heat Sink	1.0

The base plate of each module is used as a radiator and consists of an aluminum plate, with integral pads machined into the plate for mounting the low voltage components. High voltage components were mounted to the base plates across thin fiberglass-phenolic boards which provide a thermally conductive mounting. The base plate was designed for the minimum thickness commensurate with thermal and structural requirements to minimize weight.

Transformers have been potted in open cans welded to the base plate. The potting thickness is minimized so that direct heat conduction from the interior of the transformer to a metal conductor or to the exterior is through as short a path as possible.

4.10.2 Thermal Analysis

The upper limit of radiator performance is shown in Fig. 41, where radiator surface area is plotted against radiator temperature for a black radiator viewing outer space. The temperature range between 100°C and 180°C covers the possible range of peak operating temperatures for an electronic module. Two design approaches were possible: the module could be designed to operate at the highest possible radiator temperature to minimize radiator area, with components which will tolerate high temperatures; or the module could be designed for optimum efficiency, with components which generate the least amount of waste heat. The latter approach was taken on all modules, since there were no stringent radiator surface area limitations.

An "ideal" radiator is not ideal for outer space with impinging sunlight. Solar energy impinges on a surface at 1.0 A.U. in outer space at the rate of 130 watts/ft.^{2} At temperatures below 123°C a perfect black surface would absorb more heat than it would dissipate, and a 20 in.^{2} radiator surface would have to operate at a temperature of 204°C, or greater, to dissipate 20 watts in direct sunlight. Therefore, a nongray selective emissivity surface is necessary for a radiator rejecting heat to space in the presence of sunlight.

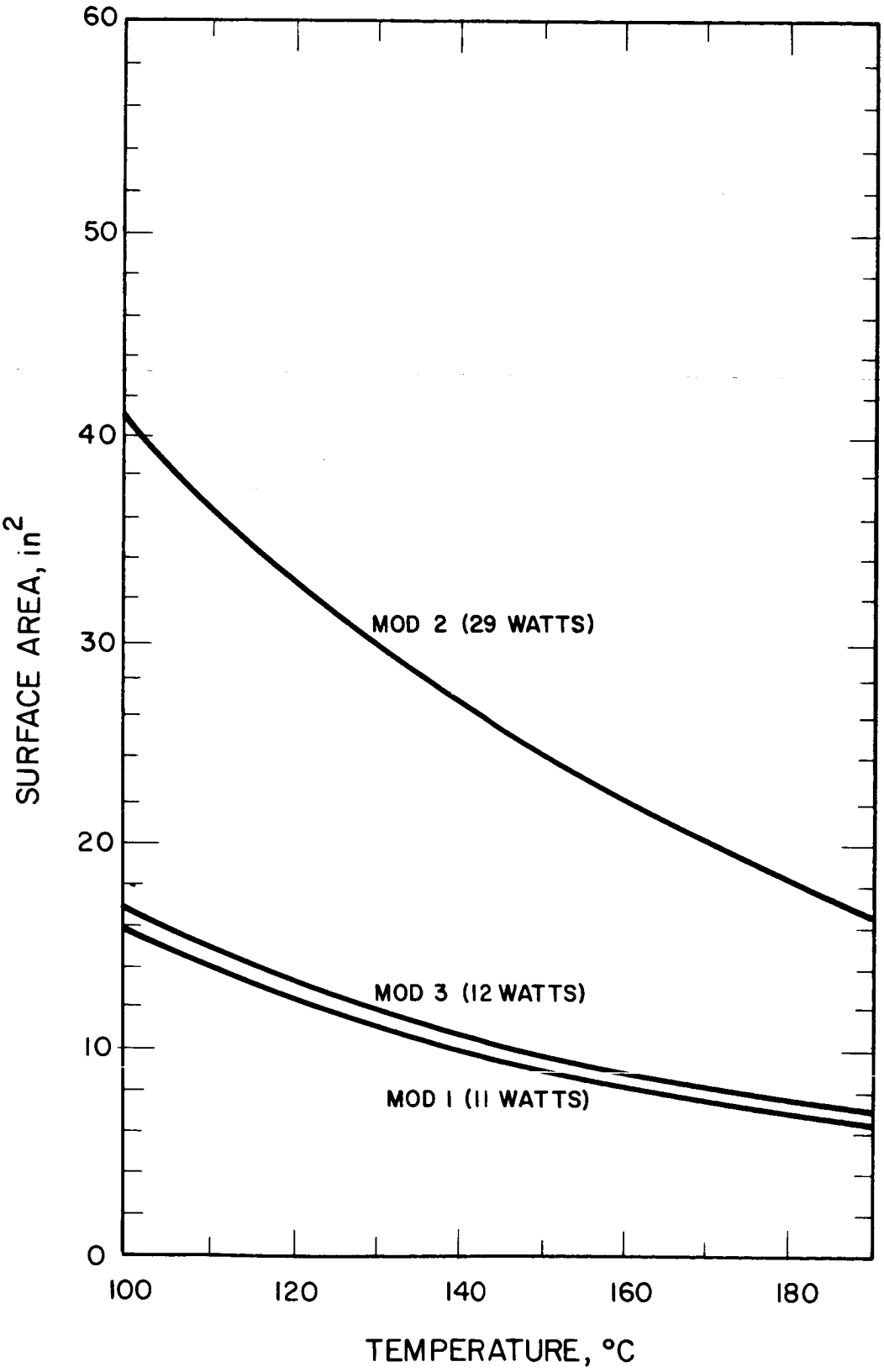

FIG. 41 RADIATOR AREA VERSUS SURFACE TEMPERATURE IDEAL LIMIT (BLACKBODY RADIATION)

EOS has built several flight test packages using selective radiator surfaces. The modules are painted with a zinc oxide-pigmented methyl silicone paint which displays an emissivity of 0.85 at the wavelengths corresponding to thermal radiation at 400°K, but an absorptivity of only 0.2 to impinging sunlight. The paint (S-13) is marketed by Transitron, Inc., an affiliate of IIT Research Institute, and possesses superior resistance to ultraviolet aging as well as desirable optical properties.

A radiator surface conforming to these conditions is analyzed by the net heat balance shown in the following equation. Surface area versus temperature using this equation is shown in Fig. 42. This figure was used to determine the required radiator surface area based on the maximum permissible radiator operating temperature.

In words, net heat out = heat lost by radiation - heat input from impinging sunlight.

This can be mathematically expressed as follows:

$$W = A_1 \sigma \epsilon_1 T_1 4 - \frac{130}{144} \alpha A_1$$

$$A_1 = \frac{W}{\sigma \epsilon_1 T_1 4 - \frac{130}{144} \alpha}$$

where,

W = heat dissipated, watts

A_1 = area, $in.^2$, of radiator surface

α = 0.2

ϵ_1 = 0.85

σ = $36.6 \times 10^{-12} \frac{W}{in.^2 \, {}^oK^4}$ (Boltzmann's constant, in convenient units)

Next, the projected operation of this radiator surface in space is compared to the actual operation of the test module in a laboratory environment. NASA requirements specified that this

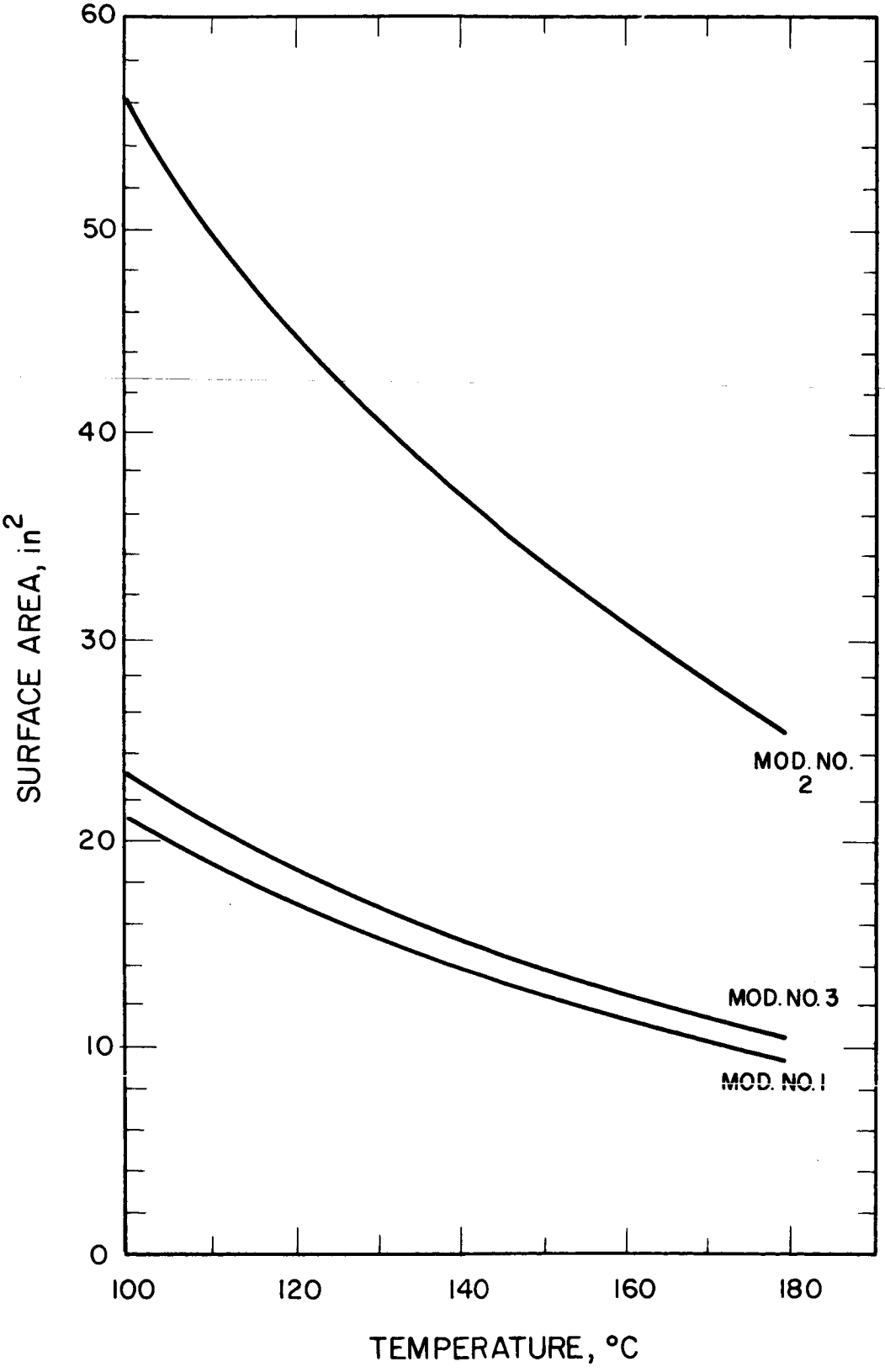

FIG. 42 RADIATOR AREA VERSUS SURFACE TEMPERATURE SPACE WITH NORMAL SUNLIGHT AT 130 W/ft^2

module be tested in a vacuum of 10^{-4} torr or greater, and that all heat must be dissipated by radiation to a flat copper plate cooled by liquid nitrogen to $77^{o}K$. This radiator heat sink must be separated from the test module radiator surface by one inch, and must extend 6 inches or more beyond the edges of the module, so that the radiator surface does not see anything but the cooled plate. The rest of the module surface must view an ambient surrounding at $25^{o}C$. Heat transfer to the ambient surroundings must be minimized.

Thermal tests used a heat sink of 1/8 inch copper, with 10 feet of 1/2 inch diameter copper tubing welded to the back and the surface viewing the modules painted with 3M black velvet over a zinc chromate primer. A continuous flow of liquid nitrogen through the tubing maintained sink temperature. Temperature versus radiator area for the test case should look like Fig. 43.

4.10.3 Thermal Design

Three factors were considered in the radiator design of these electronic modules: (1) conduction along the radiator surface must be adequate to ensure a nearly isothermal surface; (2) heat must be conducted from the mounted heat-dissipating elements to the radiator surface (through insulators, where necessary) with a minimum temperature drop; and (3) the opposite side of the module must be shielded to insure that all heat generated within the module leaves by way of the radiator surface.

Since each of the three modules generates different amounts of waste heat and has other different packaging and design requirements, the three modules were designed separately. However, since there is considerable duplication of electronic components in each module, the thermal design requirements involved in mounting and insulating these components are similar, so that the most critical components can be discussed without reference to their location. We have found that an isothermal radiator surface is easy to attain in this application.

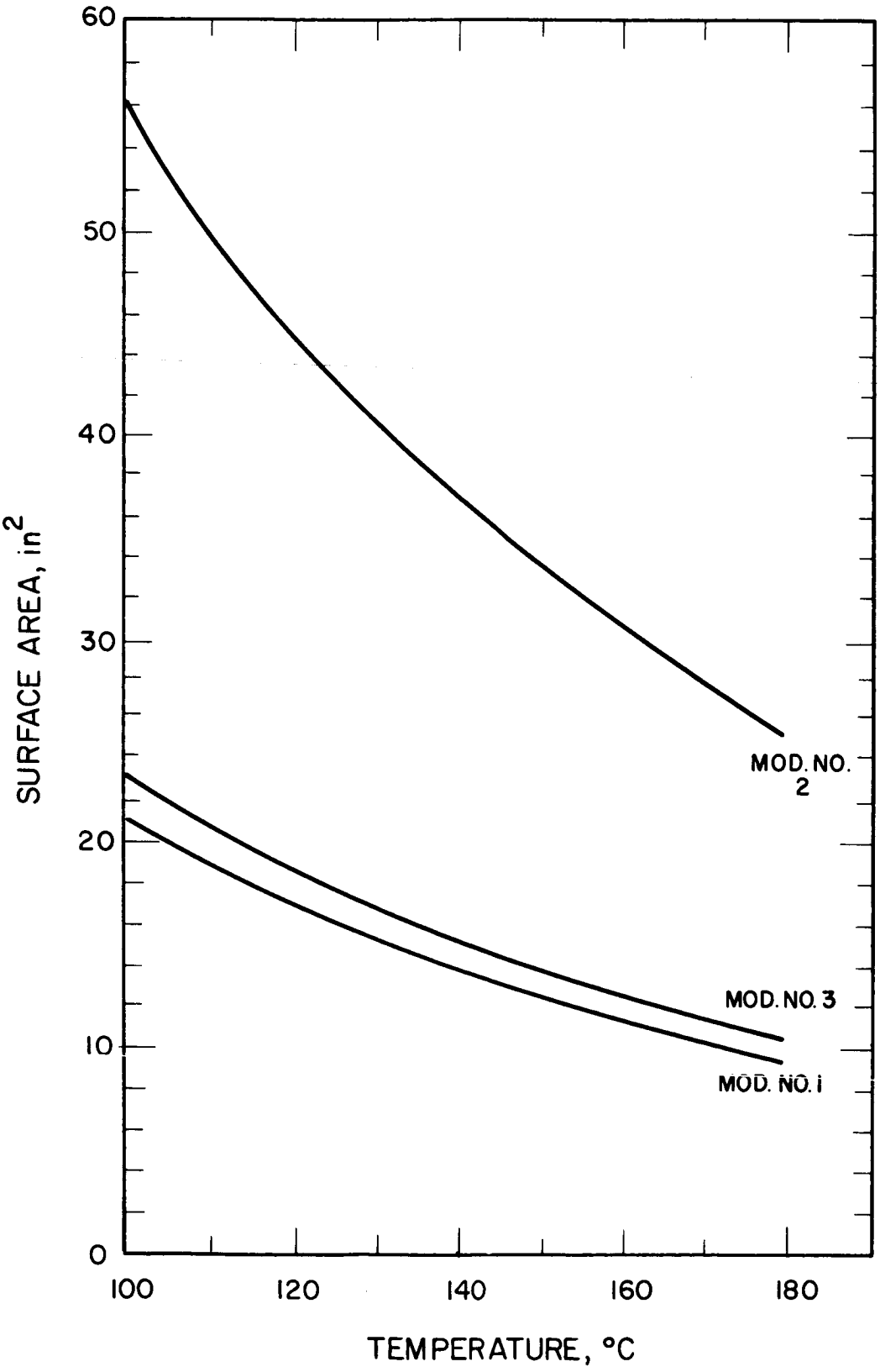

FIG. 43 RADIATOR AREA VERSUS SURFACE TEMPERATURE (TEST CONDITIONS)

In Fig. 44 the temperature drop along the radiator surface is plotted against distance from a hot spot, at three heat flow rates. A rate of 50 watts/in. corresponds to 5 watts flowing by conduction through an aluminum radiator of 0.10 inch thickness. The highest heat flow rate encountered in any of the three modules is the heat dissipation from the diode bridges through the radiator surface, which, for the thinnest portion of the radiator (1/3 inch thickness), amounts to 80 watts/in. Therefore, a temperature drop of $3^{o}C$ over a distance of 1 inch is the most that can be expected in these surfaces.

Figure 44 assumes that heat travels from the hot spot by conduction only. The analysis of a radiator losing heat by conduction and radiation is not straightforward, since it involves the solution of a nonlinear partial differential equation.

Computer solutions in graphical form are shown for some boundary values of this equation in Ref. 2. A dimensionless radiator surface effectiveness parameter (the 'profile number') is defined in Ref. 2:

$$\zeta_p = \frac{\sigma \epsilon T^3 L^2}{k \Delta x}$$

where

L = length of fin

Δx = thickness

This parameter is the ratio of heat flow out of the radiator surface by radiation to heat flow through the radiator by conduction. The parameter was less than 0.01 for the problem shown in Fig. 44, which indicated a nearly isothermal radiator.

Junction temperature drops were computed for two cases: (1) for power transistors mounted at right angles to the radiator surface; (2) for the heat-generating diode bridges on the high voltage shelf, which must be insulated electrically from the radiator

Ref. 2: MacKay, Donald B., "Design of Space Powerplants," Prentice Hall, Inc., Englewood Cliffs, N. J.

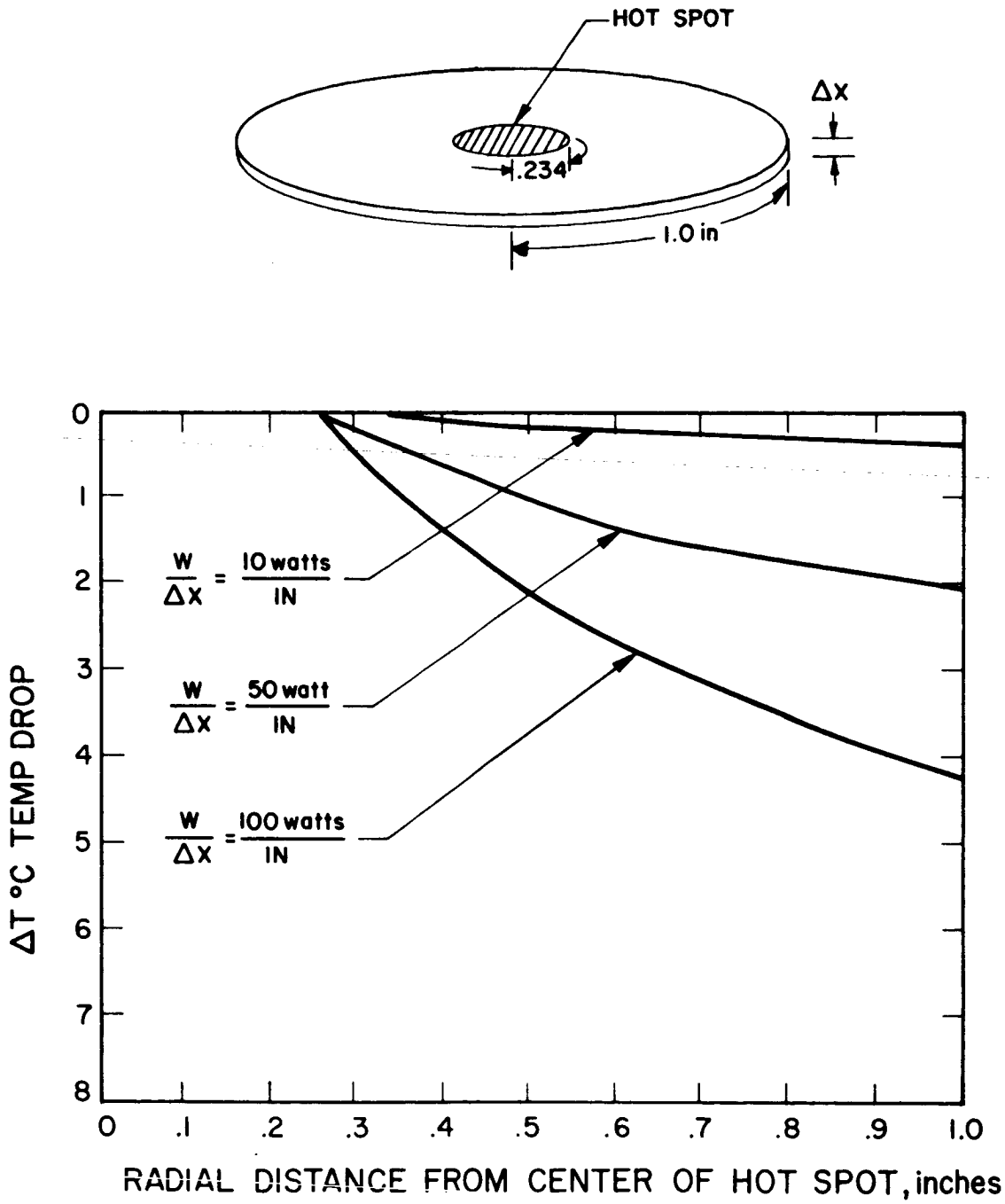

FIG. 44 TEMPERATURE DROP ALONG RADIATOR SURFACE

surface. The results of these analyses are shown in Table XL1, which presents junction resistances for the critical items. These numbers represent heat transfer by conduction only and do not take into account the heat flow by radiation which should also be appreciable, since in all cases hot bodies on the radiator surface will reflect back to it from the inner surface of the heat shield. It can be seen that a temperature drop of $5^{o}C$ is all that will be encountered in the worst case and that there should be no problems in running the heat generating components near their highest effective temperature and still maintain good heat conduction to the radiator surface.

The transformers have a large surface area contacting the radiator and the metal can was welded to the radiator so that internally generated heat could be easily transferred to a dissipating surface.

A double layer of shiny aluminum stamped from 0.005 inch sheet stock and joined together was used to shield the module. An analysis of the heat transfer through this shield shows that only 5 percent of the total heat generated within the module will escape through the shielded surfaces. This heat loss could be reduced to a negligible amount by the inclusion of a couple of layers of aluminum foil between the two shields. One advantage to shielding in a vacuum is the complete absence of convection. Another advantage is the tendency of the inner shield surface to reflect heat back to the inner radiator surface. The inner radiator surface and the components mounted on it were painted black (3M black velvet) to enhance heat transfer out of the radiator and to stabilize the interior temperature distribution.

4.11 Reliability

From a reliability standpoint, it was desirable to achieve high reliability for the high frequency converter. This end was accomplished in several ways. The number of components in the basic

TABLE XLI

THERMAL DATA

Item	Function	Junction Resistance °C/watt	Mount-Radiator Resistance °C/watt	Dissipated Watts	Temperature Drop °C
1	Q3, Q4 transistors	0.61	1.07	2.25	3.8
2	T2 transformer	0.30	0.10	2.50	1.0
3	CR1-4 Diode Bridge (Mod. 1)	1.00	0.32	1.58	2.1
4	CR1-4 Diode Bridge (Mod. 2)	0.40	0.30	1.00	7.0
5	CR1-4 Diode Bridge (Mod. 3)	1.00	0.32	2.50	3.3

converter were kept to an absolute minimum. Seventeen components are used in the basic converter circuit and a total of 45 components are used in the entire circuit which includes the overload protection circuitry.

Wherever possible, a two-to-one (100 percent) safety factor was employed for all components used in the converter circuit. The exception to this rule was in the selection of the power transistors where a 60 percent safety factor had to be tolerated as a tradeoff for fast efficient power switching.

This low parts count coupled with the use of low operating electrical stress levels resulted in a converter circuit with a very high reliability. The basic reliability of the converter circuit was computed to be 0.970.

The basic converter circuit or module can then be connected with inputs in parallel and outputs in series or parallel to achieve extremely high reliability. High reliability through redundant circuits is a major advantage in using modular high frequency converters for spacecraft applications. This is particularly true when considering missions of long duration. The modular approach provides backups for component failure. For example, the reliability of a modularized power subsystem using ten converters (10 x 100 watts = 1000 watts) in series with no standby converters is:

$$R = (0.970)^{10} = 0.707$$

With the addition of one standby converter which may be turned on in the event of a failure of any other converter, this number is increased to 0.950 and if two standby modules are added, the reliability number is further increased to 0.999.

This brief analysis has been based upon component failure rates only and it assumes that failure probabilities associated with external failure modes (such as main busses shorting to ground, etc.) have been made small (relative to component failure rates) by using sufficient design safety factors in these areas.

5. CONTROL SYSTEM

Work on the Control System began with an examination of the originally proposed system. In addition to the power conditioning system objectives of lowest possible weight, highest efficiency, and high reliability, the following objectives were considered:

1. Volume
2. Logistics
3. Maintainability
4. Cost
5. Complexity
6. Flexibility
7. Interference Susceptibility
8. Interference Generation (Radiated and Conducted)
9. Response
10. Radiation

In addition to demonstrating general system tradeoffs with the power conditioning modules, control system component tradeoffs between micro-miniature solid state devices (IC and/or MOS FET) and micro-miniature relays were made. The primary tradeoffs considered were:

1. Weight
2. Power Consumption
3. Reliability
4. Volume
5. Interference Susceptibility

The control system design was dictated by requirements of the EOS 1 kW, Df engine as shown in Table XLII.

The control system in general was divided into the following subsystems:

TABLE XLII

POWER SEQUENCING AND CONTROL
FOR A 1 kW CESIUM ELECTRON BOMBARDMENT ENGINE

Start Sequence

1. Energize reservoir, feedline, cathode, arc, and magnet supplies.
2. After the reservoir and cathode housing temperatures have reached 50°C and 350°C, respectively, energize vaporizer with feedback from arc supply. Vary vaporizer power to maintain constant arc current (20 amps). When reservoir housing reaches 50°C, de-energize reservoir supply.
3. After ion chamber housing has reached 150°C, de-energize vaporizer supply, switch vaporizer feedback loop from arc current to beam current and energize the neutralizer.
4. Energize V^+, V^- and vaporizer supplies when arc current falls below 10 amps.
5. Whenever the arc current is above 10 amps, de-energize cathode heater.
6. All supplies necessary for steady-state operation are now energized.

Maintenance of Stable Conditions

1. Maintain constant beam current by varying the vaporizer heater power.
2. Minimize drain currents by varying the arc power.
3. Maintain neutralization by varying neutralizer vaporizer power.

Module input and output control

Module failure mode detection

System input logic matrix

Timing and inhibit logic

System output logic matrix

Analog-digital circuitry

Module synchronization circuitry, fine voltage or power control

5.1 Module Input-Output Control

Several design approaches were considered to control the input power or the ON/OFF operation of the modules. The design approach applied is a combination of three control elements. Only the main switch in the overall system directly controls the power to the power conditioning modules. This single switch is utilized for all of the modules in a unit interface system. Power plant protection, or isolation for each module, is provided with an input power fuse in each module. Any catastrophic module failure will open the fuse and thus isolate the module input from the rest of the system. Static ON/OFF power control in each module is provided by micro-miniature magnetic latching relays which short the bases of the main switching transistors in the converters to ground. These relays weigh less than 0.1 ounce. Since they are magnetic latching, there is no steady state power requirement. Transient or overload ON/OFF control is provided with a parallel set of active switches (transistors).

Module output switching, where required, can also be accomplished with several different design approaches. The module outputs for the two high voltage supplies are hard-wired in series. This includes the redundant or spare modules. Isolation between module outputs is provided by the output bridge rectifier circuits. Since ON/OFF module control is provided in low level input circuitry, output switching in the interface between the power conditioning and the thrustor is not required. There are also no module output switching requirements for the cathode and reservoir heater supplies, since redundant power

conditioning modules are not utilized. Output switching, however, is required for the modules in the three remaining supplies. Since a relatively low voltage high current is required from these supplies, output load switching is required to minimize the I^2R losses. Mechanizing a hard-wire bridge configuration for these supplies could result in a 50 percent decrease in efficiency. There are other design approaches that utilize a common rectifier system. This approach, however, deviates from complete redundancy, besides adding more input switching requirements. Since the common for the vaporizer is at ground potential, a standard relay approach can be used for module output switching for this supply. The remaining two supplies, arc and vaporizer, have their outputs common to the positive high voltage. Consequently, high voltage isolation between the contacts and the actuating circuitry was required in the module output switches. There were three switch approaches that could have been implemented for these two supplies. These were:

1. Vacuum switch
2. Reed relay
3. Standard relay floating at the high potential

Based on overall system design considerations, a standard magnetic latching relay approach was selected. With this approach, the entire relay, including packaging, is referenced to the positive high voltage. Actuation of the relay is accomplished by an isolation transformer with high voltage insulation between the windings.

5.2 Module Failure Mode Detection

Module failure mode detection was accomplished via a signal from the module current sensor bridge output and a microcircuit analog-digital level detector. All possible module failure modes, with the exception of a module primary to secondary transformer short circuit that is independent of transformer secondary shorting will be detected with this scheme. Every module requires an independent A/D level detector and associated logic to distinguish between abnormal thrustor operation and abnormal module operation.

5.3 System Input and Output Logic Matrices

The input-output logic portions of the control system will program the start-up, shut-down and module replacement sequencing operations. This area was designed so that any number of system start-up and shut-down operations, in addition to module replacements, may be initiated and completed. This area is comprised of microcircuit digital logic.

5.4 Timing and Inhibit Logic

This subsystem will provide the necessary counting, time delays, and inhibit circuits for a single module sequencing operation. Energizing or deenergizing one module at a time will minimize the peak power requirements of the control system.

5.5 Module Synchronization and Fine Voltage or Power Control

Module synchronization or output voltage control is not necessary for modules No. 1 and No. 3. Regulation necessary for supplies requiring these modules will be supplied on a module addition or subtraction basis. In the case of the 1 kW, 5000 second DF engine, the +HV will be regulated to ±6.25 percent, using the module addition or subtraction technique. Supplies requiring module No. 2 will need synchronization when two or more modules in series are energized.

5.6 Analog-Digital Circuitry

Microanalog-digital circuit networks are used almost exclusively in the thrustor and power conditioning to control system interfaces. This requires, however, that the analog-signals be low level signals. Use of microcircuits resulted in large weight, volume, and power consumption savings when compared to discrete part circuitry.

5.7 Control System Modification

During the design of the control system, the NASA Technical Monitor, visited EOS. At that time (Sept. 1965) he was briefed on the design to date and a discussion was held on an optimum control system design. Mr. Gruber agreed that in order to satisfy engine requirements

at minimum system weight, several modifications had to be made to the then existing power conditioning modules. It was concluded that module No. 1, the 250 Vdc module, be incorporated as designed; module No. 2, the 5 volt module, as presently designed, could not be used effectively for any engine requirement. Three different module designs were used as substitutes for this module. The first, module 2A, is a 100 watt module and provides an 8 Vac output. This module satisfied cathode and reservoir heater requirements. Since output waveform and control are not critical for these two heaters, the weight and efficiency for module No. 2B should be comparable to module No. 1. The second design, module No. 2B, is a 200 watt arc supply module with a 6-30 Vdc output. The arc supply requirements present most of the power conditioning design problems for the electron bombardment engine. Both coarse and fine voltage control is required. Figure 45 illustrates the basic voltage-current relation for the arc supply. The coarse voltage reduction occurs when the arc strikes. After the arc strikes, fine voltage control is needed to minimize the drain currents. It should be noted that the fine voltage control is a double valued function as shown in Fig. 46. This control also has a very slow response. The third design, module No. 2C, is a 100 watt module with four separate outputs. These outputs satisfy the magnet supply, feed line heaters, discharge neutralizer heater and vaporizer heater requirements. With the exception of the feed line heaters, module No. 2C outputs have to be controllable. A constant current of approximately 2.1 amperes at about 10-12 watts is required from the magnet supply. The vaporizer power (20-50 watts) is controlled by beam current feedback (by arc current feedback during startup). The discharge neutralizer power (10-15 watts) is also feedback controlled. The -HV engine requirement is approximately 30 watts maximum at 500-600 volts. This requires some redesign to the present 100 W, 1000 volt output of module No. 3.

Power conditioning module redundancy was added where failure of a supply would result in serious degradation or complete loss of thrustor performance.

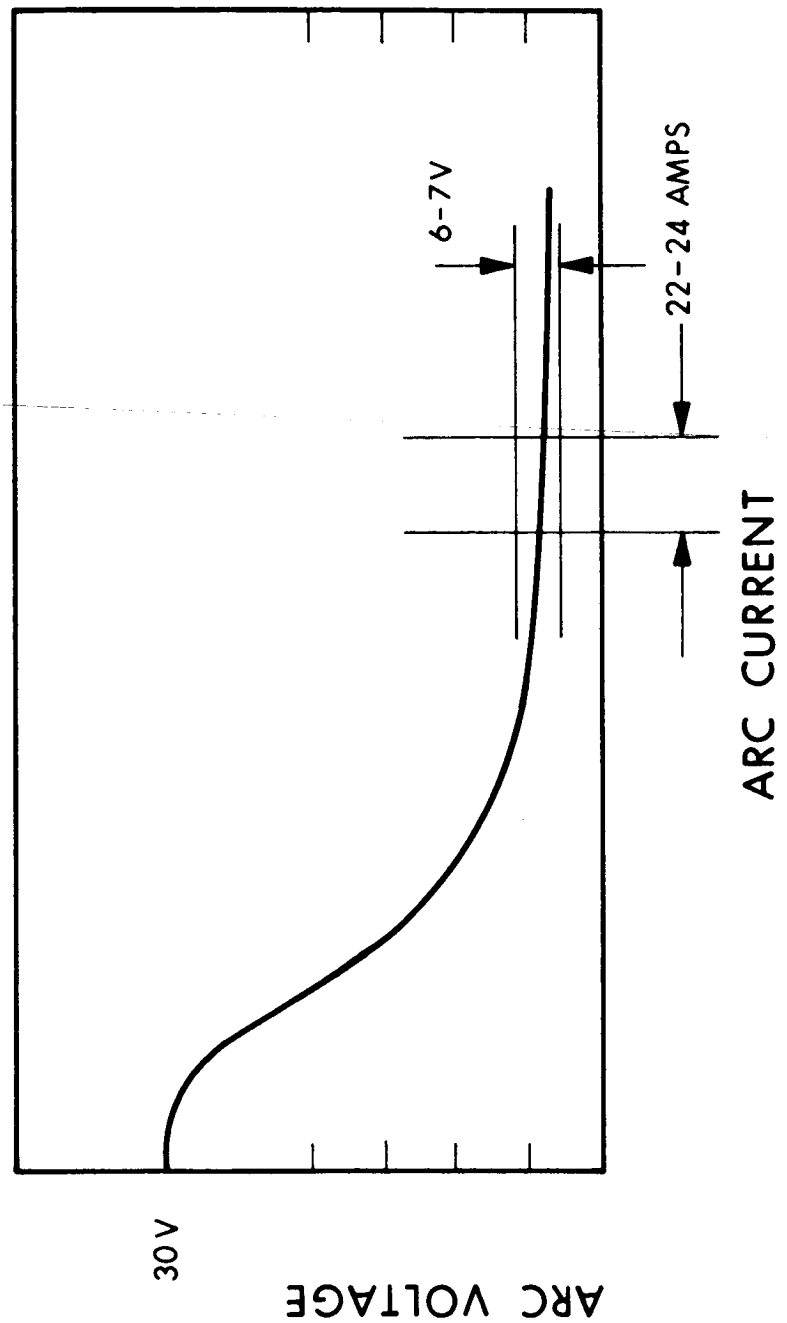

FIG. 45 ARC SUPPLY COARSE CONTROL

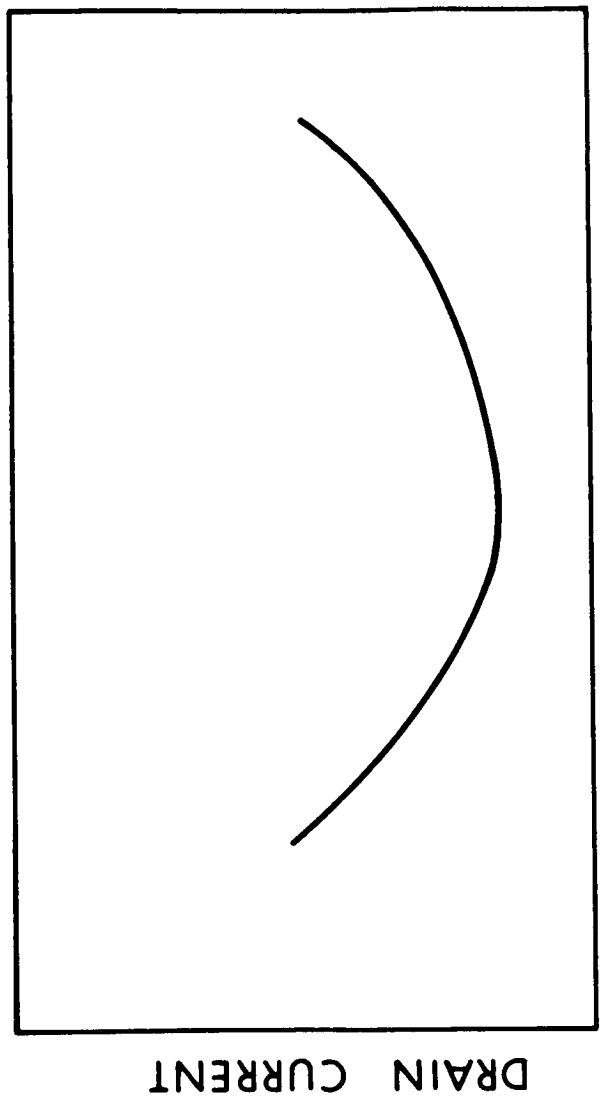

FIG. 46 ARC SUPPLY FINE CONTROL

The engine startup sequence is controlled by three engine thermistor probes and an arc supply current sensor. The startup sequence is basically a three step operation which can take as long as 90 minutes. The shutdown sequence is accomplished by simultaneous removal of all engine power. Figure 47 shows a block diagram of the modified power conditioning in control system.

5.8 Control System Summary

After the design approach for ON/OFF module control was selected, the next problem involved defining the thrustor requirements and characteristics for flight system control. A thorough investigation of engine requirements for start-up, shut-down, and transient power sequencing showed that control could be implemented as a direct function of engine parameters. Electronic or electromechanical timers used in other systems were not considered necessary and consequently were not implemented. Power control as a function of thermal and electrical characteristics of the engine during sequencing operations has distinct control, system weight, volume, control power, and response advantages over other methods. Three separate engine temperature measurements are necessary for the sequencing requirements and range from 50 to 300°C. Only one supply current is monitored, the arc supply, for sequencing operations. In addition to ON/OFF module power control, feedback loops and feedback loop control references are also controlled during sequencing operations with these same engine parameters.

A simplified block diagram of the controls for the modularized power conditioning unit is shown in Fig. 48. Figure 49 is a detailed schematic of the control system. Microcircuits are used exclusively in the control system with the exception of discrete component temperature transducers, relays for static module control, and magnetic amplifiers for current sensing.

The microcircuit networks include integrated DTL gates, DTL binaries, operational amplifiers, analog-digital comparators, and DTL power gates. Operational amplifiers are used in the two feedback loops:

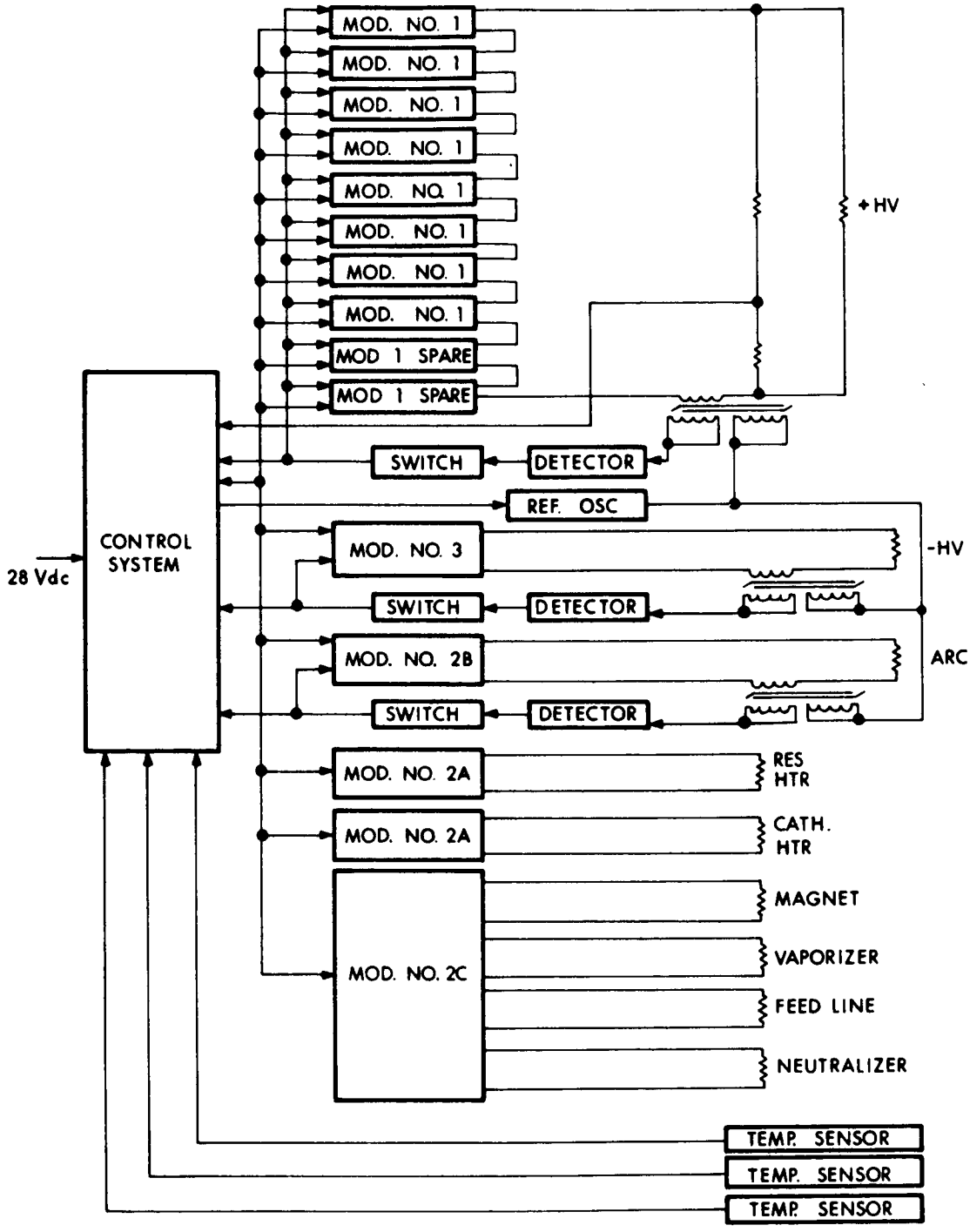

FIG. 47 DIAGRAM OF THE MODIFIED POWER CONDITIONING AND CONTROL SYSTEM

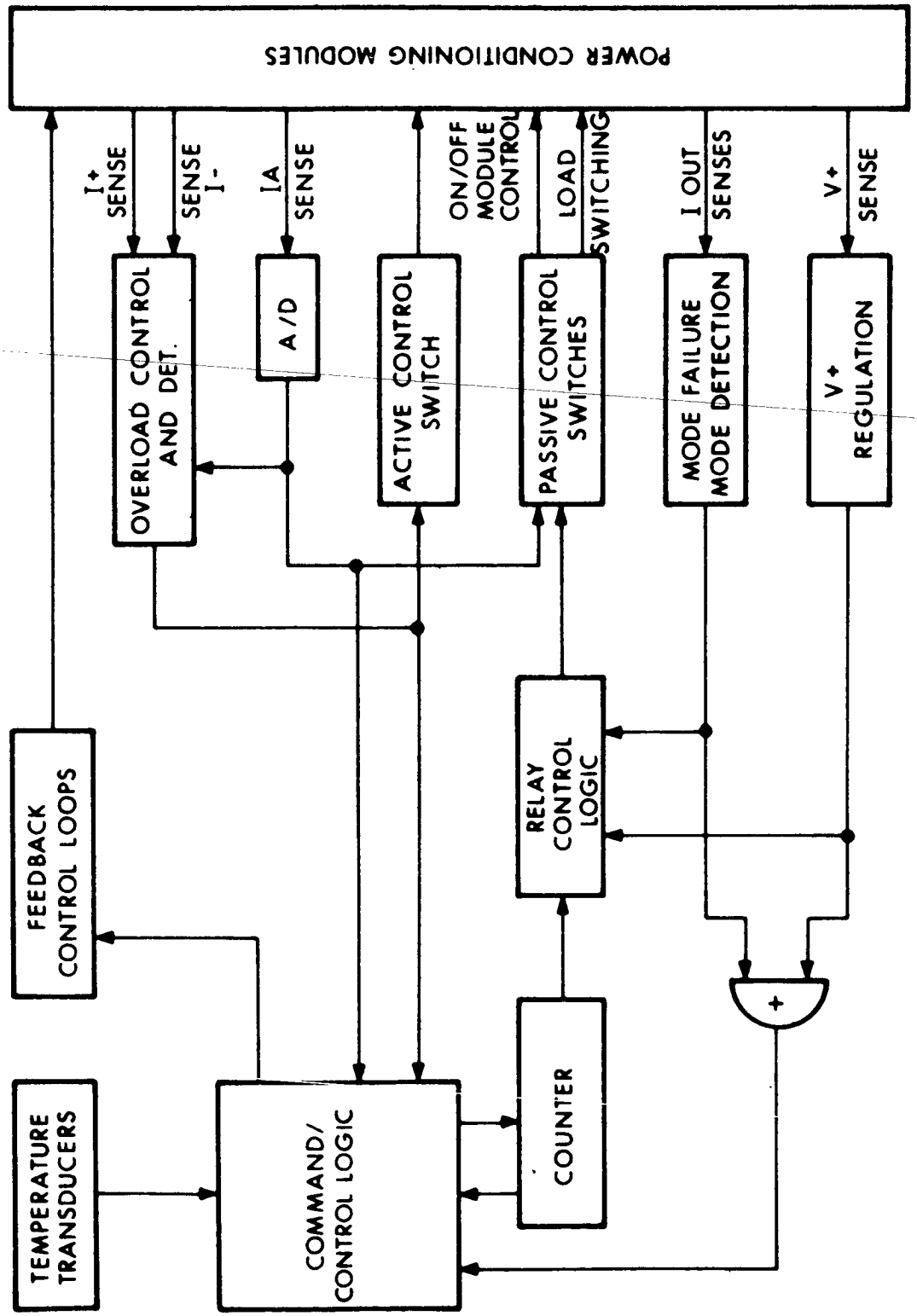

FIG. 48 CONTROL SYSTEM BLOCK DIAGRAM FOR MODULARIZED POWER CONDITIONING UNIT

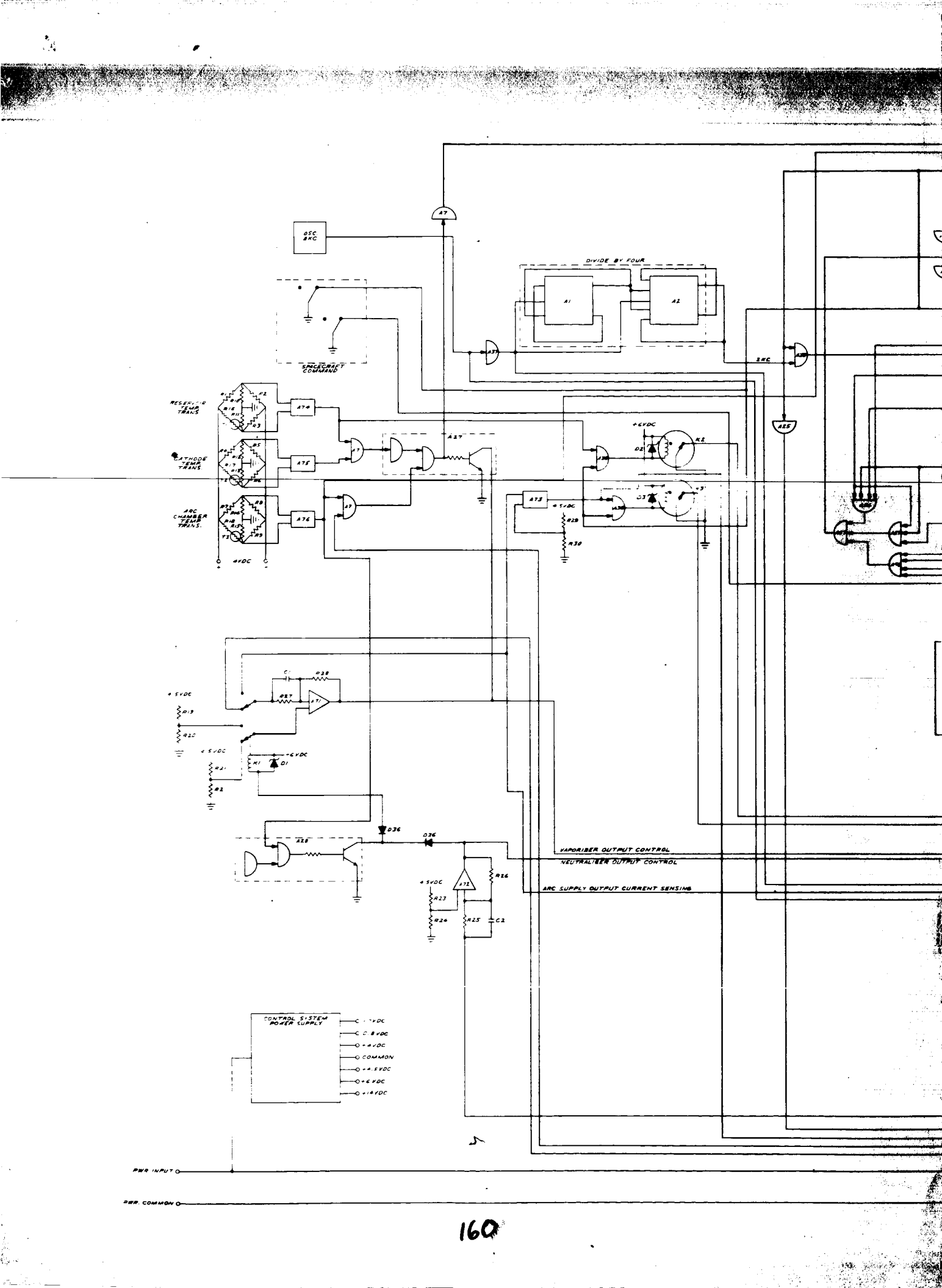
OSC & RC
DIVIDE BY FOUR
A1
A2
SPACECRAFT COMMAND
RESERVOIR TEMP. TRANS.
CATHODE TEMP. TRANS.
ARC CHAMBER TEMP. TRANS.
4VDC
+6VDC
4.5VDC
VAPORIZER OUTPUT CONTROL
NEUTRALIZER OUTPUT CONTROL
ARC SUPPLY OUTPUT CURRENT SENSING
CONTROL SYSTEM POWER SUPPLY
-7VDC
-0.8VDC
+4VDC
COMMON
+4.5VDC
+6VDC
+14VDC
PWR INPUT
PWR. COMMON

COUNTER
A3
A4
A5
A6
0.8 VDC
A77
A78
6 VDC
ARC SUPPLY MODULE
MAGNET, VAPORIZER, NEUTRALIZER, FEED LINE SUPPLY MODULE

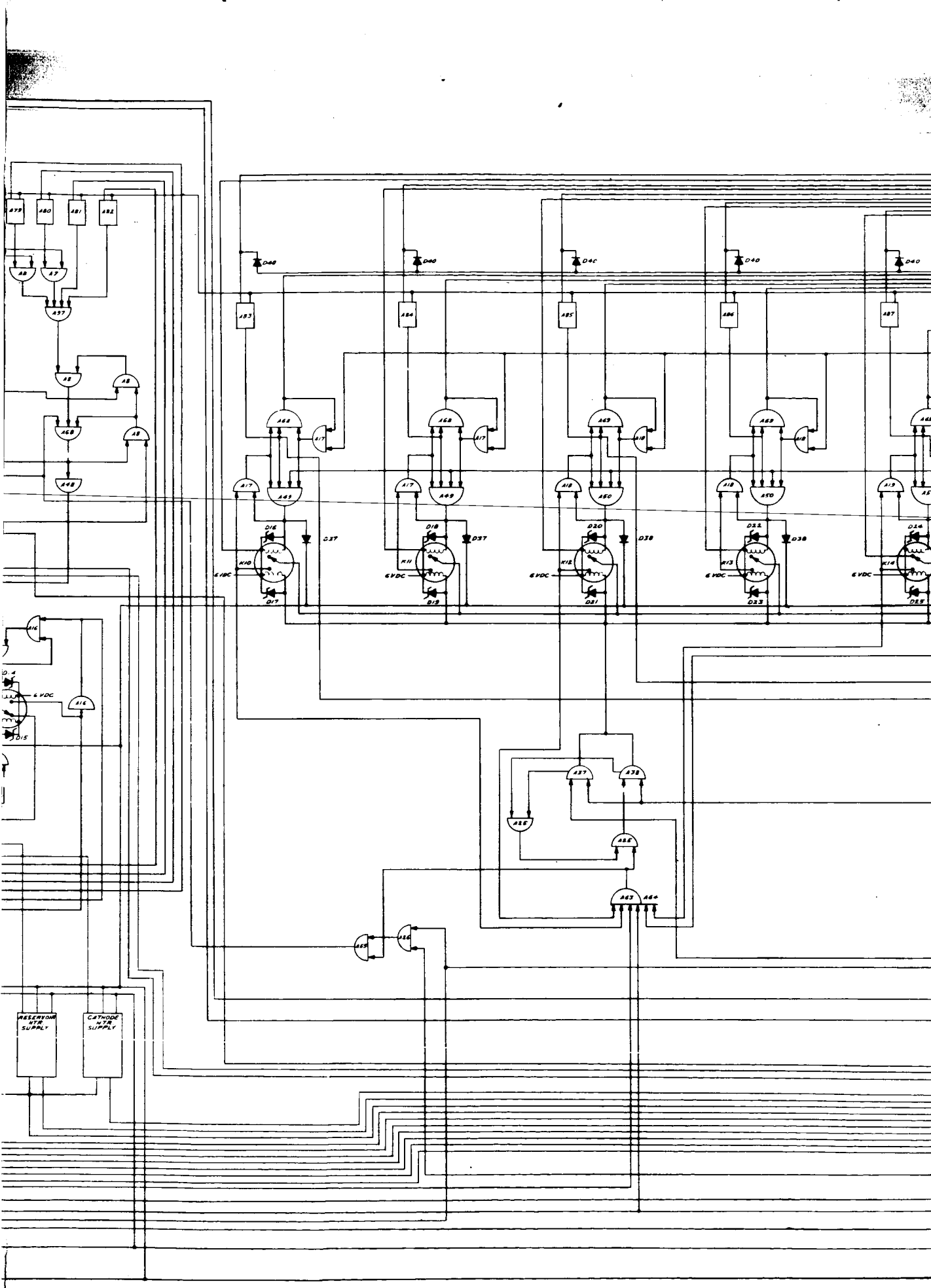
A79
A80
A81
A82
A8
A7
A97
A2
A3
A98
A1
A53
A54
A55
A56
A57
D40
A62
A63
A64
A65
A66
A17
A18
A49
A50
D16
D18
D20
D22
D24
D37
D38
K10
K11
K12
K13
K14
6 VDC
D17
D19
D21
D23
D25
A16
D15
A37
A38
A35
A36
A67
A68
A69
A70
A71
RESERVOIR HTR SUPPLY
CATHODE HTR SUPPLY

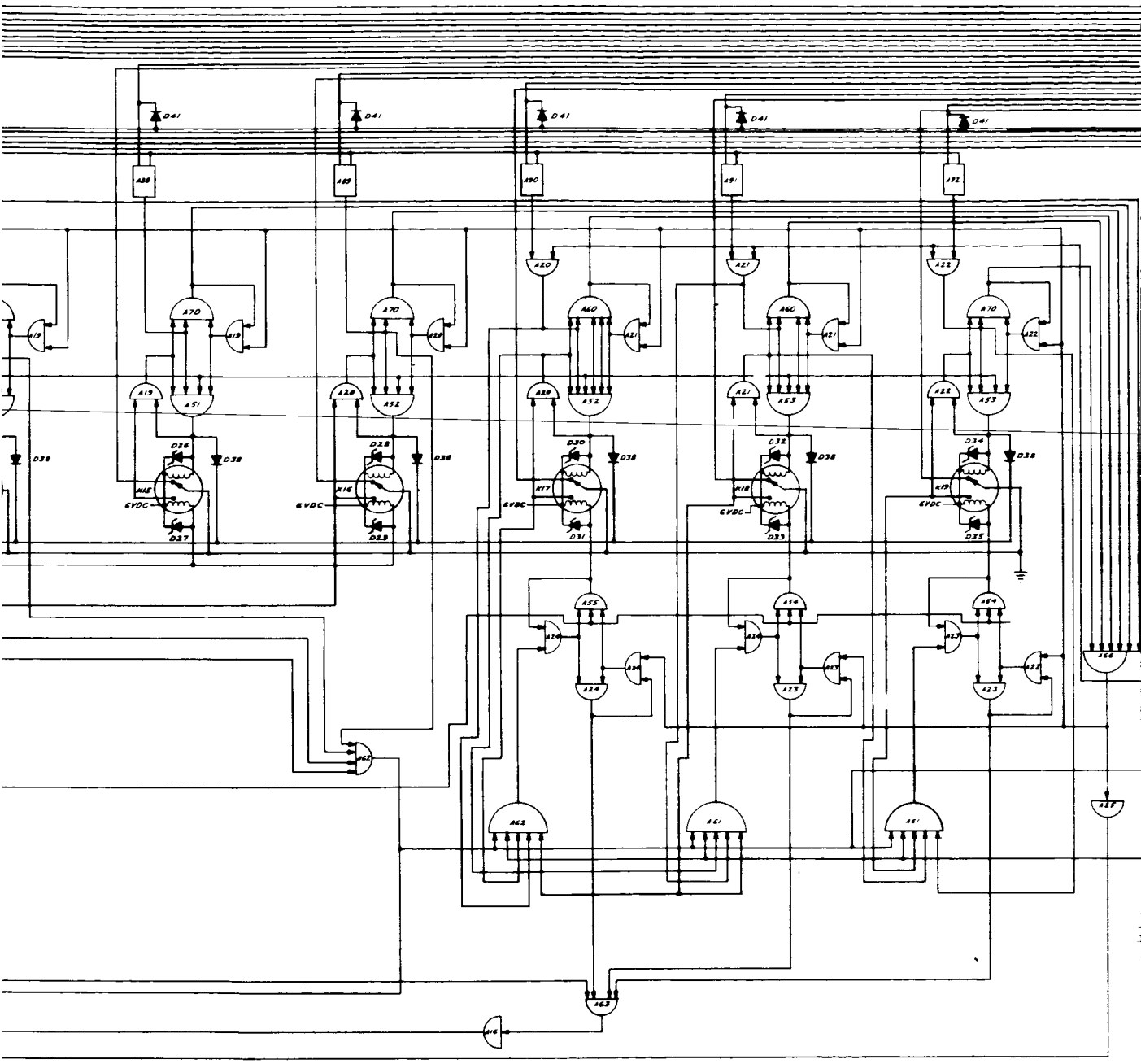

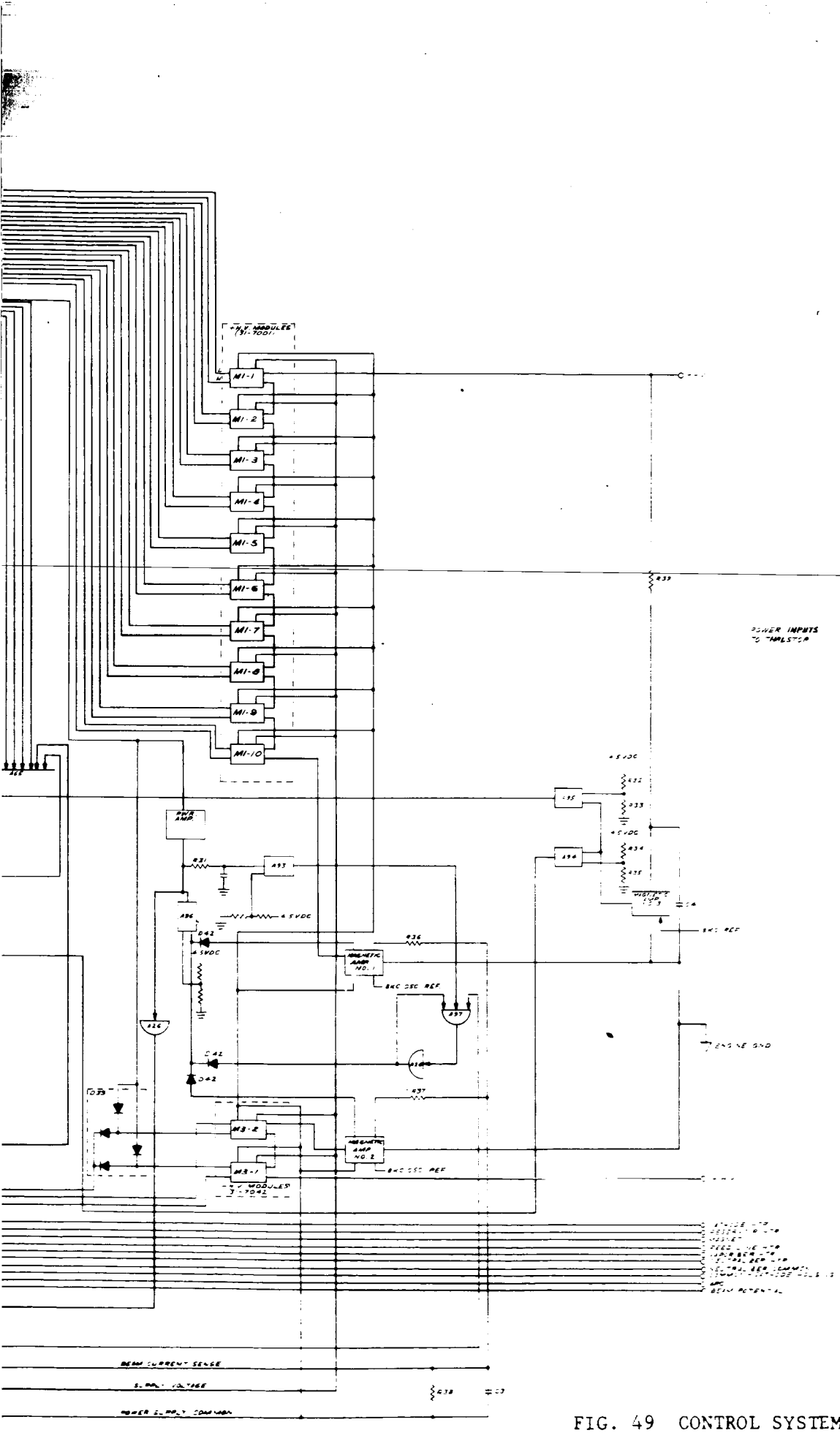

FIG. 49 CONTROL SYSTEM BLOCK DIAGRAM

beam current to engine vaporizer power, and neutralizer bias current to neutralizer vaporizer power. The A/D comparators provide the interface between the analog engine and power conditioning data and the digital section of the controls. The analog information includes failure mode detection, regulation, temperature sensing, and current sensing. Integrated circuit DTL power gates are available that have sufficient current capabilities for driving the magnetic latching relays and as such have been implemented.

The principal portion of the control system is the digital section. DTL logic was selected for this section on the basis of a compromise between power consumption, noise margin, and speed. In this section, all of the controls or coding and decoding necessary for start-up, transient protection, regulation, and failure mode sequencing are programmed into one centralized and integrated system.

The weight and power consumption of the complete control system, excluding the magnetic amplifiers, is nominally about 1.5 pounds and 2 watts for the 1 kW unit. During certain switching conditions, the power requirements will reach about 3.5 watts. For unit systems in the 1 to 5 kW range, the control system weight and power requirements should not increase significantly over that for the 1 kW unit.

6. CONCLUSIONS

The primary objectives of this research and development program have been successfully attained.

The three high frequency converter modules developed are small, lightweight, efficient, and very reliable. These modules or "building blocks" can be used to construct power conditioning subsystems of any desired voltage and power level. The resulting power conditioning system will be smaller, lighter, and more efficient when compared to a more conventional approach. Another area where modular power conditioning has clearly surpassed any conventional design is reliability. High reliability of a power conditioning subsystem is now possible through redundancy. Redundant, or spare, modules can be included in a power conditioning subsystem to provide multiple backups at fractional increases of subsystem size and weight.

A control system was designed to provide power distribution, control switching, and the necessary regulation to operate ion engines in a space environment. The exclusive use of integrated circuits in the conversion of analog to digital information and in the detection of failed modules has made possible an extremely small and lightweight control system.

BIBLIOGRAPHY

1. High Power, High Voltage, Audio Frequency, Transformer Design Manual, Navy Department, Bureau of Ships, AD 60774, p. 323

2. J. L. Jensen, "An Improved Square Wave Oscillator Circuit," IRE Transactions on Circuit Theory, Sept 1957

3. T. Roddam, Transistor Inverters and Converters, 1963, Van Nostrand, New York

4. Z. F. Chang,and C. R. Turner, "Characterization of Second Breakdown in Silicon Power Transistors," 1963, RCA Application Note, SMA-21

5. P. Ramirez Jr., "Low Input Voltage Converter Study," Electro-Optical Systems, Inc., Report 3210-Final, 1962